Joint Analysis of Gene and Protein Data

A Dissertation Presented

by

Chen Ji

to

The Graduate School

in Partial Fulfillment of the

Requirements

for the Degree of

Doctor of Philosophy

in

Applied Mathematics and Statistics

Stony Brook University

August 2007

Stony Brook University

The Graduate School

Chen Ji

We, the dissertation committee for the above candidate for the Doctor of Philosophy degree, hereby recommend acceptance of this dissertation.

Wei Zhu
Associate Professor, Department of Applied Mathematics and Statistics,
Stony Brook University
Dissertation Advisor

Nancy Mendell
Professor, Department of Applied Mathematics and Statistics, Stony Brook University
Chairperson of Defense

Esther Arkin
Professor, Department of Applied Mathematics and Statistics, Stony Brook University

Wadie Bahou
Professor, Department of Hematology, School of Medicine, Stony Brook University
Outside Member

This dissertation is accepted by the Graduate School.

Lawrence Martin
Dean of the Graduate School

Abstract of the Dissertation
Joint Analysis of Gene and Protein Data

by

Chen Ji

Doctor of Philosophy

in

Applid Mathematics and Statistics

Stony Brook University

2007

Early detection is critical in the successful treatment of life threatening diseases such as cancer. A vital component of this research is the identification and correlation of disease-related genetic and proteomic biomarkers based on gene micro-array data and proteomic mass spectra data from diseased and control subjects. Such knowledge is crucial in discovering the underlying genetic disease pathways, in drug development and in early diagnosis.

In this work, we first propose a quality control algorithm to improve proteomic data acquisition from the mass spectrometer. We then demonstrate a novel variance component approach for biomarker detection and for population homogeneity examination.

A major contribution of this thesis is the development of the scoring method that would yield the predictive disease probability rather than the traditional crude binary (yes/no) diagnosis. We present the s-CART and s-RF classifiers - the improved scoring variants of the binary classification and regression tree (CART) and Random Forest (RF) classifiers. Finally, we illustrate the biological and statistical process of integrating the genomic and proteomic data through a human platelet study conducted at the Stony Brook University Medical Center.

To my parents.

Contents

List of Figures

List of Tables

Acknowledgements

I cannot begin but by expressing my endless gratitude to my adviser, Professor Wei Zhu, not only for her valuable advice and support, but also for her warm understanding. I would have been nowhere without them.

I am also deeply indebted to the support of Doctor Wadie Bahou from School of Medicine. This thesis would not be possible without his guidance and unquestioning support.

I would like to thank Professor Nancy Mendell and Professor Estie Arkin, from whom I have learned many important scientific and mathematical skills.

I would like to thank my dear parents for constantly standing beside me and for keeping alive the place that I will always call *home*. My thoughts go to you in all I do.

Many good friends from Stony Brook and some old friends from Boston have smiled and bestowed me with various graces, through good times and rough. Dr. Dmitri Gnatenko, Peter Perotta and Melissa Monaghan, I learned a lot from you, especially on microarray technologies and biological knowledges. Dr. Jim Ma, Dr. Bin Xu, Dr. Xuena Wang, Dr. Valentin Polishchuk, for your listening and advice. Kith Pradhan, Xiangfeng Wu, Meimei Wu, Yue Zhang and Yue Wang. Thank you for your suggestions and help.

My aunt Ye Wu and her family, for their care and optimism. Thank you Larry and Dan, for all you are.

My thanks, my love to all.

Chapter 1

Introduction

1.1 Genomics and proteomics

The fundamental working units of every living system are defined as cells. All the instructions needed to direct their activities are contained within the chemical DNA (deoxyribonucleic acid). Whilst DNA from all organisms is made up of the same chemical and physical components, the DNA sequence is the particular side-by-side arrangement of bases along the DNA strand (e.g., ATTCCGGA).

This order spells out the exact instructions required to create a particular organism with its own unique traits. The genome is an organism's complete set of DNA. Genomes vary widely in size: the smallest known genome for a free-living organism (a bacterium) contains about 600,000 DNA base pairs, while human and mouse genomes have some 3 billion. Except for mature red blood cells, all human cells contain a complete genome. DNA in the human genome is arranged into 23 distinct chromosomes–physically separate molecules that range in length from about 50 million to 250 million base pairs. A few types of major chromosomal abnormalities, including missing or extra copies or gross breaks and rejoinings (translocations), can be detected by microscopic examination. Most changes in DNA, however, are more subtle and require a closer analysis of the DNA molecule to find perhaps single-base differences. Each chromosome contains many genes, the basic physical and functional units of heredity. Genes are specific sequences of bases that encode instructions on how to make proteins.

Genes comprise only about 2% of the human genome; the remainder consists of non-coding regions, whose functions may include providing chromosomal structural integrity and regulating where, when, and in what quantity proteins are made. The human genome is estimated to contain 30,000 to 40,000 genes. Although genes get a lot of attention, it's the proteins that perform most life functions and even make up the majority of cellular structures. Proteins are large, complex molecules made up of smaller subunits called amino acids. Chemical properties that distinguish the 22 commonly occurring amino acids cause the protein chains to fold up into specific three-dimensional structures that define their particular functions in the cell. Whilst humans are estimated to have between 30,000 and 40,000 genes potentially encoding 40,000 different proteins, alternative RNA splicing and post-translational modification may increase this number to in the region of 2 million proteins or protein fragments. The constellation of all proteins in a cell is called its proteome. Unlike the relatively unchanging genome, the dynamic proteome changes from minute to minute in response to tens of thousands of intra- and extracellular environmental signals. A proteins chemistry and behavior are specified by the gene sequence and by the number and identities of other proteins made in the same cell at the same time and with which it associates and reacts. Studies to explore protein structure and activities, known as proteomics, will be the focus of much research for decades to come and will help elucidate the molecular basis of health and disease. Specifically, it enables correlations to be drawn between the range of proteins produced by a cell or tissue and the initiation or progression of a disease state. As a consequence, the proteome is far more complex than the genome.

In order to enable the diagnosis for an insidious disease producing few symptoms in early stages, such as ovarian cancer, proteomics is employed to detect the protein marker pattern from the database of proteomic mass spectrometry and to make a better understanding of the molecular mechanisms of cancer development. Proteomics is a scientific discipline which detects proteins that are associated with a disease by means of their altered levels of expression between control and disease states. It enables correlations to be drawn between the range of proteins produced by a cell or tissue and the initiation or progression of a disease state. Whilst humans are estimated to have between 30,000 and 40,000 genes potentially encoding 40,000 different proteins, alternative RNA splicing and post-translational modification may increase this number to about 2 million proteins or protein fragments.

Proteins, which carry out and modulate the vast majority of chemical reactions that together constitute 'life', are the direct links to diseases and abnormalities. The proteome reflects both the intrinsic genetic program of the cell and the impact of its immediate environment.

Proteomics is the study of proteins and one of its central themes is the development of proteomic biomarker-based tests using easily accessible biological fluids such as urine, blood, feces, sputum, and bladder or bronchioalveolar lavage to identify potential diseases and to monitor the progress of certain therapeutic treatments.

1.2 Microarray technology

A DNA microarray (also commonly known as gene or genome chip, DNA chip, or gene array) is a collection of microscopic DNA spots, commonly representing single genes, arrayed on a solid surface by covalent attachment to chemically suitable matrices. DNA arrays are different from other types of microarray. They either measure DNA or use DNA as part of its detection system. Qualitative or quantitative measurements with DNA microarrays utilize the selective nature of DNA-DNA or DNA-RNA hybridization under high-stringency conditions and fluorophore-based detection. DNA arrays are commonly used for expression profiling, i.e., monitoring expression levels of thousands of genes simultaneously, or for comparative genomic hybridization.

Arrays of DNA can either be spatially arranged, as in the commonly known gene or genome chip, DNA chip, or gene array, or can be specific DNA sequences tagged or labelled such that they can be independently identified in solution. The traditional solid-phase array is a collection of microscopic DNA spots attached to a solid surface, such as glass, plastic or silicon chip. The affixed DNA segments are known as probes (although some sources such as journalists will use different nomenclature), thousands of which can be placed in known locations on a single DNA microarray. Microarray technology evolved from Southern blotting, whereby fragmented DNA is attached to a substrate and then probed with a known gene or fragment.

1.3 Mass spectrometry

The most widely used techniques for the characterization of proteins are two dimensional gel electrophoresis (2-DGE), amino acid composition analysis, peptide sequence tagging, and mass spectrometry (MS). In particular, the protein mass spectrometry technology, nicked named ”protein chips”, has given a major impetus to proteomics being the sole high-throughput technology for protein identification and sequencing. It spans the vast expanse of proteomics and drug discovery. Three unique ionization techniques facilitated the characterization of proteins by MS. One is electrospray ionization (ESI) [Fenn89] where a liquid solution of the peptide is sprayed through a fine capillary held at a high potential. This produces charged droplets that are then rapidly desolvated producing charged ions of the peptide, which are in turn directed into a quadrapole type mass analyzer. Another ionization technique, matrix-assisted laser desorption ionization (MALDI) [Kar88], involves co-crystallizing the sample with an organic matrix which strongly absorbs UV laser light. Upon irradiation under vacuum there is an energy transfer from matrix to peptide analyte, which produces gaseous ions that are typically measured by a time-of-flight (TOF) mass analyzer. The advent of these ionization techniques has extended the application of MS to study proteins in complex biological systems. The MALDI-MS method is one of the main contemporary analytical methods reviewed at length in [Gev00]. Surface-enhanced laser desorption-ionization

(SELDI), oringinally described by [Hut93], overcomes many of the problems associated with sample preparations inherent with MALDI-MS. Chiphergen Biosystems (Fremon, CA) has developed the SELDI PrtoeinChip MS technology that brings to the field of proteomics a user friendly methodology. It is rapid, highly sensitive and is readily adaptable to a diagnostic format. With the help of these biological technologies and analytical methods, researchers have been able to study the pathology of diseases and show a path to cure. [Pet02] applied the SELDI technology for the early detection of ovarian cancer. [LZR02] also applied SELDI to identify serum biomarkers for the detection of breast cancer.

[Adam02] focused on the prostate cancer and [Wads04] the head and neck cancer. A concise summary on proteomic pattern recognition methods and their applications for early cancer diagnostics can be found in [Vee04]. Despite the rapid progress in proteomic mass spectrometry technology, there is substantial room for improvement in the following areas: (1) high-quality acquisition of mass spectra data and (2) identification of significant and meaningful biomarkers. The most commonly used instrument for acquiring proteomic mass spectra is known as ProteinChip Biomarker System - II (PBS-II). It has relatively high sensitivity but low resolution and mass accuracy.

1.4 Thesis structure and overview

In Chapter 2, we present a new algorithm to improve the mass spectra acquisition quality using PBS-II. Furthermore, we also propose a systematic approach for examining the reproducibility of mass spectrometer results using repeated measures ANOVA for point-wise reproducibility test and the random field theory for multiple-test correction.

To date, many statistical groups have proposed various proteomic biomarker identification strategies. Two notable ones were [Zhu03] where they proposed a continuous marker detection method using the random field theory for multiple-test correction, and [Yasui03] where they developed a data-analytic approach to detect biomarkers based on peaks from mass spectrum only.

In Chapter 3, we propose a new strategy for significant biomarker selection by examining the total variance of each data point along the mass spectrum. Comparisons are made between the new strategy and those of [Zhu03] and [Yasui03] using the head and neck data as an example.

In Chapter 4, we develop the scoring method that would yield the predictive disease probability rather than the traditional crude binary (yes/no) diagnosis. We present the s-CART and s-RF classifiers - the improved scoring variants of the binary classification and regression tree (CART) and Random Forest (RF) classifiers.

In Chapter 5, we examine how integration of transcriptomics and proteomics improves efficiency of protein identification and study correlation between mRNA and protein expression for thoroughly selected group of genes.

Finally, we give the concluding marks and discuss future works in chapter 6.

Chapter 2

Data Acquisition and Quality Control

2.1 Data acquisition

Ciphergen's Protein Chip technology is the mot common pre-chromatography step prior to mass spectrometry analysis. Patterns are derived from surface-enhanced laser desorption and ionization (SELDI) protein mass spectra. The most common analytical platform comprises a ProteinChip Biomarker System-II (PBS-II, a low-resolution time-of-flight mass spectrometer). We present a new algorithm for PBS-II to generate a mass spectrum and show its advantage by an example.

A typical SELDI experiment is illustrated in Figure 2.1. Chip processing - i.e., adding the protein sample, washing, adding the energy adsorbing molecule (EAM). The chips are then processed in the mass reader where the bound proteins are liberated by ionization, and fly through a "time-of-flight" tube where they separate based on mass and charge. The ProteinChip Software then converts the TOF data to generate a mass spectrum profile. The two useful formats for viewing the data are the raw spectrum and the grey-scale.

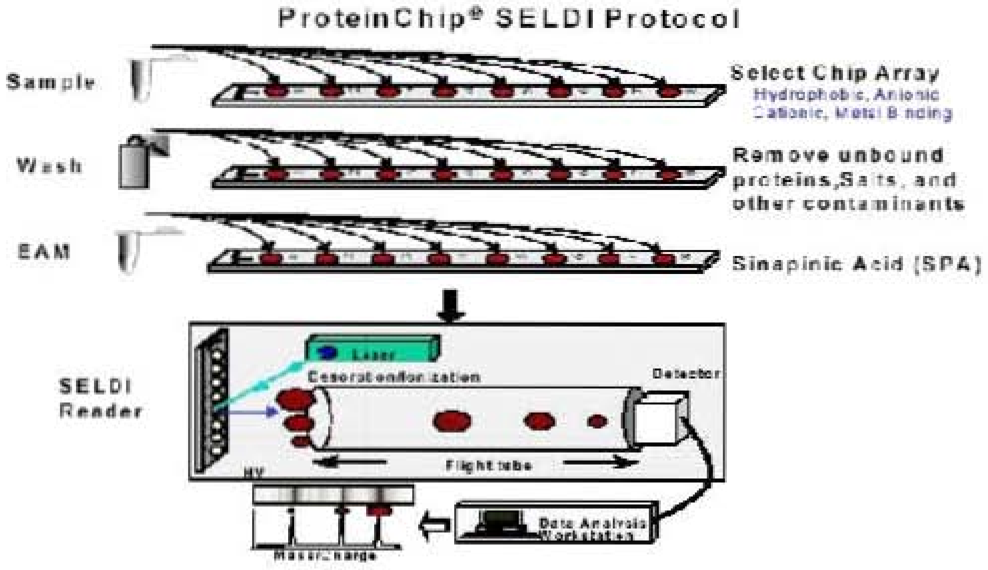

Figure 2.1: ProtinChip SELDI Protocol (Modified by William E.Grizzle,O.John Semmes et al. with permission from Ciphergen Biosystem, Inc.)

We always analyze the raw spectrum that has the markers (mass-to-charge ratio or m/z values) as the horizontal axis and intensity as the vertical axis. There are eight samples in each protein chip. The analytical platform PBS-II fires a laser beam on the middle stripe on each sample repeatedly. Each sample can be accessed through 100 different positions: position 1 is at the bottom and position 100 is at the top. The positions contain important information are called ”hot spots” and those contain no useful information are a ”cold spot”. It is expected to fire the laser on the hot spots only, but it is impossible because ”hot spots” and ”cold spots” are not easy to distinguish.

To extract the information as much as possible from ”hot spots”, PBS-II fires the laser beam several times at each chosen position, and Ciphergen's ProteinChip software takes the average of all shots of chosen positions and the

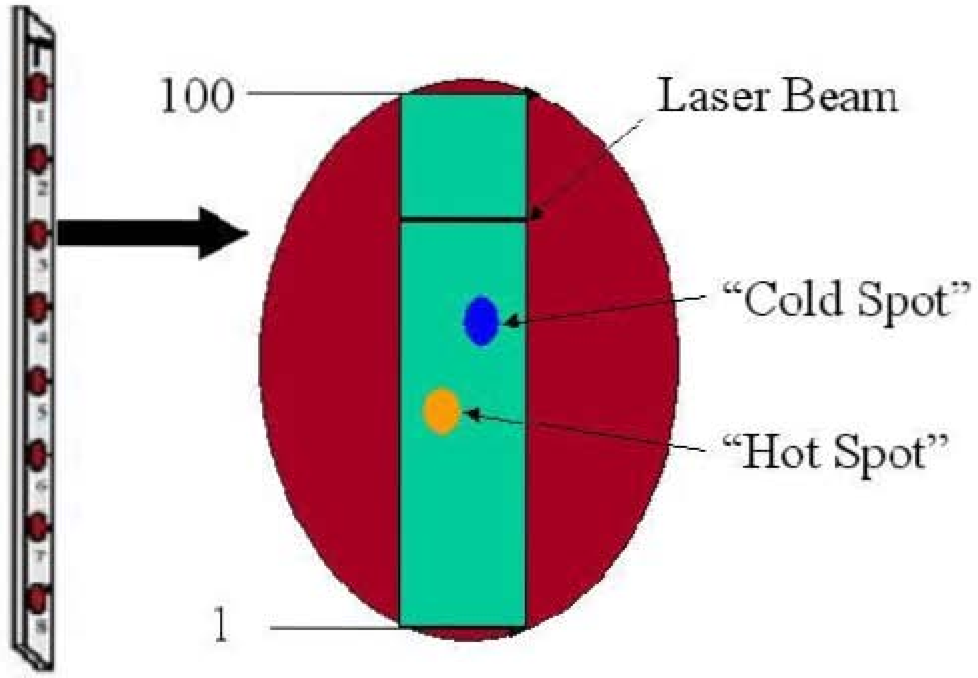

Figure 2.2: "Cold spots" and "Hot spots".

average will be the final mass spectrum of the sample. However, the average of all shots is not good if the laser beam fired on too many "cold spots". The garbage information is included and this is not acceptable. We use adjusted mean to generate more accurate mass spectrum:

1) Eliminate the instrument noise. For PBS-II, the intensities without sample on the protein chip are below 6.

2) Take the average of all shots between 25th percentile and 75th percentile at each m/z value. Example. Eight wild type rats are on one protein chip. The laser beam starts firing from position 19 to position 79. The interval between the starting position and ending position is 6. The laser will fire 15 times at each position. Therefore the total number of shots is 11*15 = 165. The m/z range is (0, 20,000). There are many instrument noises at each m/z

Sample	M/Z = 5997.97	M/Z = 8195.01
1	72%	59%
2	37%	15%
3	38%	25%
4	27%	0%
5	2%	4%
6	3%	8%
7	10%	0%
8	1%	3%

Table 2.1: Proportion of 165 shots that have intensities <6.

value.

For example, five samples have more than 10% shots below the noise level at m/z = 5997.97 and 3 samples have same situation at m/z = 8195.01, more than half of shots for sample number 1 are noises(Figure 2.3). We should not use those noises to generate mass spectra.

After eliminating the noises, we take the average of shots between 25th percentile and 75th percentile at each m/z. This algorithm considers only those stable shots after excluding the noise with small intensities. Therefore the mass spectra have higher intensities and are more accurate.

In Figure 2.4 Regular means taking the average of all 165 shots and then subtract baseline. Improved means eliminating the instrument noise and take the average of shots between 25th percentile and 75th percentile, finally subtract the baseline.

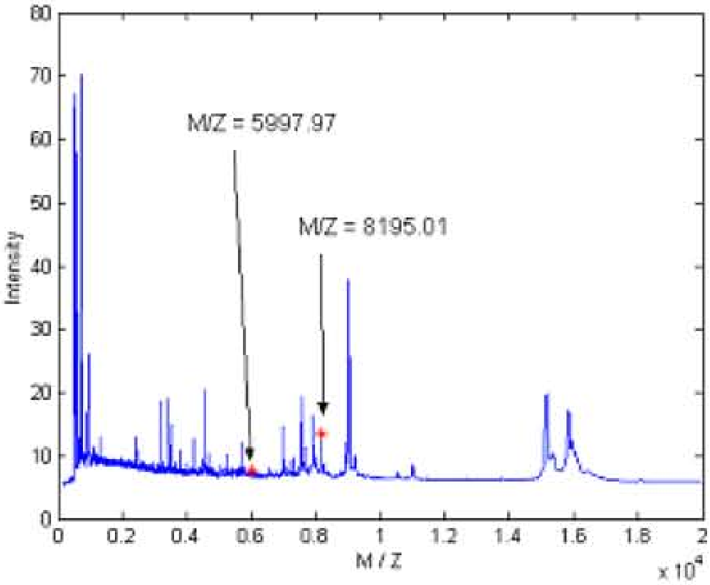

Figure 2.3: m/z = 5997.97 and m/z = 8195.01.

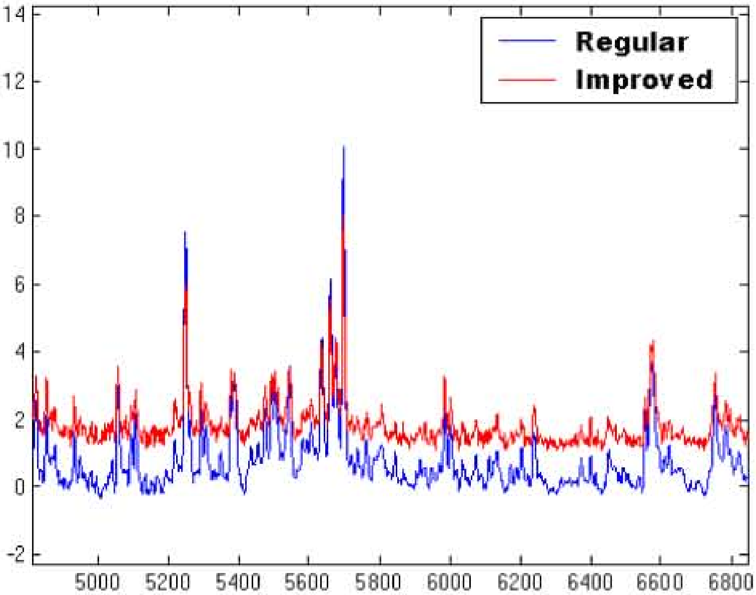

Figure 2.4: Comparison between the regular and improved methods on sample 3.

2.2 Data quality control

In many mass spectrometry datasets, each protein serum sample is generated multiple times. If the spectra of the same serum sample are not reproducible, we cannot trust them and do further analysis. One-way repeated measure ANOVA is implemented to perform the reproducibility test.

Method. Suppose we have N protein serum samples, and the mass spectrum of each sample contains intensities at M markers (mass-to-charge ratio or m/z). The intensity of each sample has the model:

$$Y_{ij} = \alpha_i + \beta_j + \epsilon_{ij}, i = 1, \ldots, N, j = 1, \ldots, M.$$

where α_i is the ith subject effect (random effect), β_j is the jth repeated measure effect (fixed effect), and ϵ_{ij} is the random error.

The null hypothesis for test is that data is reproducible, which means the repeated measure effects are equal.

$$H_0 : \beta_1 = \beta_2 = \cdots = \beta_m$$

It is rejected if

$$F_0 = \frac{MSw}{MSr} > F_{M-1,(N-1)(M-1)}$$

This test is performed at each marker. Considering the interactions among markers, the multiple test correction should be done when we calculate the F-threshold. It is derived by the Gaussian random field theory:

$$\begin{aligned}\alpha = \ & \int_f^\infty \frac{\Gamma(\frac{v+w-2}{2})}{\Gamma(\frac{v}{2})\Gamma(\frac{w}{2})}\frac{w}{v}(\frac{wu}{v})^{\frac{w}{2}-1}(1+\frac{wu}{v})^{-\frac{v+w}{2}}du \\ & +\frac{2M\sqrt{ln2})}{\sqrt{\pi}(FWHM)}\frac{\Gamma(\frac{v+w-2}{2})}{\Gamma(\frac{v}{2})\Gamma(\frac{w}{2})}(\frac{wf}{v})^{\frac{w-1}{2}}(1+\frac{wf}{v})^{-\frac{v+w}{2}}\end{aligned}$$

where f is the threshold, α is the significant level, FWHM is the smoothing kernel, v and w are the degrees of freedom. v = N-1, w = (N-1)(M-1).

Rat Age	Subjects	Replicates	Total
Inputs	4	19	47
Classes	3	7	2
8 Weeks	22	2	44
10 Weeks	22	3	66
12 Weeks	22	3	66
14 Weeks	22	2	44
21 Weeks	22	3	66

Table 2.2: Description of rats data.

Example. Five groups of mass spectra are generated from twenty-two wild type rats at their different ages, from 8 weeks to 21 weeks (Data is provided by Department of Pharmacology, SUNY at Stony Brook. Table 2.2). Each rat sample is divided into two or three equivalent parts and randomly assigned to the ProteinChip arrays. The m/z range is from 0 to 20,000 and there are about 13,500 m/z values for each sample. We will test if those two or three replicates are reproducible for the rats at different age.

There are less than 40 out of 13,500 markers at which the null hypothesis is rejected. Thus the data of rats is reproducible. However, when rats are 14 weeks, the mass spectra are relatively less reproducible than those of rats at other ages. This difference can also be seen in the F-Map(Figure 2.5), where the red line is the F-threshold by the Gaussian random field theory.

Data Set	1st d.f.	2st d.f.	F threshold	No. Markers Reject H0
8 Weeks	1	21	26.85	0
10 Weeks	2	42	12.94	11
12 Weeks	2	42	12.94	2
14 Weeks	1	21	26.85	37
21 Weeks	2	42	12.94	3

Table 2.3: Result of the reproducibility test.

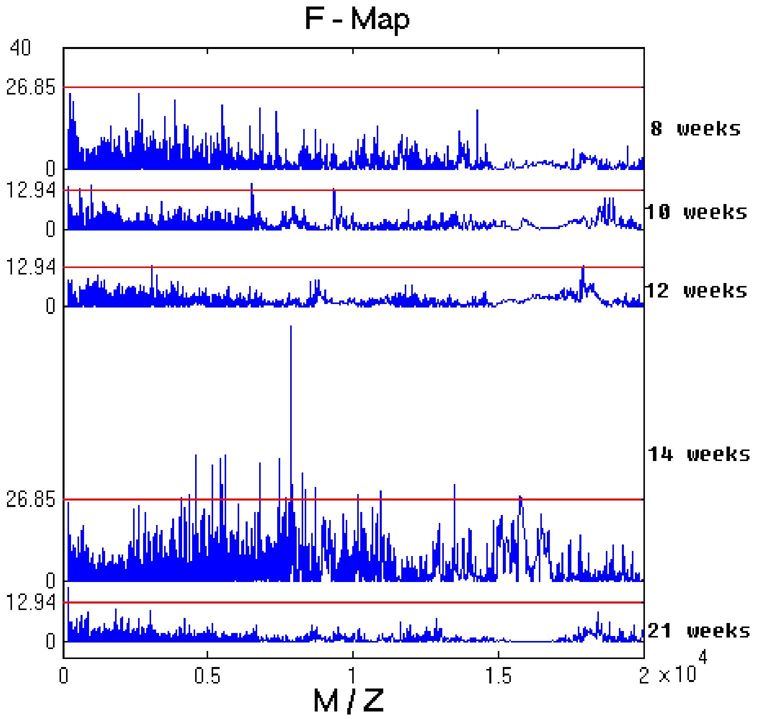

Figure 2.5: F-map of the reproducibility test.

Chapter 3

Data Preprocessing, Biomarker Detection and Classification

In this chapter, we will use the head and neck cancer data set (Table 3.1) to illustrate the three steps in proteomic biomarker analysis. The flow chart of the whole procedure is shown in Figure 3.1.

For biomarker detection, we developed a novel method based on variance analysis. In comparison with two previous methods, it improved the classification results. We proposed a new classification method called majority k-nearest neighbor which is better than the traditional k-nearest neighbor method. A new classifier combination scoring system is also developed.

Head & Neck Data Set	
M/Z Range	$0 \sim 100{,}000$
# M/Z	34,378
HSNCC	73
Normal Control	76
Blinded	49

Table 3.1: Head and neck cancer data.

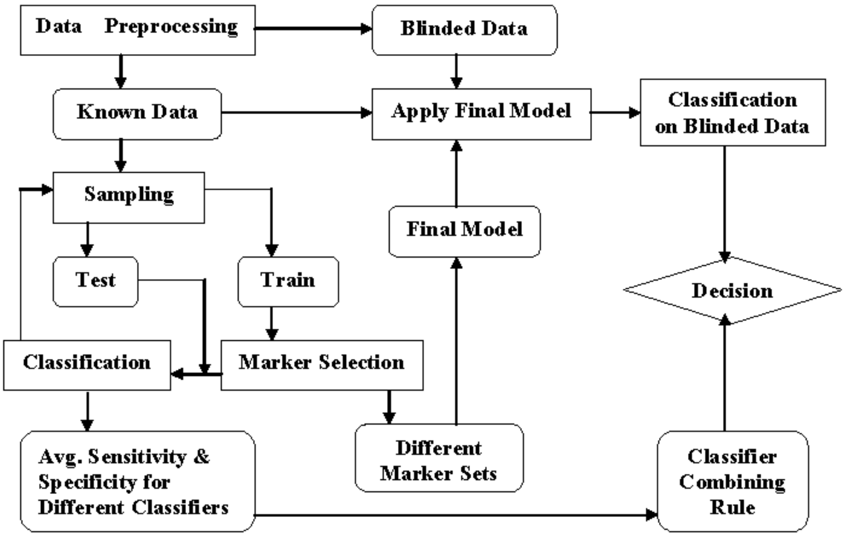

Figure 3.1: Flow chart of the proteomic mass spectrometry analysis.

3.1 Data preprocessing

Preprocessing is an important step for mass spectra based data analysis. The goal is to remove experimental noise and adjust mass spectra baseline.

1) Calibration and smoothing. Each original mass spectrum has to be externally calibrated to be in the same coordinate system and to be smoothed via a Gaussian filter.

2) Baseline subtraction. Eliminate the baseline signal caused mostly by chemical noise from matrix molecules without contamination of true protein or peptide peaks. The result is a spectrum with a spectrum with a baseline signal hovering slightly above zero with protein peaks maintaining their true intensity.

3) Normalization. Adjust for the system effects between samples due to varying amounts of protein or degradation over time in the sample or variation

in the instrument detector sensitivity. Each spectrum is divided by the average intensity.

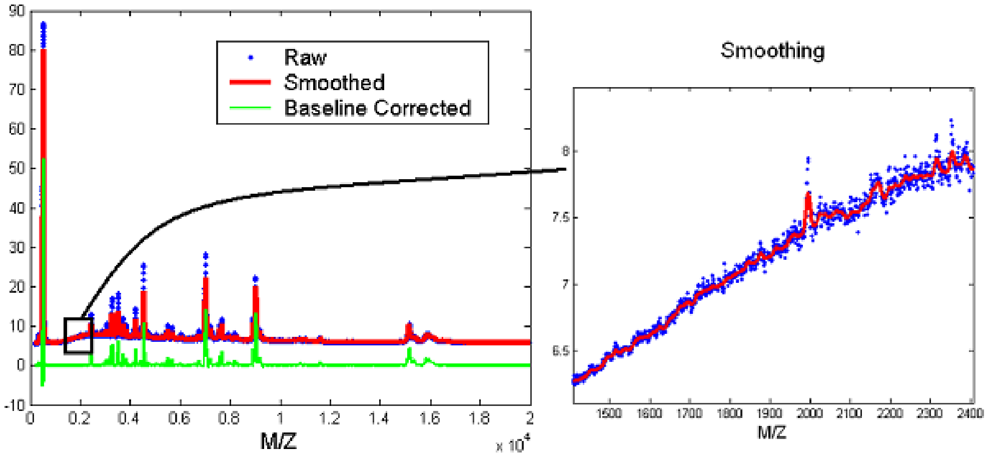

Figure 3.2: Data preprocessing.

In the head and neck cancer study, each raw mass spectrum consists of 34,378 mass-to-charge ratios (m/z values) ranging from 0 to 100,000. The m/z range of 2,000 to 20,000 is selected because the lower MS range is too noisy and the signal is too sparse in the higher MS zone. These mass spectra were also standardized and smoothed using the method developed by Zhu and colleagues (2003, Figure 3.2). Now the mass spectra are aligned on a common scale and ready for the next two steps of analysis.

3.2 Biomarker detection

We will present three algorithms. All of them are based on the statgram. Method 1 detects the biomarkers over the entire m/z range. Method 2 employs a peak detection algorithm and look for the significant biomarkers at the peak with maximum intensity. The focus of Method 3 is on those disease related markers that highly appear in the peak region. The new biomarker is the peak area instead of a single marker intensity. This method is applied by the variance component analysis. In the last section Head and Neck data is investigated by the three methods. There are 73 samples that have head and neck squamous cell carcinoma (HNSCC) and 76 are normal control. In the validation set, 49 samples (22 HNSCC and 27 control) will be classified using the detected biomarkers.

Method 1.*Zhu's continuous biomarker approach.* (1) Statgram(t-Map). A two-independent samples t/z test was performed at each m/z value to compare the intensities between the two training samples (disease and normal control). The null hypothesis is that the intensities are equal between the two groups for each particular biomarker, and the alternative one is they are different. For each biomarker, we calculated a test statistic (t value) and then generated the t-Map by t values versus m/z values. Suppose n_1 and n_2 samples are drawn from the disease group (X) and the control group (Y) respectively. The samples are independent within and between groups. At each biomarker, m, the test statistic t(m) is

$$t(m) = \frac{\bar{X}(m) - \bar{Y}(m)}{\sqrt{S_1^2(m)/n_1 + S_2^2(m)/n_2}}$$

where $\bar{X}(m)$, $\bar{Y}(m)$, $S_1^2(m)$ and $S_2^2(m)$ are the sample means and variances of the training samples. When both samples are large ($n_1 > 30$ and$n_2 > 30$), by the central limit theorem the test statistic followed approximately the standard normal distribution under the null hypothesis. Because the mutiple tests are performed, there is also a false positive problem. Namely, we need to determine a suitable significance level for each test such that at least 95% of all significant differences identified are real. Traditional methods as Tukey or Bornferroni tend to be conservative. Thus a less conservative correction method is applied based on Gaussian random field theory. The threshold t is given by

$$\alpha = \int_f^\infty \frac{\Gamma(\frac{v+1}{2})}{\Gamma(\frac{v}{2})}(1+\frac{u^2}{v})^{-\frac{v+1}{2}}du + \frac{K\sqrt{ln2})}{\pi(FWHM)}(1+\frac{t^2}{v})^{-\frac{v+1}{2}}$$

where α is the corrected experimentwise error rate, u and v are the degrees of freedom of F statistic, f is the threshold of the test and FWHM determines the Gaussian kernal and it is a constant indicating the number of biomarkers averaged in the smoothing.

(2) Stepwise Discriminant Analysis. It begins like forward selection with no variables in the model. At each step the model is examined. If the variable in the model that contributes least to the discriminantory power of the model as measured by the following rule fails to meet the criterion to stay, then the variable is removed. Otherwise, the variable not in the model that contributes most to the discriminantory power of the model is entered. When all variables in the model meet the criterion to stay and none of the other variables meets the criterion to enter, the stepwise selection process stops. During the process of the stepwise selection, only one variable can be entered into the model at each step. The selection process does not take into account the relationships between variables that have not yet been selected.

Sequential F Test Based on a Fixed α Level is the rule. Suppose that individuals belong to one of the two groups, G_1 and G_2, and $\bar{x} = (x_1, \cdots, x_p)'$ represents a full set of p measurements (variables). Assume that the prior probabilities of group membership are equal and that, in G_k, $\bar{x}$ has a p-variate normal distribution with mean vector $\bar{\mu}_k$ and positive definite covariance matrix Σ. The reference samples yield measurements $\bar{x_{ki}} = (\bar{x_{ki1}}, \cdots, \bar{x_{kip}})', i = 1, \cdots, n_k, k = 1, 2$ with sample means $\bar{x_k}$ and pooled sample covariance matrix $S, (n_1 + n_2 - 2 \geq p)$. Let $\Delta^2_{(q)}$ be the corresponding q-variate Mahalanobis distance between the two groups given by

$$\Delta^2_{(q)} = (\bar{\mu}_{1(q)} - \bar{\mu}_{2(q)})'\Sigma^{-1}_{(qq)}(\bar{\mu}_{1(q)} - \bar{\mu}_{2(q)}))$$

And $D^2_{(q)} = (\bar{x}_{1(q)} - \bar{x}_{2(q)})'S^{-1}_{(qq)}(\bar{x}_{1(q)} - \bar{x}_{2(q)}))$ is the usual estimate of $\Delta^2_{(q)}$. Test the sequential hypothesis $H_{(q)} : \Delta^2_{(q)} = \Delta^2_{(q+1)}, q = 0, 1, \cdots, (p-1)$,

$$F_{(q)} = \frac{(n_1 + n_2 - q - 2)n_1 n_2 (D^2_{(q+1)} - D^2_{(q)})}{(n_1 + n_2)(n_1 + n_2 - 2) + n_1 n_2 D^2_{(q)}}.$$

where F_α is selected as the best subset either the full set or $\bar{x}_{(q)}$ for which q is the first step and $F_{(q)} \leq F_{1-\alpha}(1, n_1 + n_2 - q - 2)$. The Monte Carlo results showed that for a fixed α level between .10 and .25, it performs better than the use of a much larger or a much smaller significance level.

Method 2. *Yasui's peak extraction method.*

(1) Peak detection (Yasui, et al 2003). Define peaks by judging, at each m/z point, whether or not the intensity at that point is the highest among its nearest ±N-point neighborhood set. Select the peaks above the noise level. Count the total number of peaks at each m/z, in all samples, that are within the window of potential shift for the m/z point. The m/z point that has the highest total number of peaks within its window of potential shift is entered in

the new m/z set as a calibrated m/z value. Construct the calibrated dataset that consists of intensities of each sample that correspond to the points in the new m/z set. For each sample i, and for each point in the new m/z set, j, we take the maximum intensity of the sample i, among the intensities corresponding to the window of potential shift for the point j, as the intensity at the calibrated m/z point j.

2)Statgram (t-Map). Same as in method 1. The significant peak maximums are the new biomarkers. Classification example SELDI -TOF spectrometry ProteinChip system was used to screen for differentially expressed proteins in serum from 73 patients with HNSCC and 76 normal controls. The mass spectrometer is QSTAR which has high resolution. The data was preprocessed. We applied the three methods to detect biomarkers on the 149 training samples. There are 49 serum samples in the validation set, among which 22 are with HNSCC and 27 are normal controls. Support Vector Machines is applied to do the classification and the sensitivity and specificity are reported.

Method 3.*Marker selection via the variance component analysis.* A good biomarker must be in the peak area and related to the disease, which means it can differentiate the disease group and the control group. We use the total variance of all subjects and independent t/z test to detect the disease related markers at peak

The idea behind the variance component method for marker selection is that disease related biomarkers tend to have larger variance over the pooled sample of control and diseased subjects than markers unrelated to the disease. Suppose we have N subjects, among which n_1 are from the disease group and n_2 are from the control group. The intensity for a subject at one specific marker is $X_{ij}, i = 1, \ldots, N, j = 1, \ldots, M$, where M is the number of markers.

For a marker unrelated to the disease, it is sensible to assume that it follows a common distribution for both the control and the diseased subjects as follows:

$$X_i \sim iid(\mu, \sigma^2), i = 1, \ldots, N(\text{All subjects}).$$

For a marker related to the disease, however, it is logical to assume that its distribution differs between the two groups as follows:

$$\begin{aligned} X_i &\sim iid(\mu_1, \sigma_1^2), i = 1, \ldots, n_1. && \text{(Control)} \\ X_i &\sim iid(\mu_2, \sigma_2^2), i = n_1 + 1, \ldots, N. && \text{(Disease)} \end{aligned}$$

Subsequently, the expected value of the sample variance is derived as

$$E(S^2) = \begin{cases} \sigma^2, \quad \text{for a marker unrelated to the disease.} \\ \dfrac{N(n_1\sigma_1^2 + n_2\sigma_2^2) + n_1 n_2(\mu_1 - \mu_2)^2}{N(N-1)}, \\ \qquad \text{for a marker related to the disease.} \end{cases}$$

In the special case of $\sigma_1^2 = \sigma_2^2 = \sigma^2$, the expected variance for a marker related to the disease is reduced to

$$E(S_2) = \sigma^2 + \frac{n_1 n_2(\mu_1 - \mu_2)^2}{N(N-1)}$$

Thus the disease-related markers have larger variance and the discrepancy is proportional to the squared mean signal intensity difference between the groups. It is therefore, reasonable to apply the variance component analysis to identify disease related biomarkers.

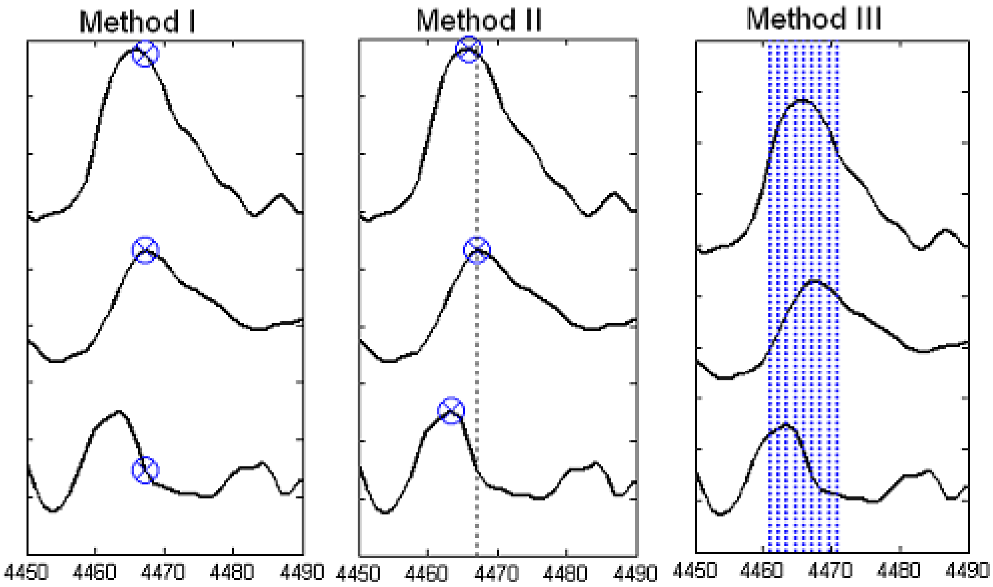

Figure 3.3: Biomarker comparison.

The biomarkers selected by these three different methods are shown in Figure 3.3. Method I is Zhu's approach. Method II is by Yasui and colleagues. Method III is our newly proposed method. The continuous markers (for Methods I and III) are not necessarily located at the most prominent peak region. Yasui's peak method selects peak apex as potential biomarkers only.

3.3 Classification methods

After selecting biomarker pattern in the previous section, we need to validate the pattern by applying classification methods to distinguish the disease-related group from disease-unrelated group.

Majority k-nearest neighbor (MKNN). MKNN classifier is a generalization of the k-nearest neighbor classifier. The kNN classifier uses only one integer parameter k. Given an input $x \in \mathbb{R}^n$, it finds the k nearest neighbors of x in the training set and then predicts the label of x as the most frequent one among the k neighbors. Extended to multi-category case, the principle of kNN is to use the majority vote of their labels to assign a label to x. MKNN extends kNN by using the majority vote of a range of k rather than just one k.

Table 3.2 shows that MKNN has sensitivity of 82% and specificity of 96% which are much better than the results of original k-NN classifier.

	Sensitivity	Specificity	Accuracy
Average KNN	68.18%	88.89%	79.59%
Majority KNN	81.82%	96.30%	89.80%

Table 3.2: Comparison of MKNN and classic kNN.

Multi-layer perceptron neural network (MLPNN). The multi-layer perceptron is a hierarchical structure of several perceptrons, and overcomes the shortcomings of those single-layer networks. It is an artificial neural network that learns nonlinear function mappings. The multi-layer perceptron is capable of learning a rich variety of nonlinear decision surfaces. Nonlinear functions can be represented by multi-layer perceptrons with units that use nonlinear activation functions. Multiple layers of cascaded linear units still produce only linear mappings.

General regression neural network (GRNN). GRNN is Donald Specht's term for Nadaraya-Watson kernel regression, also reinvented in the NN literature by Schioler and Hartmann. (Kernels are also called "Parzen windows".) One can view it as a normalized RBF network in which there is a hidden unit centered at every training case. These RBF units are called "kernels" and are usually probability density functions such as the Gaussian. The hidden-to-output weights are just the target values, so the output is simply a weighted average of the target values of training cases close to the given input case. The only weights that need to be learned are the widths of the RBF units. These widths (often a single width is used) are called ”smoothing parameters” or ”bandwidths” and are usually chosen by cross-validation or by more esoteric methods that are not well-known in the neural net literature (Specht, 1991, Rutkowski, 2004).

Support vector machine(SVM). SVM is a supervised learning method used for classification and regression. The observed m/z ratio for the ith subject $X_i \in \mathbb{R}^n$. An binary classifier would be to construct a hyperplane separating cancer subjects from normal subjects in this $\mathbb{R}^n$ space. The algorithm we applied here is described by Chang and Lin(2003).

We calculate a score for each classifier. The score is usually a classification probability and always bounded between 0 and 1. If the score is greater than 0.5, the subject is often classified as diseased, if a binary decision must be given. If the score is less than 0.5, the subject is classified as normal. To combine The decisions from the four classifiers, we take the median of the four scores. The binary decision is derived following the same threshold of 0.5 using the median score.

3.4 Results

The training set consists of 73 patients with cancer and 76 normal controls. The training data is randomly split into two equal parts and we train the classifiers using one part (37 of the cancer cases and 38 of the normal cases) and test using the remainder. We repeat this procedure for thousand times. The average classification sensitivity and specificity are reported in Table 1. We then train the classifiers using the entire training set and classify a blinded data set of 49 subjects. The prediction sensitivity and specificity for the blinded data are shown in Table 2.

Training	Method I		Method II		Method III	
Classifier	Sen	Spe	Sen	Spe	Sen	Spe
MKNN	.82	.89	.84	.96	.75	.96
GRNN	.91	.78	.93	.93	.96	.93
MLPNN	.91	.85	.93	.95	.89	.94
SVM	.91	.89	.93	.93	.93	.93
Score	.87	.91	.96	.96	.92	.95

Table 3.3: Training classification via cross-validation. Method I is Zhu's approach, Method II is Yasui's and ours is Method III. "Sen" = "Sensitivity" and "Spe" = "Specificity".

Testing	Method I		Method II		Method III	
Classifier	Sen	Spe	Sen	Spe	Sen	Spe
MKNN	.82	.89	.82	.96	.82	.96
GRNN	.86	.78	.86	.81	.82	.89
MLPNN	.86	.89	.86	.81	.86	.89
SVM	.86	.85	.86	.73	.86	.96
Score	.86	.85	.86	.81	.86	.96

Table 3.4: Testing classification on blinded data(information disclosed after analysis). Method I is Zhu's method, Method II is Yasui's and ours is Method III.

For the training dataset, our method is better than the other two for GRNN only. However, for the testing data using blinded subjects with a sensitivity of 86% and a specificity of 96%.

3.5 Extension to multiple-group classification

Our approach can be easily extended to the multiple-group classification problem. For example, if we have two disease stages and one set of normal control, a marker unrelated to the disease would be

$$X_i \sim iid(\mu, \sigma^2), i = 1, \ldots, N = n_1 + n_2 + n_3 (\text{All subjects}).$$

If a marker is related to the disease, then we have

$$\begin{aligned} &X_i \sim iid.(\mu_1, \sigma_1^2), i = 1, ..., n_1. && (\text{Disease Stage 1}) \\ &X_i \sim iid.(\mu_2, \sigma_2^2), i = n_1 + 1, ..., n_1 + n_2. && (\text{Disease Stage 2}) \\ &X_i \sim iid.(\mu_3, \sigma_3^2), i = n_1 + n_2 + 1, ..., N. && (\text{Normal Control}) \end{aligned}$$

The expected sample variance of a disease-unrelated marker is σ^2. The expected sample variance of a disease-related marker is

$$E[S_r^2] = \sigma^2 + \frac{1}{N}\Big[*\Big] > \sigma^2$$

where

$$\begin{aligned} \Big[*\Big] = \quad & n_1\Big[n_2(\mu_1 - \mu_2) + n_3(\mu_1 - \mu_3)\Big]^2 \\ & + n_2\Big[n_1(\mu_2 - \mu_1) + n_3(\mu_2 - \mu_3)\Big]^2 \\ & + n_3\Big[n_1(\mu_3 - \mu_1) + n_2(\mu_3 - \mu_2)\Big]^2 \end{aligned}$$

In summary, we propose a novel approach to identify proteomic biomarkers using the variance component analysis method. Our approach is suitable to not only two-group but also multi-group classification. Furthermore, it can be utilized to examine the consistency between the known data and the blinded data by comparing the pooled-variance at each marker between the testing and the training data sets. This would indicate whether it is reasonable to classify the training data using the given testing data.

Chapter 4

Scoring Method for CART and Random Forest

The tree based classification and regression method is called CART. It learns to extract the hidden patterns in the training data and can provide the predictive information for the future data. Random Forest(RF) combines many classification trees. Conventionally those two classifiers give binary classification results. In this chapter, we first introduce CART and RF briefly in Section 4.1 and Section 4.2. Then the scoring methods to improve those two classifiers are presented in Section 4.3. In Section 4.3.2, we compare and show the results.

4.1 Classification and regression trees

Basically *CART* has two steps: recursive partitioning to grow the tree, and prune to select the correct size of the tree.

4.1.1 Tree growing

The the tree growing step of *CART* is a top-down divide-and-conquer procedure. A binary decision tree will grow by learning the hidden pattern of the training samples.

```
Require node $n$, dataset $D$, split selection measure $v$
Build classification tree $T$
GrowTree (Node $n$, dataset $D$, split selection measure $v$)
If $n$ meets the stop criteria
    label of $n \Leftarrow$ the majority class label of $D$;
Else
    apply $v$ to $D$ to find the "best" split attribute $\varphi$ for node $n$;
    partition $D$ into $D_l$, $D_r$ by $\varphi$;
    create children nodes $n_l$ with $D_l$; $n_r$ with $D_r$;
    label the edge $(n, n_l)$ with predicate $q(n, n_l)$ and $(n, n_l)$ with
  predicative $q(n, n_r)$ based on split attribute $\varphi$;
    GrowTree ($n_l$, $D_l$, $v$)
    GrowTree ($n_r$, $D_r$, $v$)
End If
End GrowTree;
```

Table 4.1: Recursive tree growing schema for *CART*.

In Table 4.1 n is the input root node and D is the training data set. *CART* generates a binary tree. This schema shows only two children after each split. But it can be modified slightly to describe other decision algorithms (*CHAID*, *ID4.5*, *FACT*) that can generate multiple children at each split.

The split selection method v takes a very important role in tree growing. There are over ten different methods. The most general used are Entropy/Information gain, Gini Index, Gini Ratio and Marshall Correction [Min89].

1. Entropy/Information Gain

Entropy/Information Gain is used by Quinlan in *ID3*, *ID4.5* decision tree.

Entropy for a node T is

$$entropy(T) = -\sum_{j=1}^{J}\{P[j|T] \cdot \log(P[j|T])\} \tag{4.1}$$

Where T is the node. J is the number of response categories. $P[j|T]$ is the probability of observing an outcome as the j^{th} category in node T. $(0 \cdot \log 0 = 0.)$

Information Gain (IG) of a split at node T is

$$IG(T, X, Q) = entropy(T) - \sum_{k=1}^{K}\{P[q_k(X)|T] \cdot entropy(T_k)\} \tag{4.2}$$

Where X is the split attribution. Q is the branch set of node T on the split attribution X, which will leads the child nodes generated from node T. K is the child number of node T (e.g. in binary split, it is 2). T_k is the k^{th} child node. $P[q_k(X)|T]$ is the probability of descending to the k^{th} branch from T.

2. Gini Index

   Gini Index is also called Gini Diversity Index. It is the main split algorithm used in *CART*.

Gini Index for a node T is

$$gini(T) = 1 - \sum_{j=1}^{J} P[j|T] \tag{4.3}$$

Gini Index of a split at node T is

$$GI(T, X, Q) = gini(T) - \sum_{k=1}^{K} \{P[q_k(X)|T] \cdot gini(T_k)\} \tag{4.4}$$

In Eq. (4.3) and Eq. (4.4), all legends are same as Eq. (4.1) and Eq. (4.2).

3. Gini Ratio

   Gini Ratio is developed and used to counteract the bias caused of unbalanced data [Qui86].

   Gini Ratio of a split at node T is based on Information Gain, Eq. (4.2).

$$GR(T, X, Q) = \frac{IG(T, X, Q)}{-\sum_{k=1}^{|Dom(X)|} \{P[X = x_k|T] \cdot \log P[X = x_k|T]\}} \tag{4.5}$$

4. Marshall Correction

   In comparison to the Gini Ratio, Marshall Correction [Mar86] favors attributes which split the examples evenly and avoids those that produce small splits. It multiplies the splitting method by the product of the row totals, $x_{i\cdot}$. Thus it will be the maximum when the row totals are equal.

Marshall Correction

$$MarshallCorrection = \frac{x_{1\cdot}}{N} \times \frac{x_{2\cdot}}{N} \times \cdots \times k^k \tag{4.6}$$

Besides above four common split methods, there are several other methods such as Misclassification rate, χ^2 statistic, F statistic, G statistic, Twoing criterion, etc.

The stopping criteria of CART growing are as follows:

1. A certain tree depth is reached

2. The number of samples at a node is less than a predefined threshold

3. The node is pure: all samples in the node are in same category.

4. All potential splits of the node are nonsignificant, a F statistic as measure is given:

$$F = \frac{SS/(n-1)}{(SS_l + SS_r)/(n-2)}$$

The tree depth, the leaf node size and the threshold for F statistic are control parameters to avoid overfitting a tree. The machine learning is the ideal procedure to find such parameters through the study on the training data.

4.1.2 Tree pruning

One should not make more assumptions than the minimum needed. Thus the tree pruning is an important step. It means we require the tree as simple as possible. Usually the misclassification rate will decrease when the tree grows but it will increase again if the tree continues to grow and gets too big.Figure 4.1

Pruning will use the Minimal Cost-Complexity criteria. The key is to find the weakest-link cutting (WLC). It generates a decreasing sequence of subtrees: $T_1 \succ T_2 \succ T_3 \succ \cdots \succ t_1$ where t_1 is the tree which contains the root node only. It has been proved that the results are the minimum cost subtrees for a given number of terminal nodes [Bre84].

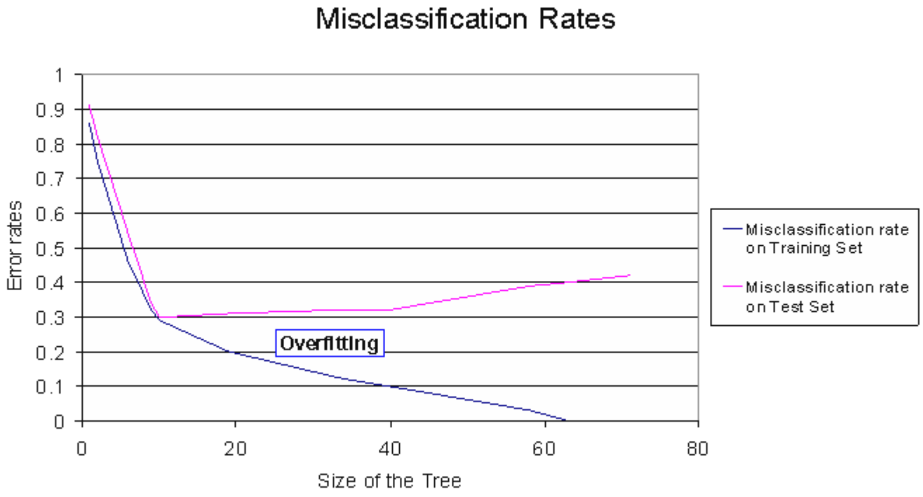

chch

Figure 4.1: Tree pruning for head and neck cancer data.

The cost-complexity measure $R_\alpha(T)$ is defined as:

$$R_\alpha(T) = R(T) + \alpha|\tilde{T}| \tag{4.7}$$

where R(T) is the misclassification rate of tree T, $|\tilde{T}|$ is the number of leaf nodes. It is also considered as the tree size and α is the complexity cost.

There are two methods for seeking the minimal cost-complexity.

- Independent testing samples, if an independent data set is given, or the original training data set is big enough to draw out a independent testing set.
- The v-fold cross-validation method, if the data set is small.

When the best tree is found by the tree growing and pruning, its misclassification rate can be given by resubstitution error rate $R^{ts}(T)$. A criteria to estimate the variance of the error rate is *1 SE Rule*: $SE(R^{ts}(T)) = [R^{ts}(T)(1 - R^{ts}(T))/N_2]^{1/2}$. This rule can also be used to select the right size tree. The purpose of the selection is (1) reduce the instability in pruning; (2) select a simplest but accuracy-comparable tree. [Bre84] gives more detail decriptions.

4.2 Random forests

A random forest is "a classifier consisting of a collection of tree-strutured classifiers" [Bre01]. The random forest algorithm is based on *CART* and *bagging sampling.*

Bagging sampling causes the first randomness of the random forests algorithm. The second randomness is the variables for selecting the best split in each tree. There are two methods of random forests, Forest-RI, which uses a random input selection and Forest-RC, which uses linear combination of inputs. The voting system is used for the multi-classifier system of Random Forest.

4.2.1 Bagging sampling

Bagging is the acronym of **b**ootstrap **agg**regat**ing**. It was introduced by L. Breiman in [Bre96]. In recent years, bagging became quite popular as the other sampling methods: boosting (including Adaboosting), v-fold cross-validation, leaf-one cross-validation, randomization, etc. [Die00, HL03, HLBR04, DF03]

It has two steps:

- sampling

  Each tree is constructed on the different training data set, $\mathcal{L}^{(B)}$. Each training sample is drawn with replacement from the original training set, $\mathcal{L}$, about one-third of the samples are left out. The left-out sample will be the testing data set, called out of bag(OOB) samples.

- voting

  Suppose the predictor of the classifier is $\varphi(\vec{x}, \mathcal{L})$, the vote is

$$\varphi_B(\vec{x}) = \begin{cases} av_B\varphi(\vec{x}, \mathcal{L}^{(B)}) & y \text{ is numerical variable;} \\ vote\varphi(\vec{x}, \mathcal{L}^{(B)}) & y \text{ is categorical variable.} \end{cases}$$

The Step 1 is the kernel and the first randomness in Random Forests. In paper [Die00], bagging has been simplified only its first phrase, sampling phrase. And that is been widely accepted. Accuracy and generalization error (*PE.*) estimation are two major advantages of using bagging.

Out-of-bag (*OOB*) is the most exciting technique developed in Random Forest, because it can be used for many purposes, such as generalization error estimation, outlier detection, variable importance rank, scaling coordinates, etc. Each bagging sampling result contains only two third of original training data set, and the left samples are organized together as *OOB* data set. Since the error rate decreases as the number of tree predictions increases in combination, the out-of-bag estimates will tend to overestimate the real error rate on the testing sample. In [Bre96], the empirical study on error estimates for the bagged classifiers shows that *OOB* is as accurate as using a test set of the same size as the training set.

After generating hundreds of trees, random forest needs apply them predicting the new case. Each individual tree will classify the new case independently. [Bre01] uses majority vote for gathering these internal predictions and giving its final classification.

Besides the majority vote, the weighted vote can also be applied. It applies the out-of-bag estimate on the combination of tree decision. Since out-of-bag is an unbiased estimator, it is used in research for estimating the strength of each tree [Bre96, Bre01]. In this thesis we take it as the weight on voting to combine the prediction of the trees vote.

4.2.2 Random forests generation

Random forests is a multi-classifier system consists of numerous trees as sub-classifiers (or internal classifiers). Each tree is a unpruned *CART*. The advantage of using the unpruned tree than using a pruned one is decreasing the correlation among tress. The unpruned tree has less strength but the reduced correlation improves the final accuracy after combining all trees. Without pruning, each tree generation will be much simpler and quicker.

Tree generation is a partition process of each node. There are two approaches for split selection in each partition [LS97].

1. For the training data set, all possible splits on each independent variable will be examined. The most impurity reduction split will be selected as the best split and used for partition. There are many impurity measures, such as Entroy/Information gain, Gini (diverse) index, Gini ratio, etc. as discussed in Section 4.1.

2. Split rule: $f(\vec{X}) \leqslant c$, where f is a linear combination function. *FACT* and *QUEST* are based on this split selection. Both of them use *ANOVA* F-statistic to find the split variable, which F-statistic is largest. Then *FACT* uses linear discriminant analysis (*LDA*), while *QUEST* uses modified quadratic discriminant analysis (*mQDA*), to find out the split point.

Both above approaches seek the "global" best split variable from all input independent variables (denoted as M). Instead of that, seeking a "partial" best split will introduce the the second randomness of Random forests. At each node, only a partial group of input variables is randomly selected to find the split rule. They are called random features. There are two types of Random Forests based on the complexity of random features:

1. **Forest-RI** is the simplest type of random features. At each node, A "partial best split" is found by the impurity measure same as *CART* from the selected group of variables. It recursively grows the tree until the tree reaches the maximum size. The number of the variable F in

the group is pre-defined, usually $\log_2 M + 1$. The selection space of Forest-RI is C_F^M.

2. **Forest-RC** is suitable for the data set consists of a small number of independent variables M. There are two problems when using *Forest-RC*. First, the chance of random feature repeat will be significantly increased and it will reduce randomness. Second, the variable number in the group (F) may take big fraction, which leads to much higher correlation. And such will cause the accuracy reduction.

   In Forest-RC, random feature is no longer a variable selected from the group. It is a linear combination of several variables. Two parameters are introduced to control the search scope, L and F. From the whole independent variables M, L variables are selected randomly. Then inside these variables, F coefficients is uniformly randomly picked from the range of $[-1, 1]$ and be used to compose the combination of the L variables. Then we use the same idea of impurity reduction as in *CART* and *Forest-RI* to find the best combination as the split rule. In [Bre01], L is suggested as 3, and F is suggested as 2 and 8.

4.2.3 Variable importance

Our study is not only limited to the considering of accuracy of predicting a new case, but also on the importance of variables. Since *OOB* can be used on the testing data set, we can derive variable ranking by removing the error change from classification. That is, we permute randomly all values at variable m in the *OOB* after each tree generation. We then classify new *OOB* on the tree to get the error rate. Repeat this procedure for all variable and all trees. Then the variable ranking is the average of error rate on all tree.

The pseudo code of algorithm is given in Table 4.2.

When viewing the outcome of a variable, the value is the average of the margin misclassification rate. This rate is raised by permuting the variable, so it shows the variable role in classification. If the outcome is big, removing it causes a high misclassification rate, and it plays an important role. On the contrary, smaller outcome means a lower importance.

4.3 score-CART and score-Random Forest

4.3.1 From s-CART to s-RF

In [Bre84], Gini Diverse Index is used in CART as the splitting method to construct the tree. However, there are several other splitting methods [Min89] to grow the tree. Each splitting method has different strength and will generate different tree. There is no significant advantage that one over another in general data sets.

We design a new scoring method achieving the benefit from the performance variance of different splitting method. It gathers and combines the decisions from different CART to give the score. Using the same tree generation technique, it is derived as an *internal multi-classifier system.*

Some splitting methods are described in Section 4.1.1. Similar as [Bre96, Bre01], usually vote system will produce a more accurate classification than that from each individual classifier. Also with the vote system, a probability

```
Require tree number $TN \geq 0$, variables $M$, training sample size $X$,
  category number of dependent variable $C$
Ensure Variable Importance array $\overrightarrow{VI}, (1..M)$
Variable Importance (tree number $TN$, variable number $M$)
/* initialize: $ME$ is to save classification result;*/
/* $times$ is to count the times of sample $x$ been selected in OOB */
$ME[X][TN][M] = 0$;      $times[X] = 0$;
for $i = 1$ to $TN$
    $T_i \Leftarrow RF$ tree construction;
    for$m = 1$ to $M$
    /* $OOB[\ ][m]$: array of all $OOB$ sample value at variable m */
       $OOB_m \Leftarrow$ randomly permute $OOB[\ ][m]$
         Classify $OOB_m$ on $T_i$, $c[i,x] \leftarrow$ predicted category for case $x$;
         for all$x$ such that $x \in OOB_m$
             $ME[x][i][m] = c[i,x]$; /*count as majority vote*/
             $times[x] = times[x] + 1$;
         end
    end
end
for$m = 1$ to $M$
    for$x = 1$ to $X$
    /* initialize: $cc$ is category counter to sum classification result */
        $cc[C] = 0$;
        for$i = 1$ to $TN$
            $cc[ME[x][i][m]] = cc[ME[x][i][m]] + 1$
        end
        $ct \leftarrow$ true category of x
        $cm \leftarrow$ maximum category in $cc$
        $Proportion[ct] = cc[ct]/times[x]$;
        $Proportion[cm] = cc[cm]/times[x]$;
        /* for any $m$, summary the misclassification rate for all $X$ */
        $VI[m] = VI[m] + (Proportion[cm] - Proportion[ct])$
    end
    $VI[m] = VI[m]/X$; /* average */
end
End Variable Importance;
```

Table 4.2: Variable importance schema for *RF*.

will be generated from the votes.

Figure 4.2 shows how the s-CART system works. In this thesis we adopt Information Gain, Gini index, Gini ratio, and their Marshall Correction algorithms as splitting methods. Six different trees are generated using different splitting methods. When a new case is input, it will travel down all trees to get the classification results.

Besides the majority vote to give the final classification of the case, the probability will be also derived from the vote. it will be regarded as the score in the scoring system.

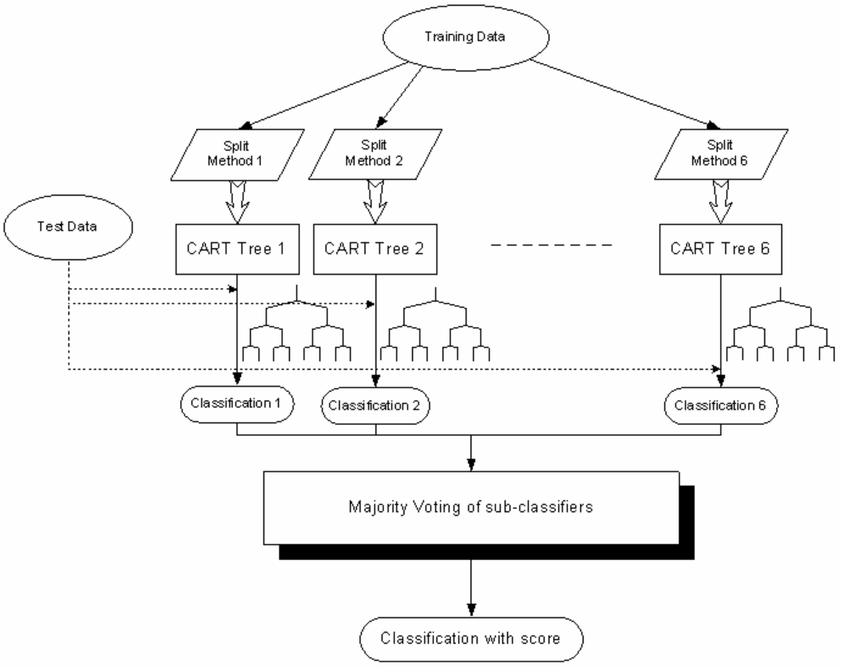

chch

Figure 4.2: s-CART mechanism.

The scoring method is more accurate because (1)it may generate different scores for different cases even if they fall into a same node of a tree. They may fall into a different node in another tree. (2)it utilizes more information from the internal characters of each case when achieving score. The cases travel through several different CART trees and internal characters have been checked and utilized for several times.

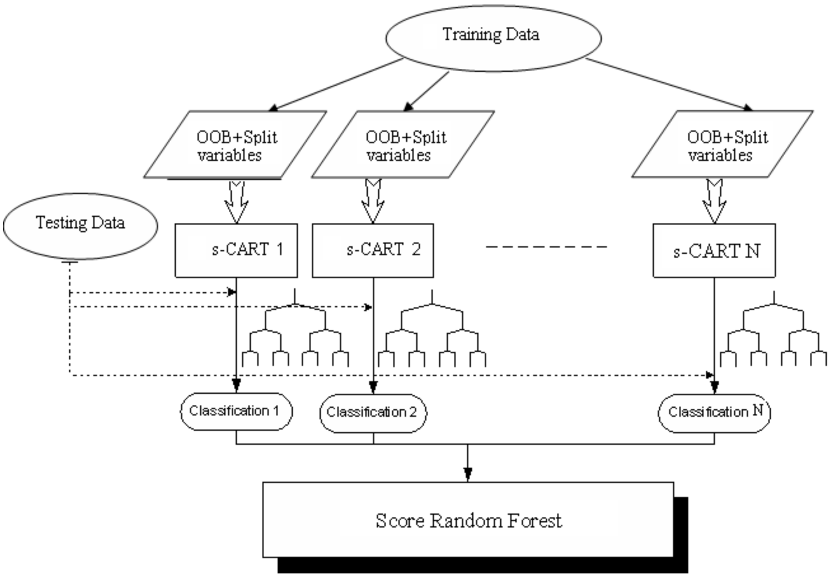

chch

Figure 4.3: s-RF mechanism.

The score-Random Forest is developed based on score-CART. In the first step, score-Random Forest applies the same OOB technique as Random Forest in generating samples. Unlike Random forest, a score-CART is grown instead of CART. Each s-CART will give a score as the classification result. The score of the Random Forest is derived by taking the average on scores of all s-CART. This is a simple idea but it builds on the strength of s-CART so that it has more power on classification.

4.3.2 Test results

We use the Head-Neck cancer data as the study object. The data is described in Chapter 3. Forty seven biomarkers are selected by proteoExplorer^{TM}(See the Appendix for the software manual).

In Table 4.3, the classification results are shown on the testing samples of these different CART trees. s-CART takes the proportion of the vote as the score. If the score is greater than 0.5 the subject has the disease otherwise it is normal. Three samples are misclassified: the disease subject #38 is classified as normal and the normal subjects #17 and #49 are classified as disease. Table 4.4 shows the number of nodes and the classification accuracy of each splitting method. s-CART combines all methods and gives the best accuracy of 93.88%.

ID	Truth	entropy	index	ratio	entropy$^+$	index$^+$	ratio$^+$	s-CART
1	1	1	0	0	1	1	1	0.667
2	1	1	1	1	1	1	1	1
3	1	1	1	1	1	1	1	1
4	1	1	1	1	1	1	1	1
5	0	1	0	0	0	0	1	0.333
6	0	0	0	0	0	0	0	0
7	0	0	0	0	0	0	0	0
8	0	0	0	0	0	0	0	0
9	0	0	0	0	0	0	0	0
10	0	0	0	0	0	0	0	0

Continued on next page

Table 4.3 – continued from previous page

ID	Truth	entropy	index	ratio	entropy$^+$	index$^+$	ratio$^+$	s-CART
11	0	0	0	0	0	0	0	0
12	0	0	0	0	0	0	0	0
13	1	1	0	0	1	1	1	0.667
14	0	0	0	0	0	1	0	0.167
15	0	0	0	0	0	0	0	0
16	0	0	0	0	0	0	0	0
17	0	1	0	1	1	0	1	0.667
18	0	0	0	0	0	0	0	0
19	0	0	0	0	0	0	0	0
20	0	0	0	0	0	0	0	0
21	0	0	0	0	0	0	0	0
22	0	0	0	0	0	0	0	0
23	0	0	0	0	0	0	0	0
24	1	1	1	1	1	1	1	1
25	0	0	0	0	1	0	0	0.167
26	0	0	0	0	0	0	0	0
27	1	1	0	0	1	1	1	0.667
28	0	0	0	0	0	0	0	0
29	1	1	1	1	1	1	1	1
30	1	1	1	1	1	1	1	1
31	0	0	0	0	0	0	0	0

Continued on next page

Table 4.3 – continued from previous page

ID	Truth	entropy	index	ratio	entropy$^+$	index$^+$	ratio$^+$	s-CART
32	1	1	1	1	1	1	1	1
33	0	0	0	0	0	0	0	0
34	0	0	0	0	0	0	0	0
35	0	0	0	0	0	0	0	0
36	1	1	1	1	1	1	1	1
37	0	0	0	0	0	0	0	0
38	1	0	0	0	1	1	0	0.333
39	1	1	1	1	1	1	1	1
40	1	1	1	1	1	1	1	1
41	1	1	0	0	1	1	1	0.667
42	1	1	1	1	1	1	1	1
43	1	1	1	1	1	1	1	1
44	1	1	1	1	1	1	1	1
45	1	1	1	1	1	1	1	1
46	1	1	1	1	1	1	1	1
47	1	1	1	1	1	1	1	1
48	1	1	1	1	1	1	1	1
49	0	1	0	0	1	1	1	0.667

Table 4.3: Classification results on testing samples of different CART tree constructed by different splitting method. ID is the testing sample index. *entropy* is Quinlan's entropy/information gain method. *index* is gini diversity index. *ratio* is gini ratio. *entropy*$^+$ is entropy information gain with Marshall correction. *index*$^+$ is gini diversity index with Marshall correction. emphratio$^+$ is gini ratio with Marshall correction.

Splitting method	Node Number	Classification Accuracy
Entropy/Information Gain	11	83.67%
+ Marshell Correction	23	87.76%
Gini Index	3	87.76%
+ Marshell Correction	13	91.84%
Gini Ratio	3	89.90%
+ Marshell Correction	13	91.84%
s-CART	64	93.88%

Table 4.4: Splitting method comparison for head and neck cancer study.

The score Random Forest is generated by running 200 score CART trees. The average scores are reported in Table 4.5. In comparison with sCART, s-RF misclassified one subject #38 and improved the accuracy. Table 4.6 shows the comparison of eight classifiers in the head and neck cancer study. s-CART achieves a better classification than a single CART tree while s-RF is better than Random Forest. The average score gives s-RF the advantage to achieve the best classification accuracy among the eight classifiers.

ID	Truth	CART	s-CART	s-RF
1	1	1	0.667	0.84
2	1	1	1	0.74
3	1	1	1	0.69
4	1	1	1	0.78
5	0	1	0.333	0.47
6	0	0	0	0.20

Continued on next page

Table 4.5 – continued from previous page

ID	Truth	CART	s-CART	s-RF
7	0	0	0	0.03
8	0	0	0	0.02
9	0	0	0	0.00
10	0	0	0	0.41
11	0	0	0	0.46
12	0	0	0	0.37
13	1	0	0.667	0.74
14	0	0	0.167	0.10
15	0	0	0	0.12
16	0	0	0	0.45
17	0	1	0.667	0.39
18	0	0	0	0.09
19	0	0	0	0.25
20	0	0	0	0.03
21	0	0	0	0.07
22	0	0	0	0.01
23	0	0	0	0.43
24	1	1	1	0.58
25	0	0	0.167	0.31
26	0	0	0	0.17
27	1	1	0.667	0.83

Continued on next page

Table 4.5 – continued from previous page

ID	Truth	CART	s-CART	s-RF
28	0	0	0	0.34
29	1	1	1	0.86
30	1	1	1	0.50
31	0	0	0	0.11
32	1	1	1	0.95
33	0	0	0	0.12
34	0	0	0	0.22
35	0	0	0	0.17
36	1	1	1	0.83
37	0	0	0	0.13
38	1	0	0.333	0.21
39	1	1	1	0.73
40	1	1	1	0.58
41	1	1	0.667	0.74
42	1	1	1	0.91
43	1	1	1	0.93
44	1	1	1	0.98
45	1	1	1	0.91
46	1	1	1	0.63
47	1	1	1	0.60
48	1	1	1	0.52

Continued on next page

Table 4.5 – continued from previous page

ID	Truth	CART	s-CART	s-RF
49	0	1	0.667	0.38

Table 4.5: Comparison on head and neck cancer testing samples by different method. ID is the testing sample ID; *CART* is classification result by original CART; *s-CART* is the classification result by score-CART; *s-RF* is score Random Forest classification given by this thesis.

Head Neck Data Set			
Classifiers	Sensitivity	Specificity	Total Accuracy
MKNN	95.91%	88.89%	91.84%
MLPNN	86.36%	74.07%	79.59%
GRNN	86.36%	88.89%	79.59%
SVM	90.91%	85.19%	87.76%
CART	90.91%	88.89%	89.80%
RF	86.36%	92.59%	89.80%
s-CART	95.45%	92.59%	89.90%
s-RF	95.45%	100.00%	97.96%

Table 4.6: Comparison of sensitivity and specificity head and neck cancer study on eight classifiers.

Chapter 5

Correlation of Proteomic and Genomic Data

Only mRNA expression levels were considered for most of the pathway models analyzed due to the lack of protein expression data [Bay02, Bay04]. Variables representing protein concentrations were either excluded or substituted with the corresponding mRNA expression levels. With the newly emerging LC-MS/MS technology, the protein expression data can now be readily obtained [Banfi06], including from plants such as Arabidopsis thaliana [Sch05]. Since the technique is much more sensitive, significantly lower sample amounts are required for LC-MS/MS than for 2-D protein gel electrophoresis. Our gene-protein integration software module will enable the automated matching of mRNA's and their corresponding protein products. A fundamental and pressing question is the correspondence of transcriptional responses (mRNA level) to cellular protein abundance, which are also influenced by translational and post-translational mechanisms [Gyg99, Cox05]. Quantification of the gene product (mRNA and protein) correlation/concordance strength and their difference in abundance would offer a unique insight on how the information encoded by a myriad of gene products is integrated at the molecular, cellular and organism levels. However, the few comparison studies published [Gyg99, Cox05] yielded inconsistent results.

The integration of gene and protein data would reveal the correspondence of cellular protein abundance to transcriptional responses and provide insight into molecular pathways that determine and link gene and protein expression patterns.

In this chapter, we fist explain how to obtain the proteomic MS data and gene microarray data (Section 5.1) and build the correspondence between the gene and protein data using the human platelet example (Section 5.2). In Section 5.3 three correlations are calculated in correlation analysis. A codon adaptation index(CAI) is also introduced as a tool to predict expression level of a particular protein or a group of proteins(Section 5.4). In Section 5.5, we propose a new method, use the triptic number to adjust the measurement of protein abundance which is proved to be a useful method in improving the correlation. Finally, we applied two techniques to do clustering protein-gene pairs in Section 5.6.

5.1 Data acquisition

Mass spectrometric analysis. Platelet samples are drawn from four different donors and then pooled for proteomic studies. They were completed in duplicate using liquid chromatography coupled to tandem mass spectrometry (LC-MS/MS), in which the LC steps are interfaced with a fused silica capillary to maximize peptide resolution and detection sensitivity by tandem MS/MS.

The mass spectrometric analysis was completed using a QSTAR Pulsar i quadrupole-TOF MS (Applied Biosystems, Foster City, CA) equipped with nano-electrospray source. The loading and elution of the peptides to and from the cation exchange column, to the reverse phase column, and to the mass spectrometer were fully automated, and individual sample runs were completed in 24 - 36 hours. MS/MS acquisition was completed in a data-dependent manner by operating the ion trap instrument using dynamic-exclusion lists. Automated protein identifications were obtained using Pro ID Software 1.0 (Applied Biosystems) linked to the SwissProt database (Version XX containing XXX proteins). Information provided by the MS analysis included: (1) protein gi accession number, (2) run, indicating if it was found in the 1st or 2nd run, (3) protein name, (4) confidence in the protein match, which is based on the ”distance to next” metric, and (5) number of spectral (peptide) counts found which represents the total number of MS/MS spectra corresponding to a particular protein accession.

Spectral (peptide) counts were used as a simple, semi-quantitative means of establishing protein abundance among complex MS data sets [Cox05, Sand05]. All peptides with confidence levels greater than 70% were used for integrated proteomic abundance determinations. To ensure compatibility between both runs, spectral counts were normalized by global scaling to the average spectral count detected per protein sample; spectral counts in each experiment were then scaled to ensure compatibility across data sets. Platelet transcripts.

Gene Microarray analysis. Microarray data were derived from a subset of previously reported mRNA profiles of human platelets [Gna03]. Platelets were collected from volunteer donors (N = 5) by apheresis to obtain sufficient

RNA for hybridization to the Affymetrix U133A gene chip (Affymetrix), and expression data were analyzed using Genespring 7.0 software (Silicon Genetics, Redwood City, CA). A transcript was considered "platelet-expressed" if it was "present" or "marginal" in 4 of 5 platelet samples. Using these strict criteria, 1640 mRNAs were expressed at significant levels by platelets [Gna03]. Relative transcript abundance was established by rank-ordering the unique set of non-redundant mRNAs by determining the mean normalized signal intensities across the individual arrays, using computational algorithms as previously described.

5.2 Integration of gene and protein database

We use a comprehensive bioinformatic approach to integrate the platelet proteomic and transcriptomic datasets as in Figure 5.1. Here we applied the BLAST algorithm for sequence comparison. Figure 5.2 shows it is a heuristic search method that seeks words of length W that score at least T when aligned with the query and scored with a substitution matrix. Words in the database that score T or greater are extended in both directions in an attempt to find a locally optimal ungapped alignment or HSP (high scoring pair) with a score of at least S or an E value lower than the specified threshold. HSPs that meet these criteria will be reported by BLAST, provided they do not exceed the cutoff value specified for number of descriptions and/or alignments to report. [Bla]

Amino acid sequences for each accession number identified by LC-MS/MS were downloaded from the NCBI database [Pru05](NCBI accession could be

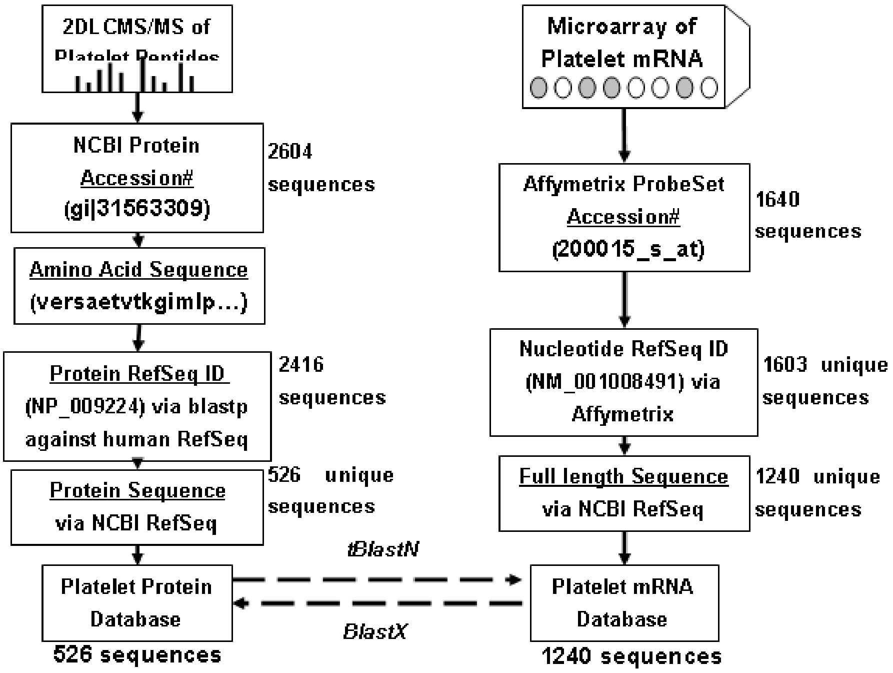
2DLCMS/MS of Platelet Peptides
NCBI Protein Accession# (gi|31563309)
2604 sequences
Amino Acid Sequence (versaetvtkgimlp…)
Protein RefSeq ID (NP_009224) via blastp against human RefSeq
2416 sequences
Protein Sequence via NCBI RefSeq
526 unique sequences
Platelet Protein Database
526 sequences
tBlastN
BlastX
Microarray of Platelet mRNA
Affymetrix ProbeSet Accession# (200015_s_at)
1640 sequences
Nucleotide RefSeq ID (NM_001008491) via Affymetrix
1603 unique sequences
Full length Sequence via NCBI RefSeq
1240 unique sequences
Platelet mRNA Database
1240 sequences

Figure 5.1: Platelet study: the process of establishing and integrating the gene/protien database.

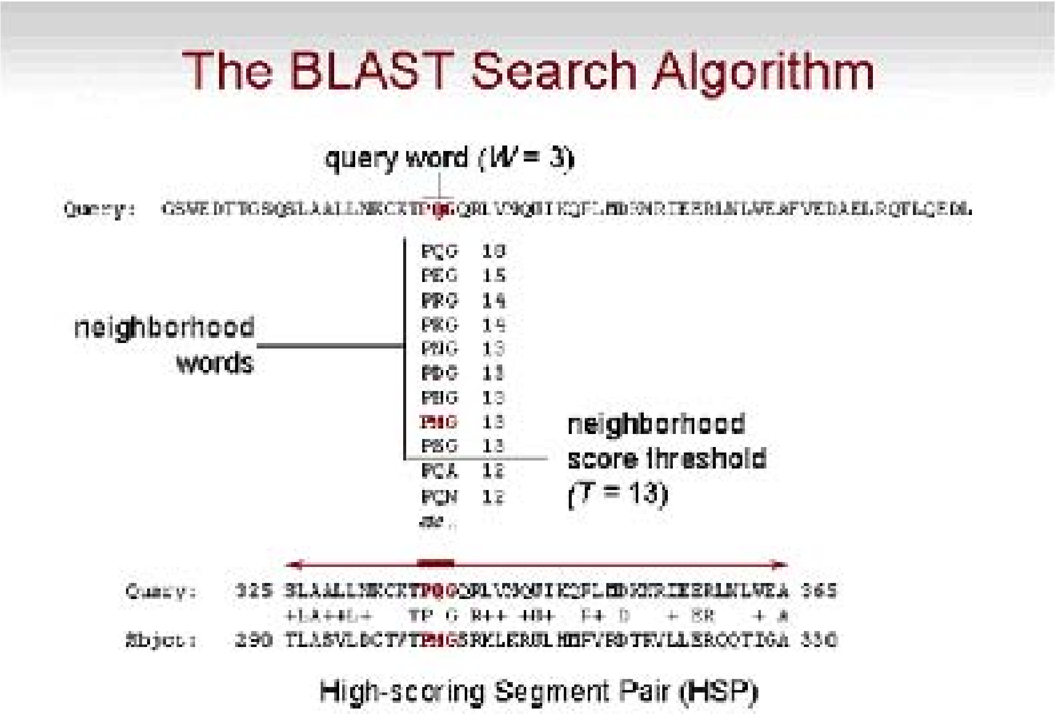

The BLAST Search Algorithm

query word (W = 3)
neighborhood words
neighborhood score threshold (T = 13)
High-scoring Segment Pair (HSP)

```
Query:  GSVEDTTGSQSLAALLNKCKTPQGQRLVNQWIKQPLMDKNRIEERLNLVEAFVEDAELRQTLQEDL

PQG 18
PEG 15
PRG 14
PKG 14
PNG 13
PDG 13
PHG 13
PMG 13
PSG 13
PQA 12
PQN 12
etc.

Query:  325 SLAALLNKCKTPQGQRLVNQWIKQPLMDKNRIEERLNLVEA 365
            +LA++L+    TP G R++  +W+  P+ D     + E R    + A
Sbjct:  290 TLASVLDCTVTPMGSRMLKRWLHMPVRDTRVLLERQQTIGA 330
```

Figure 5.2: BLAST tool.

assigned to any sequence not for protein only). A total of 2,604 unique NCBI protein accessions were identified during 2DLC/MS/MS analysis. Each sequence was queried against the protein RefSeq database for human using blastp (protein-protein BLAST, identifying a query amino acid sequence and for finding similar sequences in protein databases)program. The relative RefSeq sequences(NP ID) are used to build the protein database. 2416 of these have RefSeq accessions by using blastp against the human NCBI RefSeq database and 526 among them are unique.

The target nucleotide sequences for each Affymetrix probe set were downloaded from the Affymetrix analysis web database. 1640 of the 22,215 platelets transcripts were represented on the Affymetrix U133A microarray. These "non-full length" sequences were then used to download full length platelet nucleotide sequences from RefSeq, a curated and non-redundant collection of sequences representing genomic data, transcripts and protein citePru05. Full length sequences were available for 1,603 of the 1,640 Affymetrix accessions, of which 1,240 represented unique, non-redundant sequences. Those 1,240 sequences were used for all subsequent platelet transcript analyses.

Finally we derived two databases. The platelet protein database consists of 526 sequences and there are 1240 sequences in the platelet nucleotide database. Protein sequences were then queried against the platelet nucleotide sequence database using tBlastN (in BLAST) which allow comparison of platelet protein amino acid sequences to the six-frame translations of the platelet nucleotide database. On the other hand, nucleotide sequences were queried against the plate protein database using blastx which compares the six-frame conceptual translation products of a nucleotide query sequence (both strands)

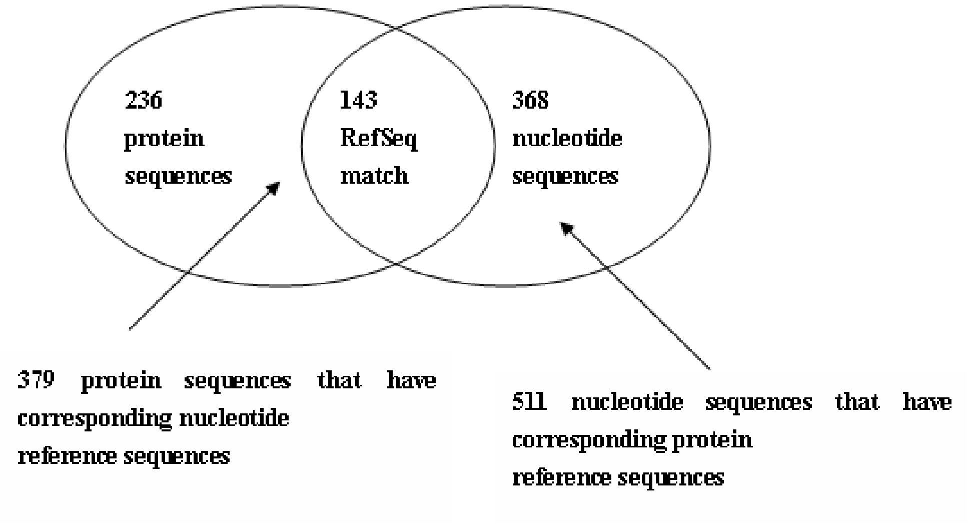
236
protein
sequences
143
RefSeq
match
368
nucleotide
sequences
379 protein sequences that have corresponding nucleotide reference sequences
511 nucleotide sequences that have corresponding protein reference sequences

Figure 5.3: Result of integrating platelet proteomic and genomic datasets.

against a protein sequence database.

As a result shown in Figure 5.3, 379 of 526 proteins (73%) have corresponding nucleotide reference sequences (E-value<0.001) while 511 of 1240 mRNA (41%) transcripts have corresponding protein reference sequences (E-value<0.001). There are 143 sequences have the same match results between nucleotide and protein references sequences as in NCBI RefSeq database for human. The reported E-values provide an estimate of the statistical significance of the match between protein and nucleotide or nucleotide and protein. An E-value of less than 0.001 was considered statistically significant. Unless other stated, all relational database analyses are derived using E-values<0.001.

For example, in the query using tblastN program, the sequence with RefSeq accession NP_004479.1 has the same corresponding nucleotide sequence as the sequence with accession NP_000164.3.(Table 5.1) However, the corresponding nucleotide accession of NP_004479.1 is NM_004488.1 in the full RefSeq database. The nucleotide sequence with accession NM_004488.1 is not in our mRNA database with 1240 sequences. Thus NP_000164.3 is one of the 143 sequences that has the same RefSeq match and NP_004479.1 belongs to the subset with 236 protein sequences.(Table 5.1)

NCBI Accession	RefSeq Accession	Nucleotide by tblastN	Actual Match	Protein Name
gi3183011	NP_004479.1	NM_000173	NM_004488.1	glycoprotein V precursor
gi121531	NP_000164.3	NM_000173	NM_000173	glycoprotein Ib alpha

Table 5.1: An example of tblastn.

Similarly, Table 5.2 shows that if we start from the nucleotide sequences, NM_000419 is one of 143 sequences and NM_003637 is among 368 sequences which have not same match as in RefSeq database.

Affymetrix Probeset No.	RefSeq Accession	Protein by blastX	Actual Match	Gene Name
216956_s_at	NM_000419	NP_000410.1	NP_000410.1	integrin alpha 2b
206766_at	NM_003637	NP_000410.1	NP_003628	integrin alpha 10

Table 5.2: An example of blastx.

Both protein and mRNA sequences were transformed to reference sequences. If one reference sequence has multiple corresponding protein or mRNA sequences, we take the average of those abundances. For instance, four protein sequences with NCBI accessions gi113606, gi113607, gi113608 and gi113609 have the same reference sequences with accession NP_000025.1. The abundance of this protein sequence is 45 which is the average of four number of peptide hits. "1/2" in the column "Run" means peptides are found in both two runs and the hit in the column 'No. of Peptide' is the average.

NCBI accession	RefSeq accession	No. of Peptide	Run
gi113606	NP_000025.1	58.5	1/2
gi113607	NP_000025.1	40	1/2
gi113608	NP_000025.1	46.5	1/2
gi113609	NP_000025.1	33	2

Table 5.3: Taking the average to get the final gene and protein abundances.

The protein abundances are denoted by number of peptide which is normalized by the median of the experiment. The mRNA abundances are denoted by the normalized signal intensities of the microarray gene chips. For the 143 genes, the protein abundances are ranged from 0.29 to 118.36 and the average gene expressions of 5 platelet chips are ranged from 0.76 to 16.75.

5.3 Correlation analysis

We investigate the gene-protein correlation using three different methods: Pearson correlation, Spearman rank correlation, and the usual canonical correlation. Among 143 gene-proteins pairs, there only 120 whose protein abundances can be detected in both runs of proteomic mass spectrometer. To calculate the canonical correlation, we will focus on these 120 pairs.

In Figure 5.5, neither protein nor gene data has normal distribution thus we perform the Box-Cox transformation[Box64]:

$$x(\lambda) = \frac{x^{\lambda} - 1}{\lambda}, \lambda \neq 0$$

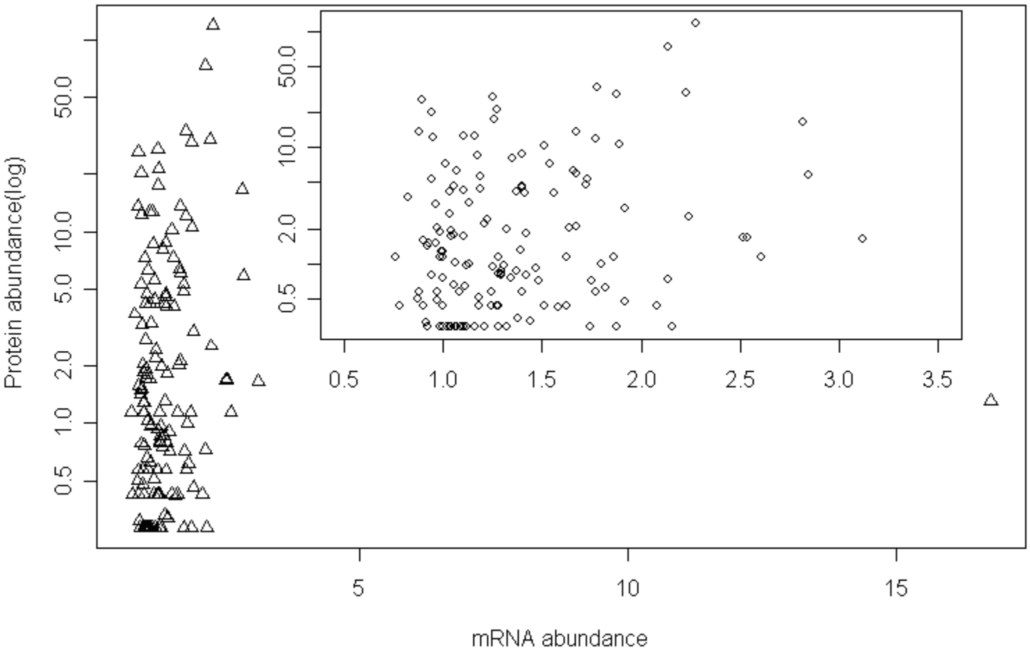

Figure 5.4: 143 gene-protein pairs.

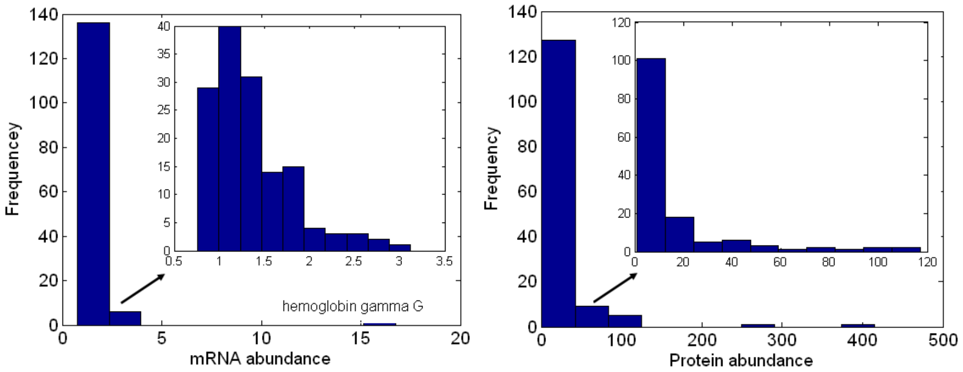

Figure 5.5: Distributions of protein and mRNA abundances.

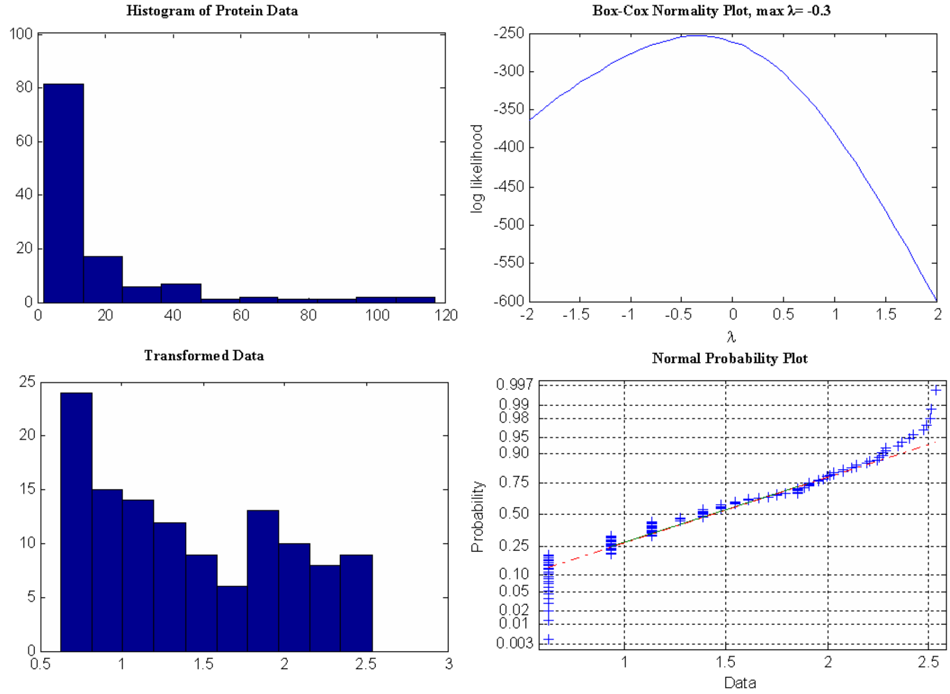

Figure 5.6: Box-Cox transformation of protein abundances.

Select λ to maximize the logarithm of the likelihood function:

$$f(x,\lambda) = -\frac{n}{2}log[\sum_{i=1}^{n}\frac{(x_i(\lambda)-\bar{x}(\lambda))^2}{n}] + (\lambda-1)\sum_{i=1}^{n}log(x_i)$$

where $\bar{x}(\lambda) = \frac{1}{n}\sum_{i=1}^{n} x_i(\lambda)$ is the mean of the transformed data.

In Figure 5.6 and Figure 5.7, we notice that the mRNA data is normal but the protein data is still not normal after the transformation. But we can still calculate p-values and confidence interval for Pearson correlation and canonical correlation by applying bootstrap method.

Before we calculate the canonical correlation, it is necessary to check the reproducibility of the five microarrays and two proteomic runs for the 120 gene-protein pairs. Figure 5.8 shows there is a high correlation(0.9) between

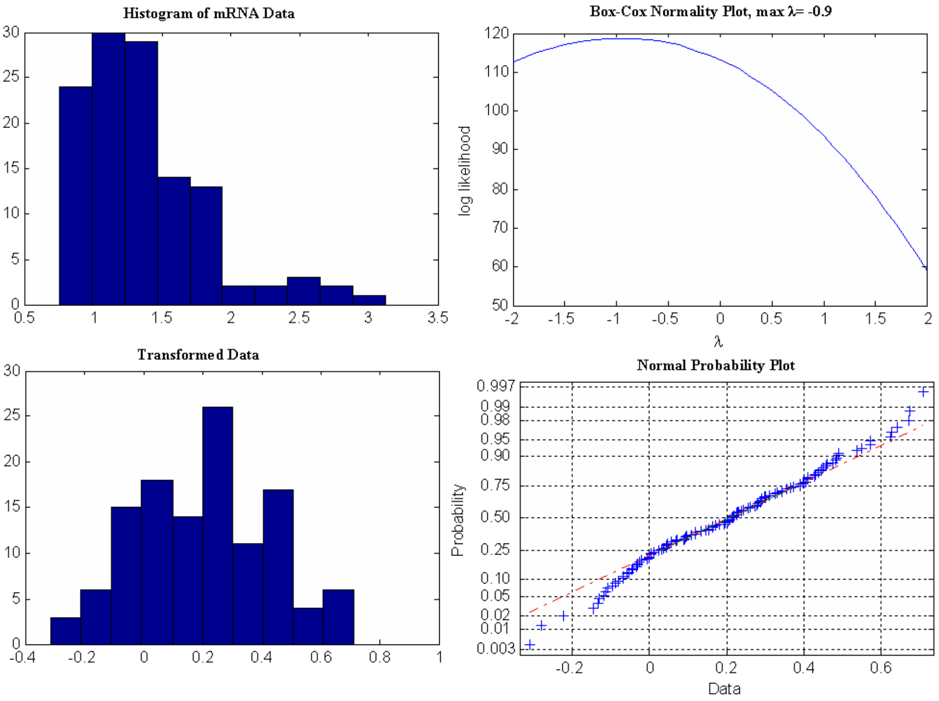

Figure 5.7: Box-Cox transformation of mRNA abundances.

the 2 runs for proteomic data generation, which means the protein data is reproducible. In Table 5.4, we notice that the five microarrays correlate very well. The correlations are all above 0.8 except those between 3rd array and the others are above 0.7.

	Array 1	Array 2	Array 3	Array 4	Array 5
Array 1	1	0.9154	0.732	0.9105	0.8076
Array 2		1	0.7636	0.9717	0.9168
Array 3			1	0.7178	0.8775
Array 4				1	0.8654
Array 5					1

Table 5.4: Correlation of gene data.

Figure 5.9 shows the gene-protein correlation result using three different methods: Pearson correlation, Spearman rank correlation, and the canoni-

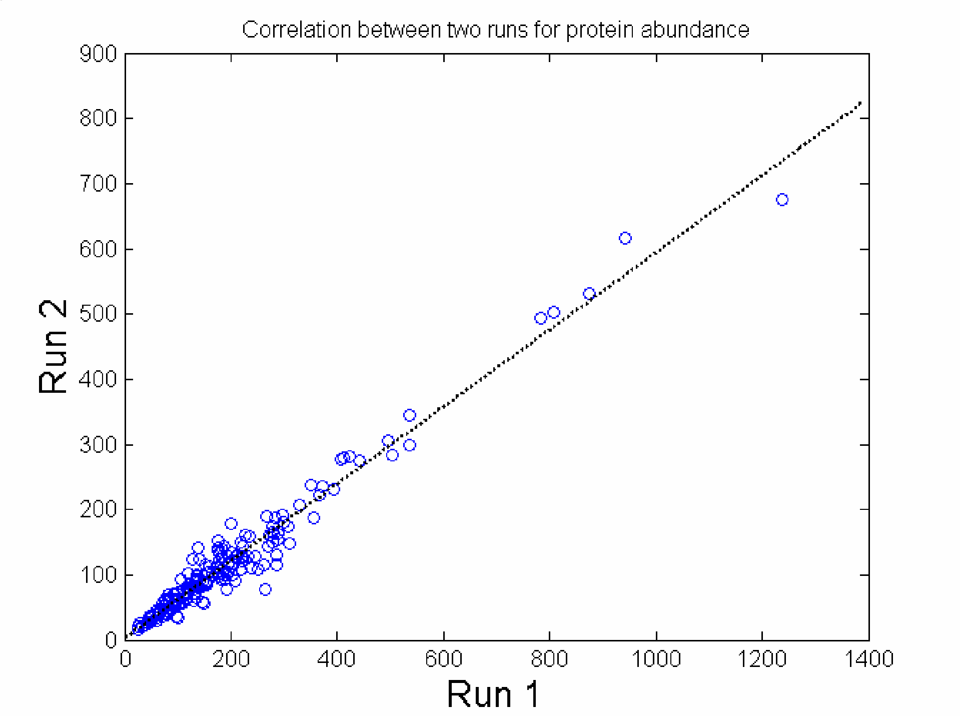

Figure 5.8: Correlation of the protein data.

cal correlation. It is evident that the Spearman rank correlation is the least powerful and the canonical correlation is the most powerful. Even for the same method, its correct and incorrect usage would yield drastically different results. Figure 5.10 depicts the Pearson correlation for the platelet study without the Box-Cox normality transformation Figure 5.10a, with the normality transformation performed on both gene and protein data Figure 5.10b, or with the normality transformation performed on the gene data only Figure 5.10c. Since both the gene and protein data were found to be non-normal, the Pearson correlation without the normality transformation indicating that the correlations are uniformly significant is incorrect Figure 5.10a. The Pearson correlation with the normality transformation done on both gene and protein data indicates that the correlations are uniformly insignificant Figure 5.10b. The Pearson correlation with the normality transformation done on the gene data only indicates that the correlations are uniformly significant again Figure 5.10c. So which one should we report? Although both Figure 5.10b and Figure 5.10c are correct, Figure 5.10b is too conservative because only one of the two variables is required to be normal for valid statistical results. Thus the correct answer is to report the findings in Figure 5.10c - the Pearson correlation sorted by the top genes are uniformly significant.

The canonical correlations aim to gauge the relationship between two sets of variables directly. Canonical correlation is essentially the Pearson correlation between the linear combination of variables in one set and the linear combination of variables from another set. The pair of linear combinations having the largest correlation is determined first. Next, the pair of linear combinations having the largest correlation among all pairs uncorrelated with

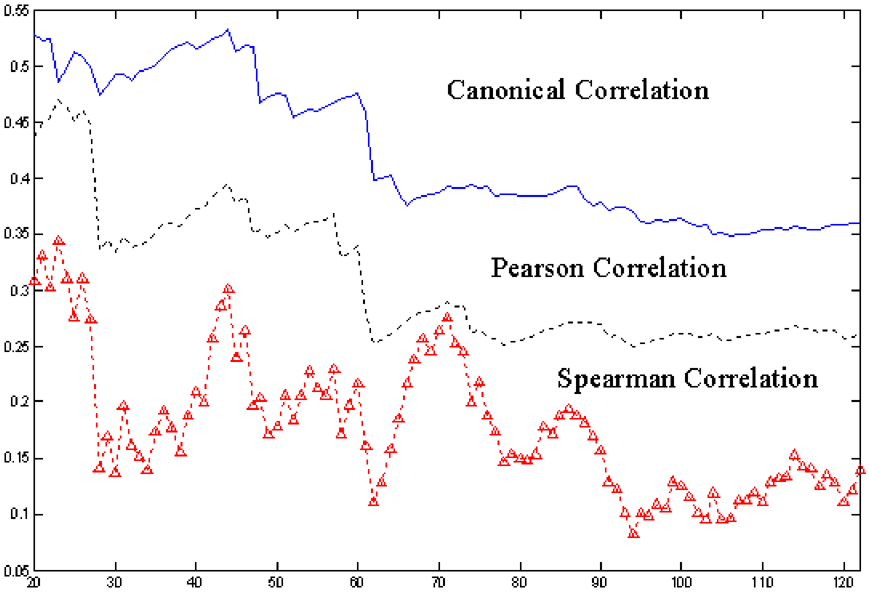

Figure 5.9: Pearson, Spearman and canonical correlations between gene-protein expression data for the platelet study.

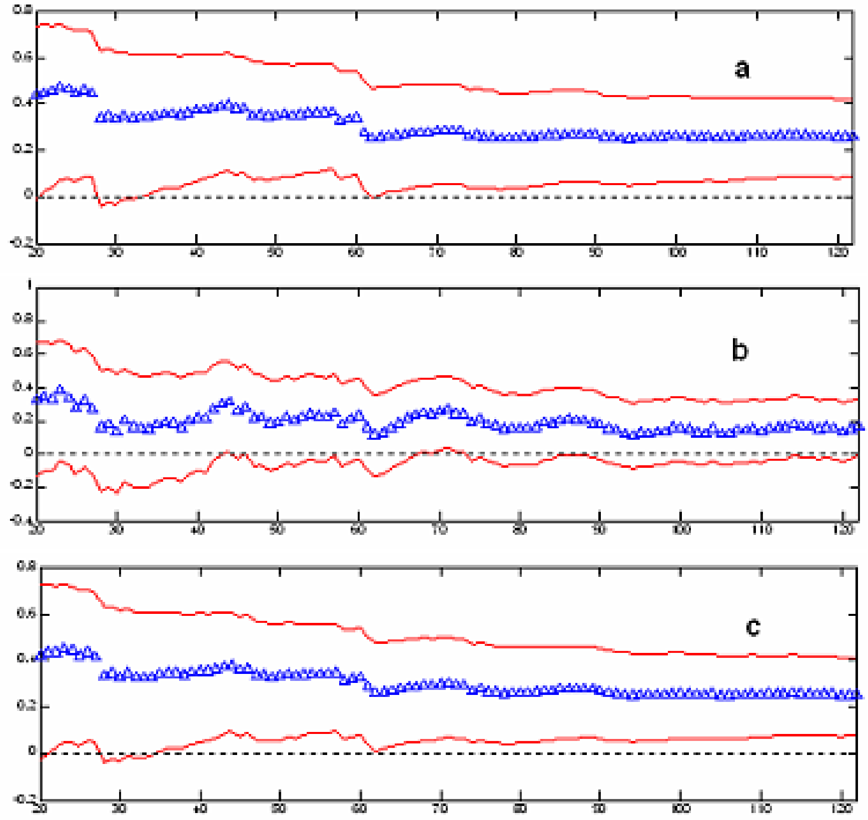

Figure 5.10: Pearson correlation between the original gene-protein expression data (a), the normality transformed data on both gene and protein (b) and the normality transformed data on gene only (c).

the initially selected pair is identified, and so on. The pairs of linear combinations are called the canonical variables, and their correlations are called the canonical correlations. The first canonical correlation, which is often the only significant one as in our case, is usually adopted to describe the interclass correlation. Here we will report the first canonical correlation, its test statistic - Wilks' Lambda, the equivalent F-statistic and the p-value. In our study, there are five sets of gene microarray data and one set of protein LC-tandem MS data. The Pearson correlation and the Spearman correlation can only gauge the relationship between the protein data and one set of the gene expression data (e.g. the average of the 5 sets of gene data). Thus they will be influenced by the quality of all the data sets involved. If one set of gene data is of poor quality and thus fail to reflect the true nature of the presumably high-correlated mRNA-protein relationship, both Pearson and Spearman correlation will be less than optimal. On the other hand, the first canonical correlation (or its nonparametric counterpart based on the ranks) will be larger than the largest Pearson (or Spearman) correlation between the protein data and each individual set of gene expression data. Thus, as long as one set of gene data is of good quality, canonical correlations will preserve and prevail. In addition, the major Principal Components can be obtained to replace the original variables to magnify the significance of canonical correlation.

Table 5.5 shows the three correlations for the 120 gene-protein pairs. The Pearson and Spearman correlations are very small and not significant. The canonical correlation is 0.53 with a significant p-value less than 0.01. We will show the adjustment technique using the number of tripsin fragments in Section 5.5. It improved the Pearson and Spearman correlations a lot.

120 gene-protein pairs	Correlation	P-value
Pearson	0.02	> 0.2*
Spearman	-0.04	0.68
Canonical*	0.53	< 0.01*

Table 5.5: Correlation of 120 gene-protein pairs before the triptic adjustment.
* p-values are calculated by bootstrapping

5.4 Codon adaptation index

Codon usage could be used as a tool to predict expression level of a particular protein or a group of proteins. The degeneracy of the genetic code enables the same amino acid sequence to be encoded and translated in many different ways. Alternative codon usage is not purely random - systemic bias of degenerate codon usage appears at different level of genetic organization. It became accepted that biased codon usage could regulate the expression levels of individual genes by modulating the rates of polypeptide elongation. Historically, the relationship between codon usage and protein/mRNA expression has been most extensively studied in yeast2. To date, several gene sequence - based computer algorithms are available to calculate the codon usage for a particular organism or tissue (EMBOSS, Jcat and etc.) We applied codon usage analysis to platelets to predict correlation between mRNA and protein abundances.

Sharp and Li ([Sha87]) proposed to use CAI (codon adaptation index) to evaluate how well a gene is adapted to the translational machinery. CAI is a single value measurement that summarizes the codon usage of a gene relative to the codon usage of a reference set of genes. A higher CAI value usually suggests that the gene of interest is likely to be highly expressed.

50 highest platelet-expressed transcripts were taken as the initial reference set in our studies. We calculated CAI for 156 highest-expressed platelet transcripts and for 156 lowest-expressed. [Wu05]

The CAI distribution of 156 highest-expressed platelet transcripts is left skewed, and the median 0.77 is greater than the mean 0.76. Similarly, the CAI distribution of the lowest-expressed platelet transcripts is right skewed, and the median 0.73 is less than the mean 0.74.

The mean CAIs for these two groups of genes were 0.76 and 0.74 respectively. The p-value of the two sample t-test is 0.003, which means the two means are significantly different.

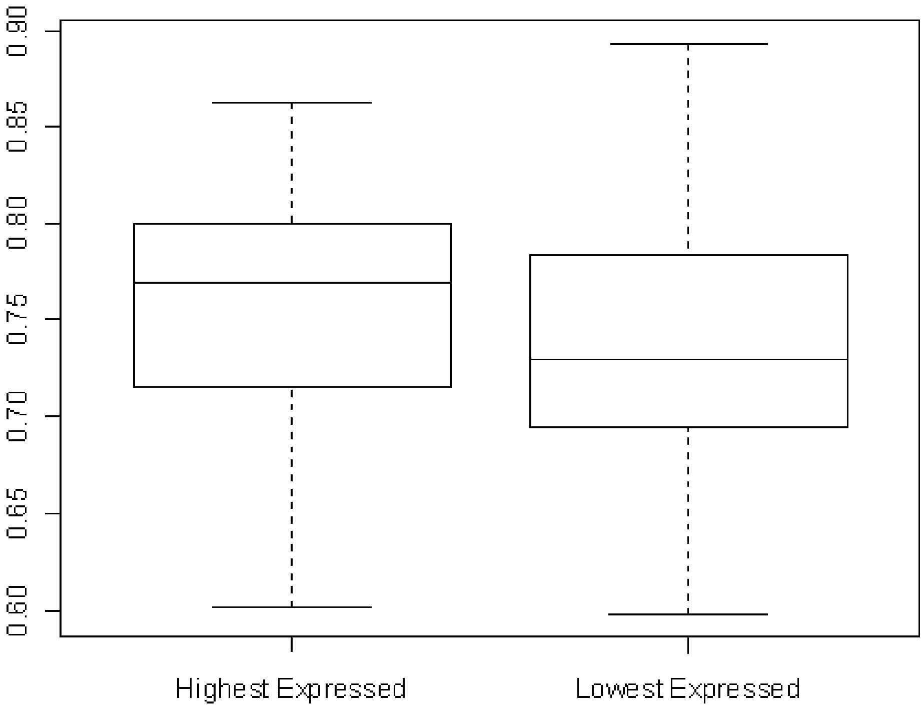

Figure 5.11: Box plot of CAI for highest and lowest expressed platelet transcripts.

At the protein level, we detected 22 proteins belonging to the group of

50 highest-expressed platelet transcripts. For the lowest-expressed transcript group only 12 proteins have been detected.

It is evident that for individual genes correlation between protein and mRNA expression is low (number). Since correlation depends on the distributions of both parameters compared, it is possible that different types of transcript and protein abundances distribution Figure 5.11. It may indicate also that our method of measurement of protein abundance (number of peptide hits per protein) is not optimal for this type of analysis. In summary, CAI analysis could be used as a tool to predict or compare protein expression levels for a group of proteins, but requires extra caution if applied to individual gene products.

5.5 Triptic adjustment

Trypsin is a serine protease found in the digestive system, where it breaks down proteins. It is used for numerous biotechnological processes. Figure 5.12 shows the crystal structure of a Trypsin. In Figure 5.13, the tripsin fragments of the protein Proflin are illustrated.

We use the number of peptide hits per protein to measure the protein abundance in previous correlation analysis. This may not be optimal and the tripsin cleavage enlightened us to make an adjustment. The new protein abundance is the peptide hits divided by the number of tripsin framents.

1. Before triptic adjustment:

   protein abundance = peptide hits.

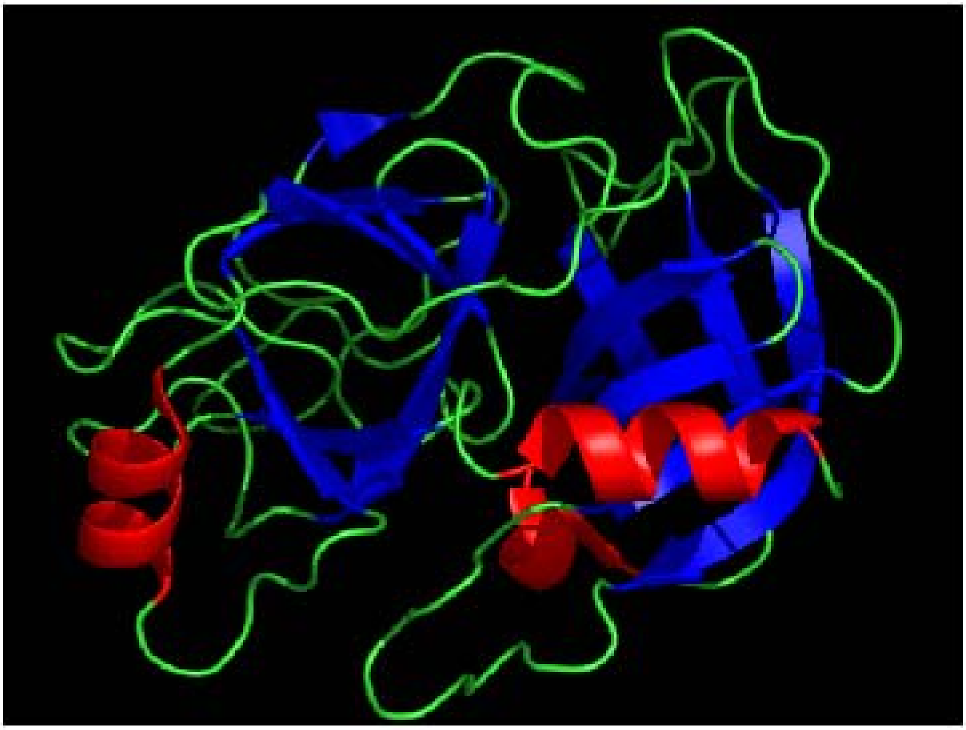

Figure 5.12: Crystal structure of tripsin.

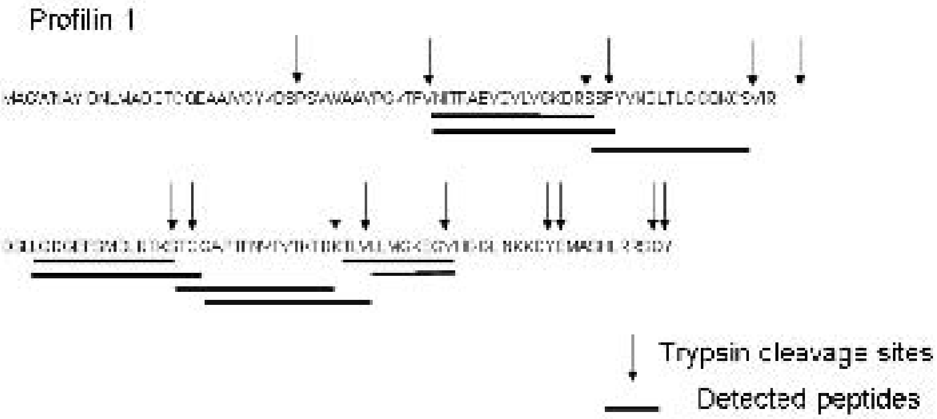

Figure 5.13: Example of triptic fragments for proflin.

2. After triptic adjustment:

$$\text{protein abundance} = \frac{peptidehits}{numberoftripsinfragments}.$$

In Table 5.6, the Pearson correlation increases from 0.02 to 0.31 and the Spearman correlation increases from -0.04 to 0.27. Both correlations are statistically significant after the triptic adjustment. There is a small change for the canonical correlation from 0.53 to 0.55 and it is still significant.

	Before Triptic Adjustment		After Triptic Adjustment	
	Correlation	P-value	Correlation	P-value
Pearson	0.02	>0.2*	0.31	<0.05*
Spearman	-0.04	0.68	0.27	0.0014
Canonical	0.53	<0.01*	0.55	< 0.01*

Table 5.6: Triptic adjustment comparison for the correlation of 120 gene-protein pairs. * p-values are calculated by bootstrapping

A hypothesis testing on the change of the correlations is performed and both p-values for Pearson and Spearman correlations are smaller than 0.01, which means there are significant changes.

5.6 Quadrant analysis and clustering

5.6.1 Quadrant analysis

First, the set of 120 proteins was ranked by the protein abundance and the correlation was calculated by including the 15 highest-abundant proteins and then decreasingly including the remaining 105 ones in order of abundance. In Figure 5.14, the top 18 highly abundant proteins have the maximum correlation of 0.44 In the other hand, the set of 120 genes was ranked by the mRNA abundance(gene expression). The correlation was calculated by including the 15 highest expressed genes and then decreasingly including the remaining 105 pairs. As shown in Figure 5.15, the most highly expressed 20 genes have the largest correlation of 0.84 with the proteins.

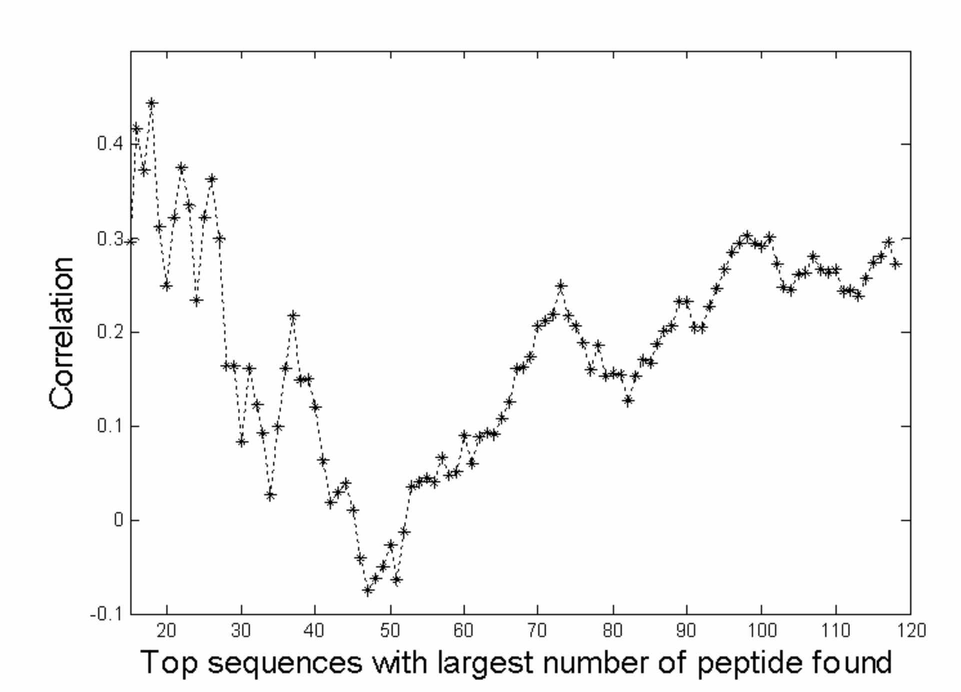

Figure 5.14: Effect of highly abundant proteins on Spearman correlation coefficient for mRNA and protein abundance in platelet. Top 18 highly abuandant proteins has largest correlation of 0.44.

Then we can divide all 120 genes into four groups. It is shown as four quadrants in Figure 5.16. The 18 most highly abundant proteins are in quadrant 1 and 2 and the 20 highest expressed genes are in quadrant 2 and 3. Table 5.7 shows that the three groups in Q1 Q3 and Q4 have very significant correlations(p<0.01).

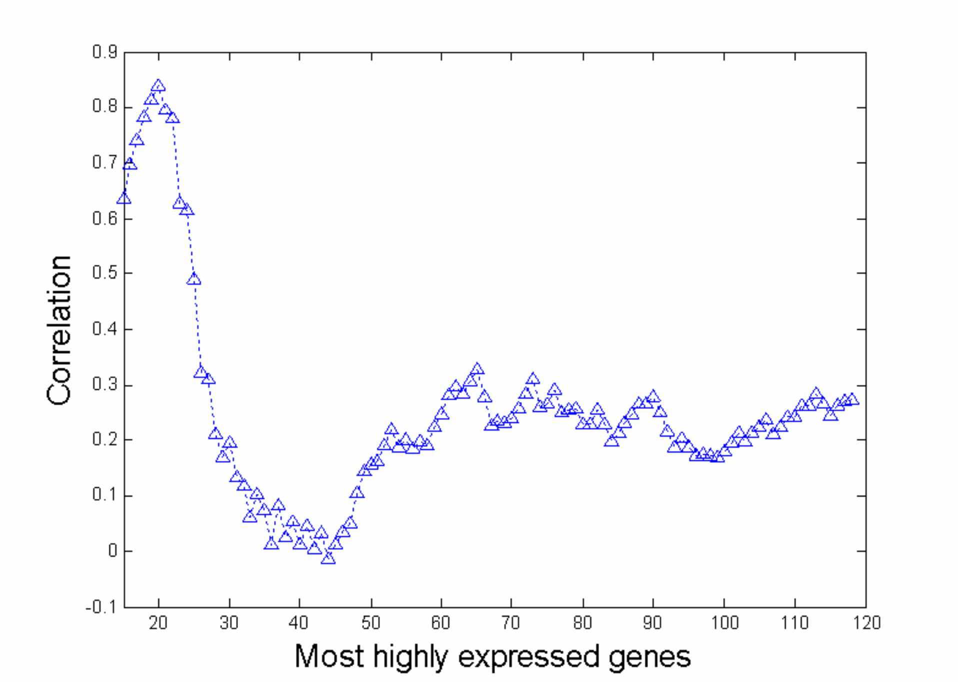

Figure 5.15: Effect of highly abundant genes on Spearman correlation coefficient for mRNA and protein abundance in platelet. Top 20 highly abundant genes has largest correlation of 0.84.

Quadrant	Number of Genes	Spearman Correlation	P-value
Q1	14	0.36	0.1015
Q2	4	0	0.54
Q3	84	0.33	0.0012
Q4	16	0.91	< 0.0001

Table 5.7: Correlations of the group in four quadrants.

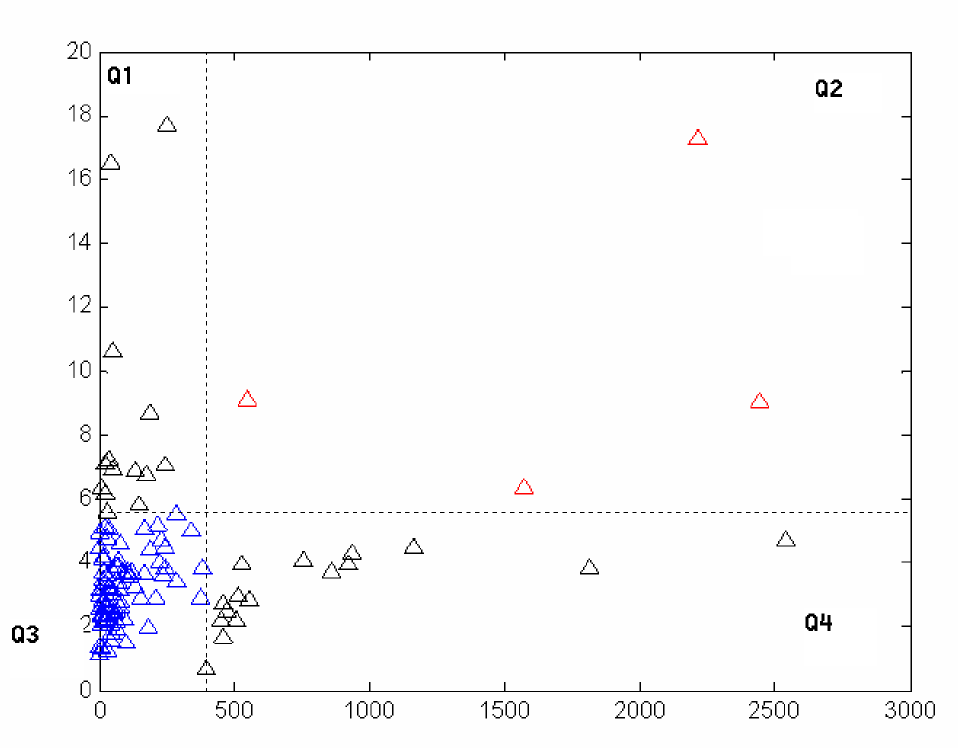

Figure 5.16: Four quadrants: Q1: highly abundant in protein but low abudant in gene; Q2: highly abundant in both gene and protein; Q4: highly abundant in gene but low abundant in protein.

5.6.2 Clustering

Co-regulated genes (proteins) are expected to have correlated expression patterns. Thus when submitted to the cluster analysis with a suitable threshold for the similarity measure, they tend to be clustered together. Figure 5.17 shows the hierarchical clustering result. The distance between subjects is 1-r, where r is the correlation between the gene and protein. The top nine cluseters are illustrated in Figure 5.18 and Figure 5.19. Cluster 4 is the largest one with 92 subjects. The details for clustering is shown in Table 5.9. This is very useful to biologists and chemists for further discussion.

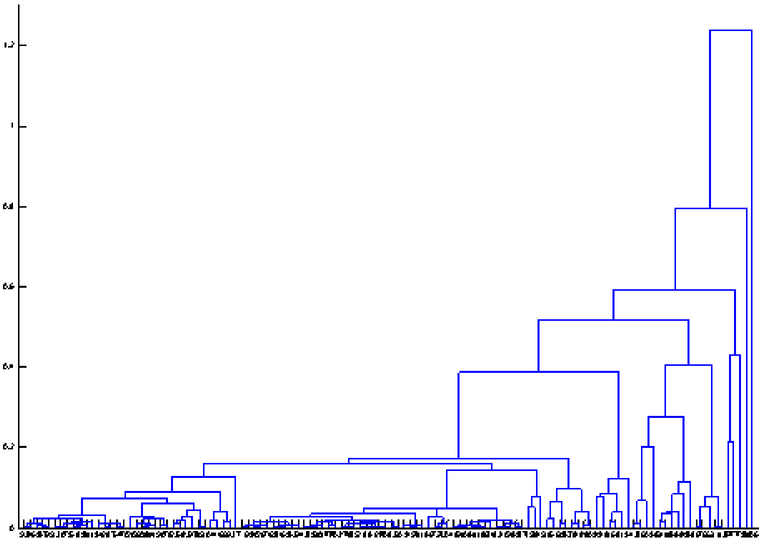

Figure 5.17: Hierarchical clustering. average Link, distance = 1-r.

Cluster No.	Number of protein-gene pairs
1	6
2	4
3	6
4	92
5	5
6	1
7	2
8	1
9	1

Table 5.8: Clustering result.

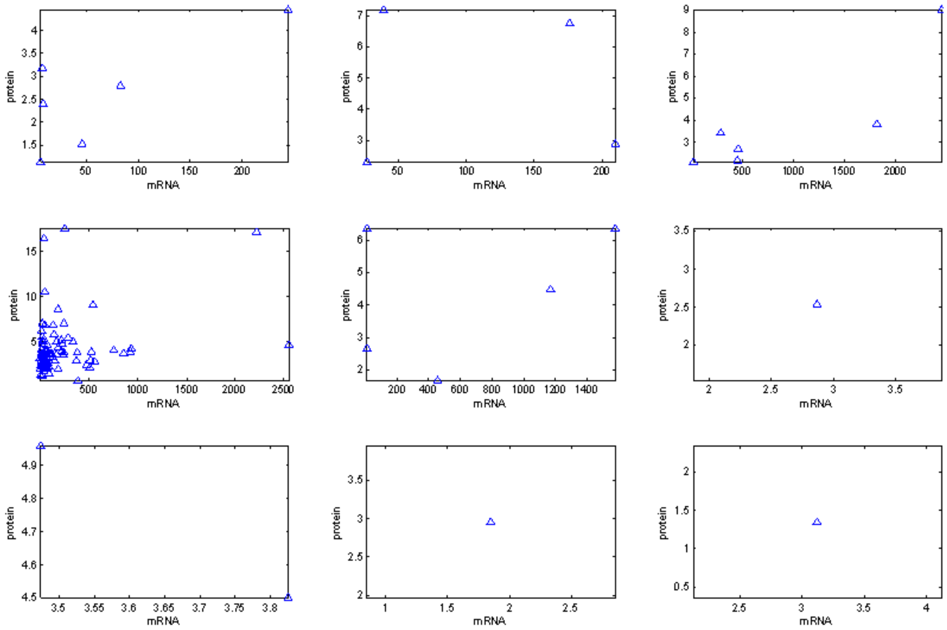

Figure 5.18: Top 9 clusters for hierarchical clustering.

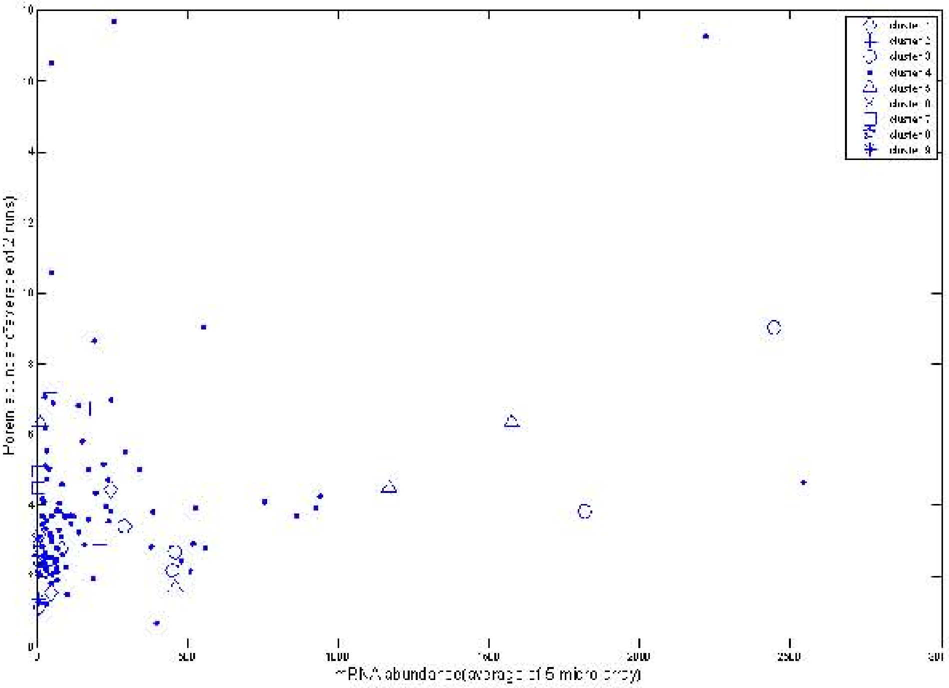

Figure 5.19: Top 9 clusters shown in the plot of mRNA abundance vs. protein abundance.

Cluster	Symbol	Name
1	EEF1G	eukaryotic translation elongation factor 1 gamma
1	GDI2	GDP dissociation inhibitor 2
1	RAB11A	Ras-related protein Rab-11A
1	ARPC3	actin related protein 2/3 complex subunit 3
1	ZNF185	heat shock 90kDa protein 1, beta
1	TUBA6	myosin regulatory light chain MRCL2
2	CA2	carbonic anhydrase II
2	UBE2L3	ubiquitin-conjugating enzyme E2L 3 isoform 1
2	ACTR3	ARP3 actin-related protein 3 homolog
2	OSTF1	ras suppressor protein 1 isoform 1
3	GSTP1	glutathione transferase
3	RGS10	regulator of G-protein signaling 10 isoform a
3	PPBP	pro-platelet basic protein precursor
3	TIMP1	tissue inhibitor of metalloproteinase 1 precursor
3	DNCL1	dynein light chain 1
3	MYL6	thymosin, beta 4
4	ALDOA	aldolase A
4	F13A1	coagulation factor XIII A1 subunit precursor
4	GP1BA	platelet glycoprotein Ib alpha polypeptide precursor
4	GSN	gelsolin isoform a
4	NP	purine nucleoside phosphorylase
4	PGK1	phosphoglycerate kinase 1

Continued on next page

Table 5.9 – continued from previous page

Cluster	Symbol	Name
4	SNCA	alpha-synuclein isoform NACP140
4	TPI1	riosephosphate isomerase 1
4	GPX1	glutathione peroxidase 1 isoform 1
4	FKBP1A	FK506-binding protein 1A
4	ZYX	zyxin
4	SEPT7	cell division cycle 10 isoform 2
4	HSPCA	heat shock 90kDa protein 1, alpha isoform 1
4	ACTB	beta actin
4	ACTN1	actinin, alpha 1
4	ARHGDIB	Rho GDP dissociation inhibitor (GDI) beta
4	CLIC1	chloride intracellular channel 1
4	ENO1	enolase 1
4	FHL1	four and a half LIM domains 1
4	FLNA	filamin 1 (actin-binding protein-280)
4	GDI1	GDP dissociation inhibitor 1
4	HSPB1	heat shock 27kDa protein 1
4	ACTG1	actin, gamma 1 propeptide isoform 4
4	ARF3	ADP-ribosylation factor 3
4	RHOA	ras homolog gene family, member A
4	ENO2	enolase 4
4	EPB49	erythrocyte membrane protein band 49

Continued on next page

Table 5.9 – continued from previous page

Cluster	Symbol	Name
4	FYN	protein-tyrosine kinase fyn isoform a
4	GAPDH	glyceraldehyde-3-phosphate dehydrogenase
4	LDHB	lactate dehydrogenase B
4	MPP1	palmitoylated membrane protein 1
4	MSN	moesin
4	MYH9	myosin, heavy polypeptide 9, non-muscle
4	PF4	platelet factor 4
4	PF4V1	platelet factor 4 variant 1
4	PFDN5	prefoldin 5 isoform alpha
4	PGAM1	phosphoglycerate mutase 1(brain)
4	PKM2	pyruvate kinase 3 isoform 1
4	LEK	pleckstrin
4	PRG1	proteoglycan 1
4	CCL5	small inducible cytokine A5 precursor
4	SH3BGRL	SH3 domain binding glutamic acid-rich
4	SPARC	secreted protein, acidic, cysteine-rich
4	THBS1	thrombospondin 1 precursor
4	TPM4	tropomyosin 4
4	TPT1	tumor protein, translationally-controlled 1
4	VCL	vinculin isoform VCL
4	YWHAH	tyrosine 3/tryptophan 5-monooxygenase

Continued on next page

Table 5.9 – continued from previous page

Cluster	Symbol	Name
4	TAGLN2	tyrosine 3/tryptophan 5 -monooxygenase
4	SNX3	sorting nexin 3 isoform a
4	SNAP23	synaptosomal-associated protein 23
4	ST13	heat shock 70kD protein binding protein
4	ACP1	acid phosphatase 1 isoform c
4	GSTO1	glutathione-S-transferase omega 1
4	PRDX6	peroxiredoxin 6
4	CAPZB	F-actin capping protein beta subunit
4	LIMS1	LIM and senescent cell antigen-like domains 1
4	PCBP2	poly(rC)-binding protein 2 isoform a
4	PFN1	profilin 1
4	CTTN	cortactin isoform a
4	CFL1	cofilin 1 (non-muscle)
4	ARPC1B	actin related protein 2/3 complex subunit 1B
4	TUBA1	tubulin, alpha 1
4	K-ALPHA-1	tubulin, alpha, ubiquitous
4	TUBB4	tubulin, beta4
4	TUBB2	tubulin, beta2
4	MYL9	myosin regulatory light polypeptide 9 isoform a
4	CAPZA2	capping protein muscle Z-line, alpha 2
4	PCBP1	poly(rC) binding protein 1

Continued on next page

Table 5.9 – continued from previous page

Cluster	Symbol	Name
4	TLN1	talin 1
4	CAP1	adenylyl cyclase-associated protein
4	MRCL3	myosin regulatory light chain MRCL3
4	TALDO1	transaldolase 1
4	YWHAE	polypeptide
4	YWHAQ	polypeptide
4	CALM1	calmodulin 1 (phosphorylase kinase, delta)
4	SUMO3	small ubiquitin-like modifier protein 3
4	STXBP2	syntaxin binding protein 2
4	HSPCB	microtubule-associated protein, RP/EB family
4	MAPRE1	osteoclast stimulating factor 1
4	RSU1	coronin, actin binding protein, 1C
4	CORO1C	EH-domain containing 3
4	MYH2	cytochrome c
4	CYCS	PDZ and LIM domain 1 (elfin)
4	PDLIM1	ubiquitin C
4	UBC	smooth muscle and non-muscle myosin alkali
4	TMSB4	X peptidylprolyl isomerase A isoform 1
4	PPIA	coactosin-like 1
4	COTL1	SH3 domain binding glutamic acid-rich
4	SH3BGRL3	tubulin alpha 6

Continued on next page

Table 5.9 – continued from previous page

Cluster	Symbol	Name
4	MRLC2	ras homolog gene family, member C
4	RHOC	tubulin, beta polypeptide
5	NP	G-gamma globin
5	HBA1	alpha 2 globin
5	HBB	beta globin
5	AKR7A2	aldo-keto reductase family 7, member A2
5	HBE1	actinin, alpha 1
6	LDHA	lactate dehydrogenase A
7	TXN	thioredoxin
7	PCMT1	protein-L-isoaspartate (D-aspartate)
8	CAPZA1	F-actin capping protein alpha-1 subunit
9	EHD3	myosin, heavy polypeptide 2, skeletal muscle, adult

Table 5.9: The gene symbols and names in nine clusters.

Chapter 6

Conclusion and Future Work

This thesis has focused on the discovery of genomics and proteomics knowledge by mining bioinformatics literature. In the last few years, there has been a lot of interest within the scientific community to help sort through this ever-growing huge volume of literature and find the information most relevant and useful for specific analysis tasks. We extend and expand the available knowledge and provide new strategy in device data acquisition, biomarker detection, classifier combination and data integration.

6.1 Original contribution to knowledge

This thesis makes the following original contributions to knowledge:

1. A new data acquisition algorithm for proteomic ProteinChip SELDI data.

2. F-random field theory to determine the threshold for the reproducibility test.

3. Majority k-nearest neighbor classification method. It loops over all

possible values for k. Based on the Mahalanobis distance, it takes the majority vote and improved the classic k-NN method.

4. Total variance analysis is a novel method to detect biomarker pattern. In comparison with previous biomarker detection approaches such as stepwise discriminant analysis and the traditional peak detection strategy, we found that the new variance component approach can better distinguish cancer from non-cancer cases with a sensitivity of 86% and a specificity of 96%.

5. Classifier combination to improve the classification result using the new biomarker pattern.

6. Conventional CART and random forest are extended to s-CART and s-RF. The scoring system improves the binary classifiers.

7. Integration of Gene and Protein Data in platelet. A significant correlation is found.

6.2 Future works

In our study, the data set only has two groups, disease and normal. The extension of the analysis to multiple disease categories can be achieved for cross-sectional classification and longitudinal profiling. We can also correlate proteomic markers with other covariates such as age and gender etc.

The limitation of the gene/protein database generation and integration process is that it was done half manually and for one platelet study only. One would have to repeat the entire time- and labor-intensive process for another study. Thus our goal is to establish a customized software module automating this process. For any future gene-protein integration study, the researchers

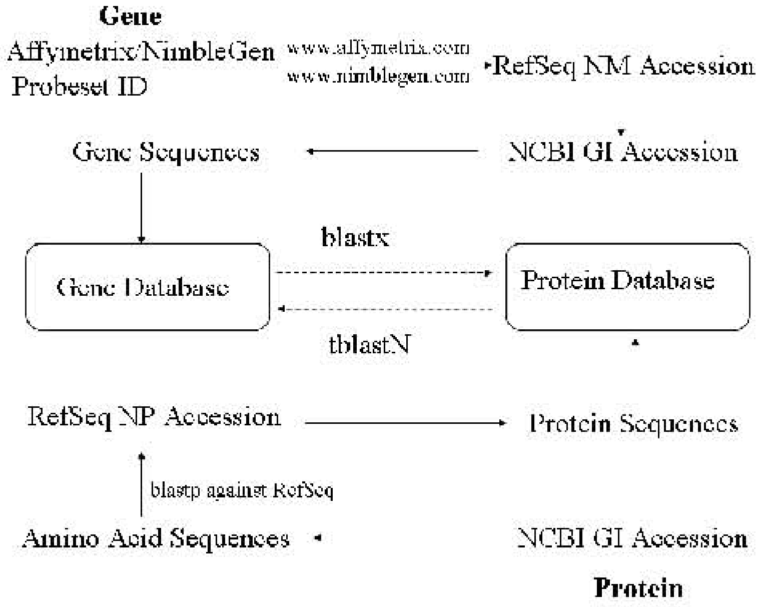

Figure 6.1: Automated gene-protein integration system.

would have the freedom to access the module on-line and integrate their own gene-protein database with ease.

Figure 6.1 illustrated the flow chart of developing a fully automatic web-based integration on matching gene-protein data. It will be done by co-referencing the microarray data and LC-tandem MS (also referred to as LC-MS/MS) data from the same study to the NCBI reference sequence database.

Bibliography

[Adam02] Adam B.L., Qu Y., Davis J.W., Ward M.D., Clements M.A., Cazares L.H., Semmes O.J., Schellhammer P.F., Yasui Y., Feng Z. and Wright G.L. Jr.(2002),*Serum protein fingerprinting coupled with a pattern-matching algorithm distinguishes prostate cancer from benign prostate hyperplasia and healthy men*, Cancer Research, **62**(13), pp 3609-14.

[Adl81] Adler R.J. (1981), The Geometry of Random Fields, John Wiley & Sons, New York.

[Alba04] Alba R, Fei Z, Payton P, Liu Y, Moore SL, Debbie P, Cohn J, D'Ascenzo M, Gordon JS, Rose JKC, Martin G, Tanksley SD, Bouzayen M, Jahn MM and Giovannoni J.(2004), *ESTs, cDNA microarrays, and gene expression profiling: tools for dissecting plant physiology and development*, Plant J., **39**, pp 697-714.

[Alt90] Altschul SF, Gish W, Miller W, Myers EW, Lipman DJ(1990), *Basic local alignment search tool*, J Mol Biol., **215**, pp 403-410.

[Ars91] Arshad, M., and W.T. Frankenberger (1991), Microbial production of plant hormones. Dordrecht, the Netherlands, Kluwer Academic Publishers.

[Banfi06] Banfi C, Brioschi M, Wait R, Begum S, Gianazza E, Fratto P, Polvani G, Vitali E, Parolari A, Mussoni L, Tremoli E(2006), *Proteomic analysis of membrane microdomains derived from both failing and non-failing human hearts*, Proteomics, 2006 Feb 13 [Epub ahead of print].

[Bar04] Barac T, Taghavi S, Borremans B, Provoost A, Oeyen L, Colpaert J, Vangronsveld J, van der Lelie D(2004), *Engineered endophytic bacteria improve phytoremediation of water-soluble volatile organic pollutants*, Nature Biotech., **22**, pp 583-8.

[Bash97] Bashan, Y., and G. Holguin (1997), *Azosprillum-plant relationships: environmental and physiological advances (1990-1996)*, Can. J. Microbiol.,**43**, pp 103-121.

[Bay02] Bay SD, Shrager J, Pohorille A, Langley P.(2002), *Revising regulatory networks: from expression data to linear causal models*, J Biomed Inform. , **Oct-Dec 35**(5-6), pp 289-97.

[Bay04] Bay SD, Chrisman L, Pohorille A, Shrager J.(2004), *Temporal aggregation bias and inference of causal regulatory networks*, J Comput Biol. , **11**(5), pp 971-85.

[Bla] http://www.ncbi.nlm.nih.gov/BLAST/.

[Box64] Box, George E. P.; Cox, D. R. (1964), *An analysis of transformations*, Journal of Royal Statistical Society, Series B 26, pp 211-246.

[Bre84] L. Breiman, J. H. Friedman, R. A. Olshen and C. J. Stone(1984), *Classification and regression trees*, Stanford University.

[Bre01] L. Breiman(2001), *Random forests*, Machine Learning, **45**(1), pp 5-32.

[Bre01a] L. Breiman(2001), *Statistical modeling: the two cultures*, Statistical Science, **16**, pp 199-215.

[Bre96] L. Breiman(1996), *Out-of-bag estimation*, Wadsworth International Group.

[Bre03] L. Breiman(2003), *RF/TOOLS: A Class of Two-eyed Algorithms*, SIAM Workshop, Statistics Department, UC Berkeley.

[CAI] http://www.evolvingcode.net/codon/cai/cais.php.

[Car03] Cartieux F, Thibaud M-C, Zimmerli L, Lesssard P, Sarrobert C, David P, Gerbaud A, Robaglia C, Somerville S, Nussaume L.(2003), *Transcriptome analysis of Arabidopsis colonized by a plant-growth promoting rhizobacterium reveals an general effect on disease resistance*, Plant J. **36**, pp 177-188.

[Cha03] Chang, C.C. and Lin, C.J.(2003). Software package LIBSVM v.2.3 . http://www.csie.ntu.edu.tw/ cjlin/libsvmtools/.

[CST00] Cristianini, N. and Shawe-Taylor, J. (2000), An introduction to Support Vector Machine and other kernel-based methods, Cambridge University Press.

[Cox05] Cox B, Kislinger T, Emili A.(2005), *Integrating gene and protein expression data: pattern analysis and profile mining*, Methods., **35**(3), pp 303-14.

[Di04] Di Bernardo D.(2004), *Modeling genetic networks from expression profiling.* SISSA-ICTP, Computational Systems Biology of the Neuronal Cell, December, pp 6-10, Trieste, Italy.

[DF03] S. Dudoit and J. Fridlyand(2003), *Bagging to improve the accuracy of a clustering procedure*, Bioinformatics, **19**(9), pp 1090-99.

[Die00] T.G. Dietterich(2000), *An Experimental Comparison of Three Methods for Constructing Ensembles of Decision Trees: Bagging, Boosting, and Randomization*, Machine Learning, **40**(2), pp 139-58.

[Fenn89] Fenn JB, Mann M, Meng CK, Wong SF and Whitehouse CM (1989). Science, **246**, pp 64-71.

[Fie00] Fiehn, O., J. Kopka, P. Dormann, T. Altmann, R.N. Trethewey and L. Willmitzer(2000), *Metabolite profiling for plant functional genomics*, Nature Biotech., **18**, pp 1157-1161.

[For02] Forster, J., A.K. Gombert and J. Nielsen(2002), *A functional genomics approach using metabolomics and in silico pathway analysis*, Biotechnology and Bioengineering, **79**, pp 703-712.

[For03] Forster, J., I. Famili, P. Fu, B.O. Palsson and J. Nielsen(2003), *Genome-scale reconstruction of the Saccharomyces cerevisiae metabolic network*, Genome Research, **13**, pp 244-253.

[Fri04] Friberg M, von Rohr P, Gonnet G.(2004), *Limitations of codon adaptation index and other coding DNA-based features for prediction of protein expression in Saccharomyces cerevisiae.*, Yeast. **21**, pp 1083-1093.

[Fun02] Fung, E.T. and Enderwick, C. (2002), *ProteinChip clinical proteomics: computational challenges and solutions*, Biotechnique,. **Suppl:34**(8), pp 40-1.

[Geo02] George E, Glimm J, Li X, Marchese A, Xu Z. A Comparison of Experimental, Theoretical, and Numerical Simulation Rayleigh-Taylor Mixing Rates.(2002), Proc. National Academy of Sci. **99**, pp 2587-2592.

[Gev00] Gevaert, K. and Vandekerckhove, J. (2000), *Protein identification methods in proteomics*, Electrophoresis, **21**(6), pp 1145-54.

[Gna03] Gnatenko DV, Dunn JJ, McCorkle SR, et al.(2003), *Transcript profiling of human platelets using microarray and serial analysis of gene expression*, Blood, **101**(6), pp 2285-93.

[Gna05] Gnatenko DV, Cupit LD, Huang EC, Dhundale A, Perrotta PL, Bahou WF.(2005), *Platelets express steroidogenic 17beta-hydroxysteroid dehydrogenases, Distinct profiles predict the essential thrombocythemic phenotype*, Thromb Haemost., **Aug 94**(2):412-21.

[Gyg99] Gygi SP, Rochon Y, Franza BR, Aebersold R(1999),*Correlation between protein and mRNA abundance in yeast*, Mol Cell Biol., **19**, pp 1720-1730.

[Har04] Hardiman G.(2004), *Microarray platforms - comparisons and contrasts*, Pharmacogenomics, **5**, pp 487-502.

[HL03] B. Lausen and T. Hothorn(2003), *Double-Bagging: Combining Classifiers by Bootstrap Aggregation*, Pattern Recognition, **36**(6), pp 1303-309.

[HLBR04] T. Hothorn, B. Lausen, A. Benner and M. Radespiel-Troger(2004), *Bagging Survival Tree*, Statistics in Medicine, **23**(1), pp 77-91.

[Hol02] Holloway AJ, van Laar RK, Tothill RW, and Bowtell DDL. (2002), *Options available -from start to finish- for obtaining data from DNA microarrays II*, Nature Genetics, **32**, pp 481-489.

[Hut93] Hutchens, T.W. and Yip, T.T. (1993), *New desorption strategies for the mass spectrometric analysis of macromolecules*, Rapid. Commun. Mass Spectrom, **7**, pp 576-580.

[Jan03] Jansen R, Bussemaker HJ, Gerstein M. Revisiting the codon adaptation index from a whole-genome perspective: analyzing the relationship between gene expression and codon occurrence in yeast using a variety of models(2003), Nucleic Acids Res., **31**, pp 2242-2251.

[Joh04] Johann, D.J., McGuigan, M.D., Tomov, S., Fusaro, V.A., Ross, S., Conrads, T.P., Veenstra, T.D., Fishman, D.A., Whiteley, G.R., Petricoin, E.F., and Liotta, L.A.(2004), *Novel approaches to visualization and data mining reveal diagnostic information in the low amplitude region of serum mass spectra from ovarian cancer patients*, Disease Markers, **19**, pp 197-207.

[Joh04a] Johann, D.J., McGuigan, M.D., Patel, A.R., Tomov, S., Ross, S., Conrads, T.P., Veenstra, T.D., Fishman, D.A., Whiteley, G.R., Petricoin, E.F., and Liotta, L.A. Clinical proteomics and biomarker discovery(2004), Annals of the New York Academy of Sciences **1022**, pp 295-306.

[Joo04] Joo J, Ahn H, Lombardo F, Hadjiargyrou M, Zhu W. (2004), *Statistical Approaches in the Analysis of Gene Expression Data Derived from Bone Regeneration Specific cDNA Microarrays*, J. Biopharm. Stat., **14**, pp 607-28.

[Kar88] Karas, M. and Hillenkamp, F. (1988), Anal. Chem., **60**, pp 2299-2301.

[Kell02] Kell, D.B.(2002), *Metabolomics and machine learning: explanatory analysis of complex metabolome data using genetic programming to produce simple, robust rules*, Molecular Biology Reports, **29**, pp 237-241.

[Kur91] Kurland CG (1991), *Codon bias and gene expression.* FEBS Lett. **285**, pp 165-169.

[LS97] Wei-Yin Loh and Yu-Shan Shih(1997), *Split selection methods for classification trees*, Statistica Sinica, **7**, pp 815-40.

[LZR02] Li, J., Zhang, Z., Rosenzweig, J., Wang, Y.Y. and Chan, D.W. (2002), *Proteomics and bioinformatics approaches for identification of serum biomarkers to detect breast cancer*, Clinical Chemistry, **48**(8), pp 1296-1304.

[Mar86] R. Marshall(1986), *Partitioning methods for classification and decision making in medicine*, Statistics in Medicine, **5**, pp 517-526.

[Mer00] Merchant, M. and Weinberger, S.R. (2000), *Recent advancements in surface-enhanced laser desorption/ionization-time of flight-mass spectrometry*, Electrophoresis, **21**, pp 1164-1167.

[Min89] J. Mingers(1989), *An empirical comparison of selection measures for decision-tree induction*, Machine Learning, **3**(4), pp 319-342.

[Per04] Perrotta PL and Bahou WF.(2004), *Proteomics in platelet science*, Curr Hematol Rep., **3**(6), pp 462-9.

[Pet02] Petricoin, E.F. III, Ardekani, A. M., Hitt, B.A, Levine, P.J., Russo, V.A., Steinberg, S. M., Mills, G.B., Simone, C., Fishman, D.A., Kohn, E.C. and Liotta, L.A. (2002), *Use of proteomic patterns in serum to identify ovarian cancer*, Lancet,**359**, pp 572-577.

[Pet02a] Petricoin, E.F. III, Ardekani, A. M., Hitt, B.A, Levine, P.J., Russo, V.A., Steinberg, S. M., Mills, G.B., Simone, C., Fishman, D.A., Kohn, E.C. and Liotta, L.A. (2002), *Proteomic patterns in serum and identification of ovarian cancer*, Lancet,textbf360, pp 169-171.

[Pru05] Pruitt KD, Tatusova T, Maglott DR(2005), *NCBI Reference Sequence (RefSeq): a curated non-redundant sequence database of genomes, transcripts and proteins*, Nucleic Acids Res., **33**(Database issue), pp D501-4.

[Qui86] J. Ross Quinlan(1986), *Induction of decision trees*,Machine Learning, **1**(1), pp 81-106.

[Sand05] Sandhu C., Michael Connor, Thomas Kislinger, Joyce Slingerland, and Andrew Emili(2005), *Global Protein Shotgun Expression Profiling of*

Proliferating MCF-7 Breast Cancer Cells, Journal of Proteome Research, **4**(5), pp 674- 689.

[Sch05] Schad M, Lipton MS, Giavalisco P, Smith RD, Kehr J.(2005), *Evaluation of two-dimensional electrophoresis and liquid chromatography–tandem mass spectrometry for tissue-specific protein profiling of laser-microdissected plant samples*, Electrophoresis, Jul;26(14), pp 2729-38.

[Sha87] Sharp PM, Li WH. (1987), *The codon Adaptation Index–a measure of directional synonymous codon usage bias, and its potential applications*, Nucleic Acids Res. ,**15**(3), pp 1281-95.

[Scha05] Schad M, Lipton MS, Giavalisco P, Smith RD, Kehr J.(2005), *Evaluation of two-dimensional electrophoresis and liquid chromatography–tandem mass spectrometry for tissue-specific protein profiling of laser-microdissected plant samples*, Electrophoresis, Jul;26(14), pp 2729-38.

[Sor03] Sorace, J.M., Zhan, M. (2003), *A data review and re-assessment of ovarian cancer serum proteomic profiling*, BMC Bioinformatics, **4**(1), pp 24.

[Sri02] Srinivas, P. R., Verma, M., Zhao, Y. and Srivastava, S. (2002). *Proteomics for cancer biomarker discovery*, Clinical Chemistry, **48**, pp 1160-1169.

[Tam00] Tamhane, A.C. and Dunlop, D.D. (2000), Statistics and Data Analysis: from elementary to intermediate, Prentice Hall, Upper Saddle River, NJ.

[Tay02] Taylor, J., R.D. King, T. Altmann and O. Fiehn(2002), *Application of metabolomics to plant genotype discrimination using statistics and machine learning*, Bioinformatics, **18**, pp S241-S248.

[Vee04] Veenstra, T.D., Prieto, D.A., Conrads, T.P. (2004), *Proteomic patterns for early cancer detection*, Drug Discovery Today, **9**(20), pp 889-97.

[Ver01] Verma, M., Wright, G.L. Jr., Hanash, S.M., Gopal-Srivastava, R., Srivastava, S.(2001), *Proteomic approaches within the NCI early detection research network for the discovery and identification of cancer biomarkers*, Ann N Y Acad Sci., **945**, pp 103-15.

[Wads04] Wadsworth, J.T., Somers, K.D., Cazares, L.H., Malik, G., Adam, B.L., Stack, B.C. Jr., Wright, G.L. Jr., Semmes, O.J. (2004), *Serum protein profiles to identify head and neck cancer*, Clin Cancer Res, **10**(5), pp 1625-32.

[WAF03] Wu, B,, Abbott, T., Fishman, D., McMurray, W., Mor, G., Stone, K., Ward, D., Williams, K., Zhao, H. (2003), *Comparison of statistical methods for classification of ovarian cancer using mass spectrometry data*, Bioinformatics, **19**(13),pp 1636-43.

[Wang06] Wang X, Zhu W, Pradhan K, Ji C, Ma Y, Semmes OJ, Glimm J, Mitchell J. (2006), *Feature Extraction in the Analysis of Proteomic Mass Spectra*, Proteomics, Apr 6(7), pp 2095-100.

[Woo04] Woo Y, Affourtit J, Daigle S, Viale A, Johnson K, Naggert J, Churchill G. 2004. A comparison of cDNA, oligonucleotide, and

Affymetrix GeneChip gene expression microarray platforms. J. Biomol. Tech. **15**, pp 276-284.

[Wright21] Wright S.(1921), *Correlation and Causation*, Journal of Agricultural Research, **20**, pp 557-585.

[Wu05] Wu G, Culley DE, Zhang W. (2005), *Predicted highly expressed genes in the genomes of Streptomyces coelicolor and Streptomyces avermitilis and the implications for their metabolism*, Microbiology, **Jul**151(Pt 7), pp 2175-87.

[Yasui03] Yasui, Y., Pepe, M., Thompson, M.L., Adam, B.L., Wright, G. L. Jr., Qu, Y., Potter, J. D. , Winget, M., Thornquist, M. and Feng, Z.(2003), *A data-analytic strategy for protein biomarker discovery: profiling of high-dimensional proteomic data for cancer detection*, Biostatistics, **4**, pp 449-463.

[Yasui03] Yasui, Y., McLerran, D., Adam, B.L., Winget, M., Thornquist, M. and Feng, Z. (2003), Journal of Biomedicing and Biotechnology, **4**, pp 242C248.

[Zhu03] Zhu, W., Wang, X., Ma, Y., Rao, M., Glimm J. and Kovach, J.S. (2003), *Detection of cancer-specific markers amid massive mass spectral data*, Proceedings of National Academy of Science, **100**(25), pp 14666-14671.

[Zhu05] Zhu, W., Zhang, Y., Neophytou, N., Pradhan, K., Chen, J., Wu, M., Xu, B. (2005), proteoExplorer - Interactive Analysis of Mass

Spectrometry-based Proteomics. Copyright application through the State University of New York.

[Zhu05a] Zhu, W., Zhang, Y., Neophytou, N., Pradhan, K., Chen, J., Wu, M., Xu, B. (2005), ViStaMSTM - Software for Gene Microarray and SAGE Analysis. Copyright application through the State University of New York.

Appendix A

User Manual of proteoExplorer

Preface

proteoExplorer$^{\text{TM}}$ is a customized software for the analysis and visualization of large-scale proteomic mass spectrum datasets. The combination of modern mathematical/statistical methodologies and advanced computer graphical technologies provides the user with a novel environment for an informative and enjoyable data-mining experience. This user manual is prepared for both the experienced data analysts as well as novice. Detailed data examples and screenshots are provided for each functionality. In particular, a flow-chart of routine analysis and visualization procedures is provided to guide new users. Behind this demo version, the software is still under development to add more functionalities, to implement the latest-developed algorithms, and to be more robust and user-friendly. We thank the State University of New York at Stony Brook for sponsoring the development of proteoExplorer.

A.1 Introduction

Structure of **proteoExplorer$^{\text{TM}}$**

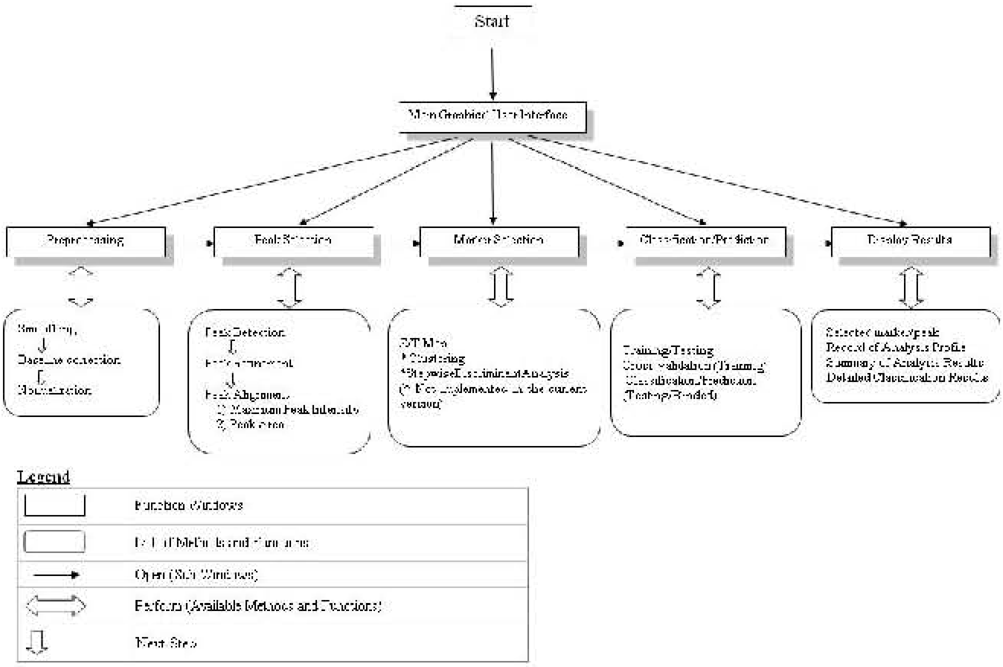
Start
Main Graphical User Interface
Preprocessing
Peak Selection
Marker Selection
Classification/Prediction
Display Results
Smoothing
Baseline correction
Normalization
Peak Detection
Peak Enhancement
Peak Alignment
1) Maximum Peak Intensity
2) Peak Area
SVT Map
* Clustering
*Stepwise Discriminant Analysis
(* Not implemented in the current version)
Training/Testing
Cross Validation (Training/
Classification/Prediction
(Testing/Render))
Selected marker/peak
Record of Analysis Profile
Summary of Analysis Results
Detailed Classification Results
Legend
Function Windows
List of Methods and Functions
Open (Sub Windows)
Perform (Available Methods and Functions)
Next Step

Analysis Procedure

Step 1. Data Quality Control by Visualization

Use the visualization tool provided by the software to easily monitor the mass spectrum individually, by group, among repeated measures or by any other experimental factors. A simple function, taking the average of multiple files or an entire directory, is also implemented in this step both for visualization and for creating the desired average spectrum (for example, group average). In this step, the user can (1) detect any abnormal-looking mass spectra /outliers; (2) check reproducibility of repeated measures; (3) compare group average spectra (e.g. the diseased group versus the control group); (4) examine whether any processing steps such as baseline correction has been performed.

Step 2. Data Processing

Data Processing usually goes in the order of smoothing, baseline correction and normalization. In all cases, smoothing is necessary as the first processing step to filter out noise. Depending on whether baseline has been correction during the generation of the mass spectrum, which is implied by the absence of negative intensity values in mass spectrum, baseline correction is an optional processing step. Normalization should be performed on smoothed and baseline corrected mass spectrum and also is necessary for all cases.

Use the Analysis ⟶ Preprocessing Window to (1) tune parameters for each processing step by visualizing the effects of different parameters; (2) save selected parameters into a profile; (3) apply the saved profile to datasets to be analyzed and run the preprocessing batches automatically.

Step 3. Select Biomarker Type

The user can choose and generate two types of biomarkers for the ensuing classification and prediction: Maximum Peak Intensity and Peak Area.

For the choice of Maximum Peak Intensity, one needs to generate the corresponding peak data using three sequential steps: peak identification, peak refinement and peak alignment. The newly generated peak data will have two measurements: peak center and maximum peak intensity (or peak area). In detail, the steps of peak data generation implemented in proteoExplorer$^{\text{TM}}$include:

(1) Peak detection: Detect all possible peaks by local maximums;

(2) Peak refinement: Refine peaks above the local noise level;

(3) Peak alignment and generation: Align refined peaks across all spectra in the data sets to be analyzed, and calculate the corresponding biomarker value - maximal peak intensity.

If Peak Area is chosen, in addition to repeat all the steps for Maximum Peak Intensity, one needs to select the area width in peak alignment and generation.

This step is performed using the Analysis ⟶ Biomarker Detection Window.

Step 4. Classification/Prediction Analysis

Once the biomarkers are determined and/or generated from Step 3, one can perform the ensuing classification and prediction analysis on the given training/testing data sets. This is done with the Analysis ⟶ Classification/Prediction Window.

Methods for choosing significant biomarkers include:

(1) Z/T test

(2) Total variance test

(3) Scoring system

(4) Clustering

(5) Stepwise Discriminant Analysis

Depending on the necessity, select all or part of the above methods to trim the biomarker pattern. The final model is applied to the classification based on the training data sets and the subsequent prediction on the testing/blinded dataset. For the current test version, only option (1) is provided for simplicity.

The proteoExplorer$^{\text{TM}}$software implemented the following 7 classifiers and each classifier will provide both binary classification outputs (e.g. 0 for control and 1 for diseased) as well as scores indicating the disease-risk probabilities for all testing samples.

The proteoExplorer$^{\text{TM}}$includes classifiers as following:

(1) Marjority K-Nearest Neighbor (MKNN)

(2) Linear Discriminant Analysis (LDA)

(3) Logistic Regression (LOGIT)

(4) Generalized Regression Neural Network (GRNN)

(5) Multiple Layer Perceptron Neural Network (MLPNN)

(6) Support Vector Machine (SVM)

(7) Spherical Support Vector Machine (SSVM)

(8) Classification and Regression Tree (CART)

Our experience indicated that no single classifier is dominantly superior to the others in protein proteomic data analysis. The performance of classifiers depends to a large degree on the characteristics of the specific datasets. This motivated us to combine the decisions from all classifiers for a unanimous and more robust decision. Several approaches have been developed by our team. In this test version, we have included the mean score approach to yield the combined decision across all classifiers. In the output HTML file, you will see the combined decision labeled as Averaged in the summary table of the training data, and Combined for the prediction of the status of each subject in the testing/blinded data set.

Step 5. Reading the Analysis Output

The final analysis output is in an html format for user's review. It can be opened by clicking on Analysis ⟶ Display Classification/Prediction Results. There are four parts in the output.

(1) Analysis Profile;

(2) Summary of cross-validation Results based on the Training data;

(3) Classification Results on the Testing/Blinded Set;

(4) Biomarker Pattern C significant biomarkers used for the classification/prediction.

Step 6. Visualize Biomarker Pattern

Finally, the user can visually examine the set significant biomarkers used in the above classification/prediction analysis by clicking on Analysis ⟶ Read Latest Biomarker Pattern. Please note that you must open up some mass spectra in the main window first. The biomarker pattern used in the latest classification/prediction analysis will then be superimposed (in red vertical lines) to the opened spectrum (spectra).

A.2 Visualization

A.2.1 Overview

Start the software by running "proteoExplorer.bat". The following is a screen shot of the main Graphical User Interface with one spectrum loaded:

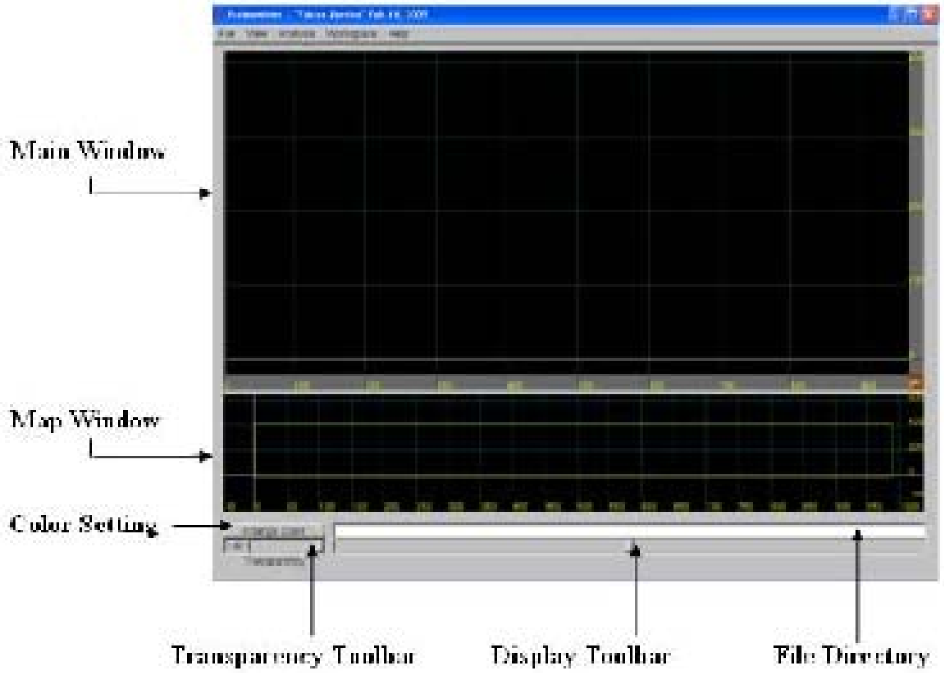

The Main Window displays one single spectrum or multiple spectra. In the Main Window, you can set up a target region and zoom in by clicking the right mouse button, click the left mouse button to enlarge/move it and the right mouse to shrink it. You may also click and drag the left mouse button on the grey axes area to enlarge or shrink the spectrum.

In the Map Window which is linked to the Main Window, the user can set (use the right mouse button), resize and move (use the left mouse button) the yellow rectangular selection bar along the horizontal and vertical axes to reveal details of the selected region in the Main Window.

The File Directory contains the directory of the file(s) opened.

The Display Toolbar (clicking or dragging by the left mouse button) allows the user to look at each spectrum when multiple spectra are displayed.

The Color Setting allows the user to change the color of a spectrum, click Change Color and choose the desired color in the color panel.

The Transparency Toolbar is for the multiple spectra display, the transparency is defined from 0 to 1.

A.2.2 Loading files

Open Single/Multiple File(s)

To open a single spectrum, go to File → Read Files, locate the directory, choose the spectrum and click OK.

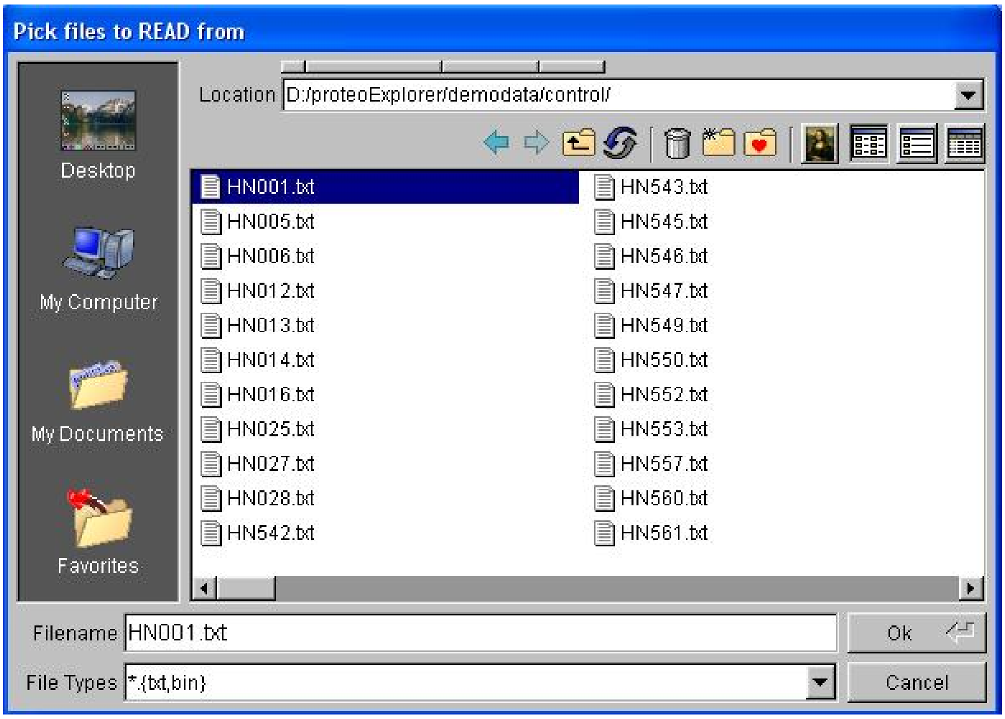

Pick files to READ from

Location D:/proteoExplorer/demodata/control/

HN001.txt
HN005.txt
HN006.txt
HN012.txt
HN013.txt
HN014.txt
HN016.txt
HN025.txt
HN027.txt
HN028.txt
HN542.txt
HN543.txt
HN545.txt
HN546.txt
HN547.txt
HN549.txt
HN550.txt
HN552.txt
HN553.txt
HN557.txt
HN560.txt
HN561.txt

Filename HN001.txt

File Types *.{txt,bin}

To open multiple spectra, press down the 'Ctrl' button in the keyboard when choosing the spectra.

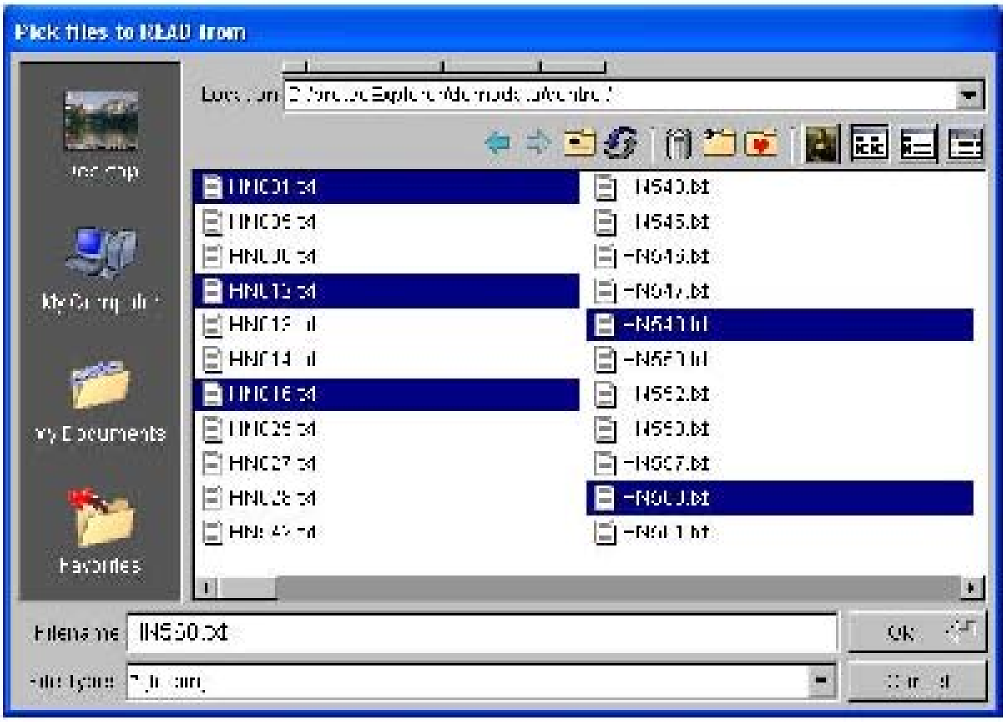

Filename: IN550.txt

Select the color in the color panel, the default color is yellow.

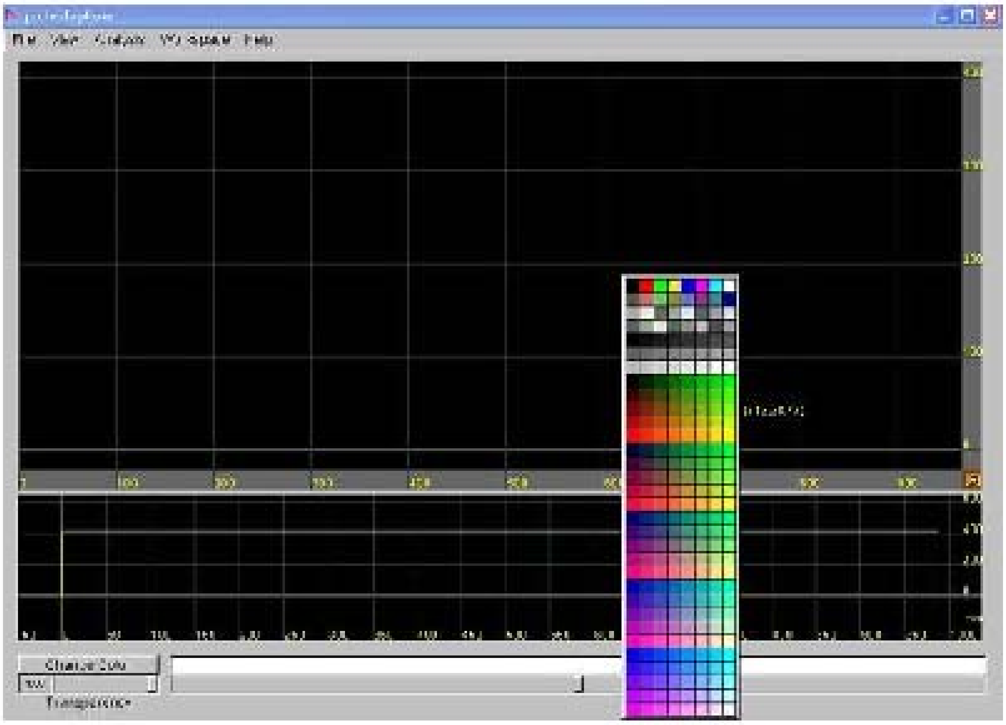

The spectrum is shown in both the Main Window and the Map Window.

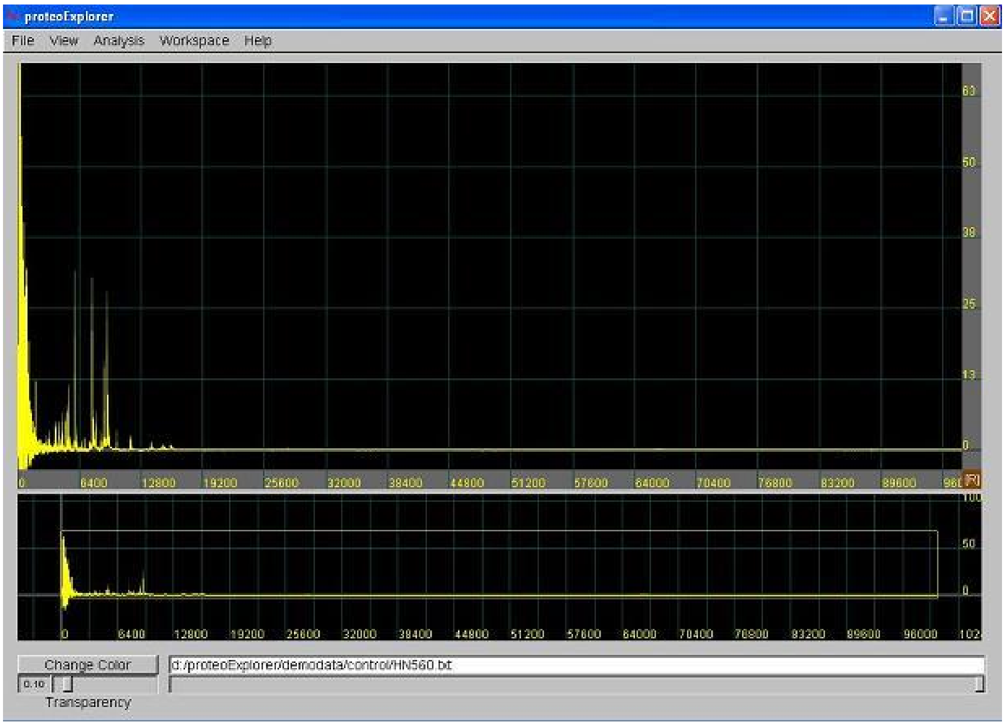

d:/proteoExplorer/demodata/control/HN560.txt

Open an Entire Directory

To display all spectra in the same directory, click File → Read Files, locate the directory and 'Ctrl' + 'A' in the keyboard. All files in the directory will be chosen and opened.

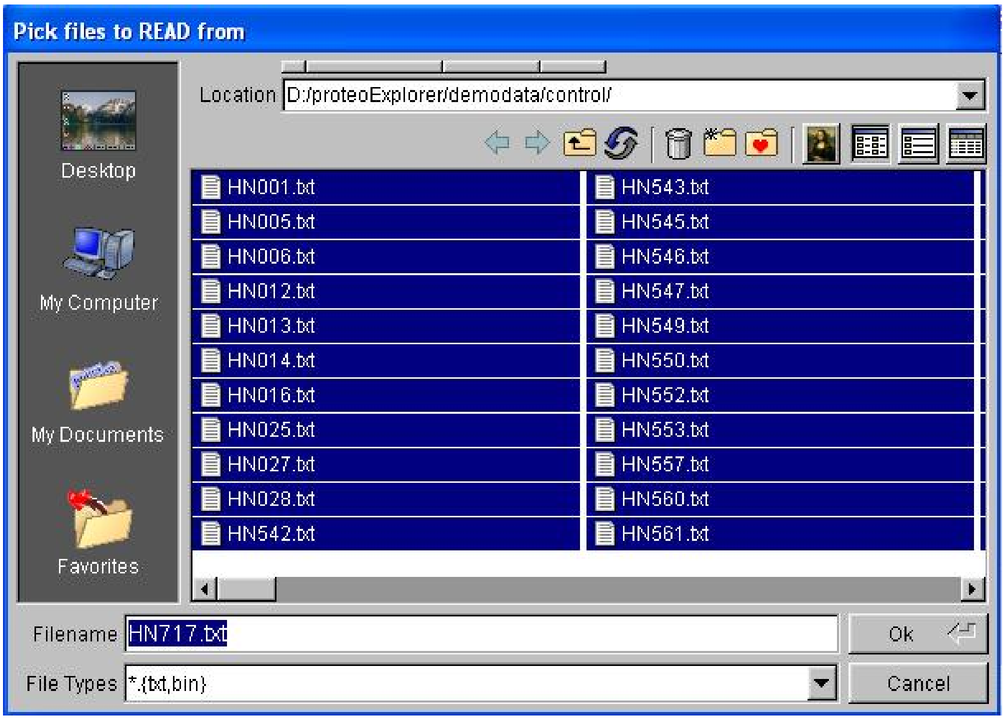

Pick files to READ from

Location D:/proteoExplorer/demodata/control/

HN001.txt
HN005.txt
HN006.txt
HN012.txt
HN013.txt
HN014.txt
HN016.txt
HN025.txt
HN027.txt
HN028.txt
HN542.txt
HN543.txt
HN545.txt
HN546.txt
HN547.txt
HN549.txt
HN550.txt
HN552.txt
HN553.txt
HN557.txt
HN560.txt
HN561.txt

Filename HN717.txt

File Types *.{txt,bin}

The program will promote you to select color for all spectra to be opened. They will be in the same color but you can change the color of any individual spectrum later on by selecting that particular spectrum using the Display Toolbar and then clicking the Change Color to reset its color.

Move the Display Toolbar below the Map Window to see each single spectrum. The location of each spectrum can bee seen in the File Directory.

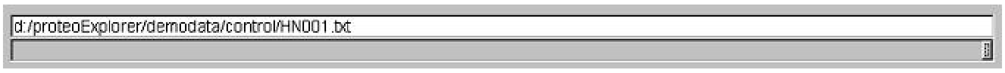

d:/proteoExplorer/demodata/control/HN001.txt

Alternatively, you can hold the "Ctrl" button in the keyboard and click the left mouse to choose the desired spectrum.

A.2.3 Average files

Display and Output Average Spectrum of Multiple Files

Choose File → Average Files, the average of all selected spectra will be calculated and displayed in the Main Window. To take the average of all spectra in a directory, choose the target directory and press 'Ctrl' + 'A' in the keyboard. The File Directory will display that this spectrum is an average.

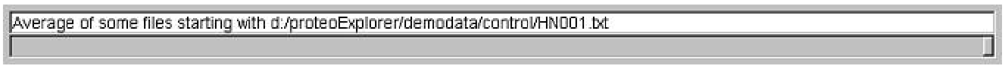

Average of some files starting with d:/proteoExplorer/demodata/control/HN001.txt

Select File → Save Spec to save this average file.

A.2.4 Display features

Zoom In/Out

Left click to zoom in, right click to zoom out. To select a target region in Main Window or Map Window, right click the mouse, hold it and drag the yellow rectangular box to zoom in.

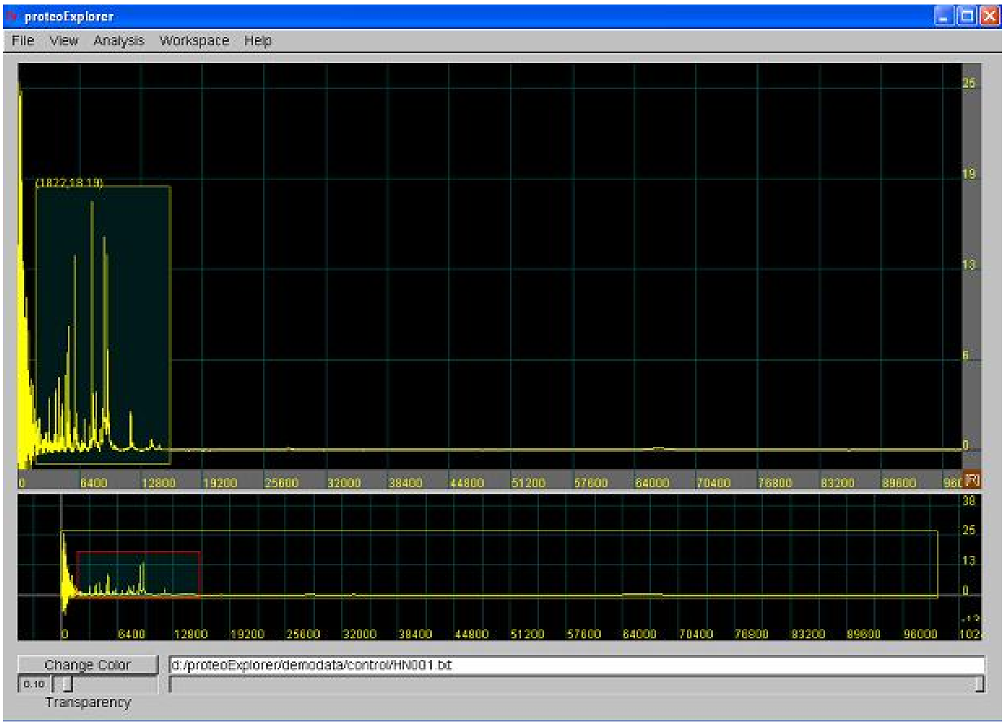

d:/proteoExplorer/demodata/control/HN001.txt

The target region is resizable in the Map Window by clicking and dragging its edges using the left mouse button. To zoom out, simply right click mouse continuously or click [R] button in the right down corner of the Main Window. (The[R] button is also available in the Preprocessing sub-window and Biomarker Detection sub-window.)

Move Spectrum

By moving the rectangular bar in the Map Window horizontally, the view of mass spectrum in the Main Window will move simultaneously as well.

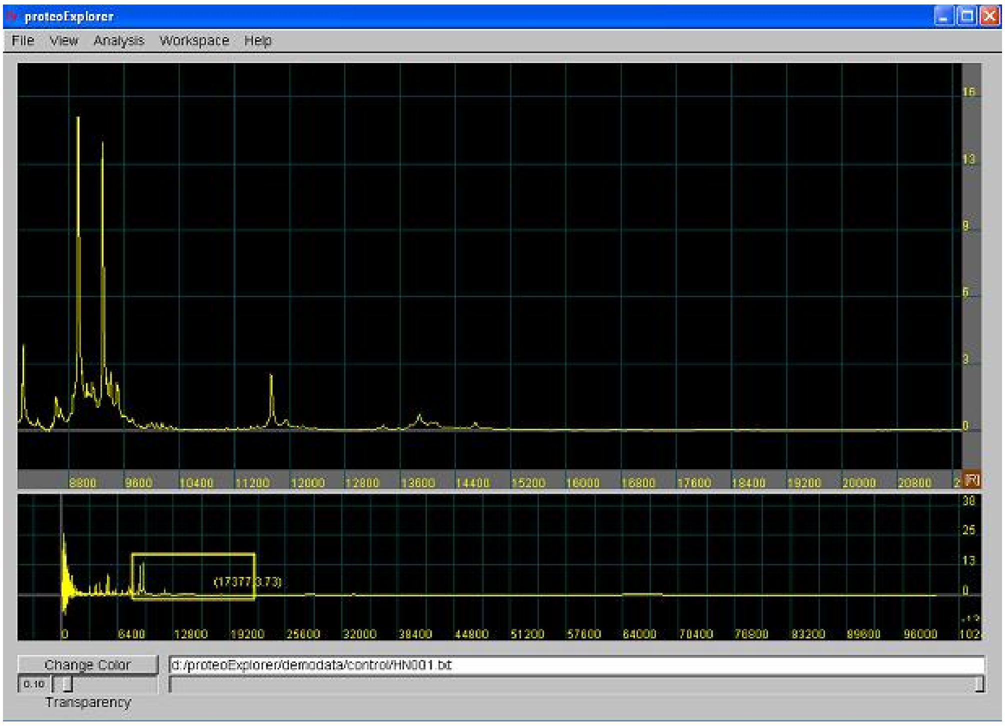

d:/proteoExplorer/demodata/control/HN001.txt

Bring a Specific Spectrum to the front of Multiple Spectra

While holding 'Ctrl' in your keyboard, left click the target spectrum will bring it to the front among the multiple spectra on display.

Change Color

The spectrum is displayed in white by default. The color can be changed by clicking Change Color and choosing the color in the color panel.

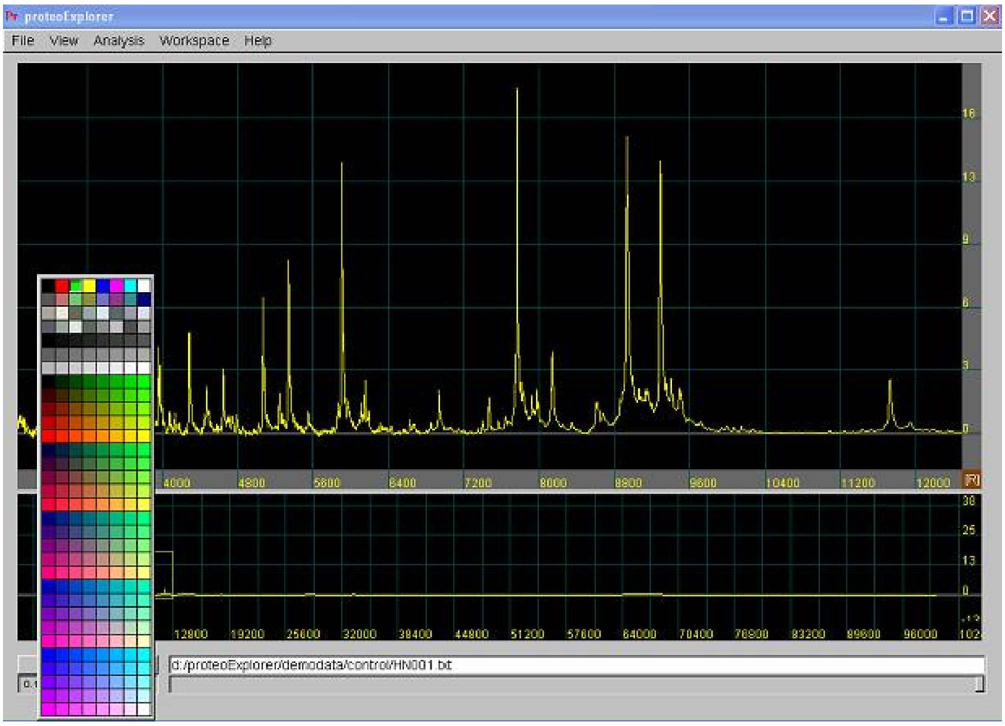

d:/proteoExplorer/demodata/control/HN001.txt

The color of the spectrum will change from yellow to green.

A.2.5 Display options

Single/Multiple - Spectrum Display

View → Multi Spec: Check this option to display multiple spectra in the same time. The following example has three spectra on display. They are colored green, yellow and red for distinction.

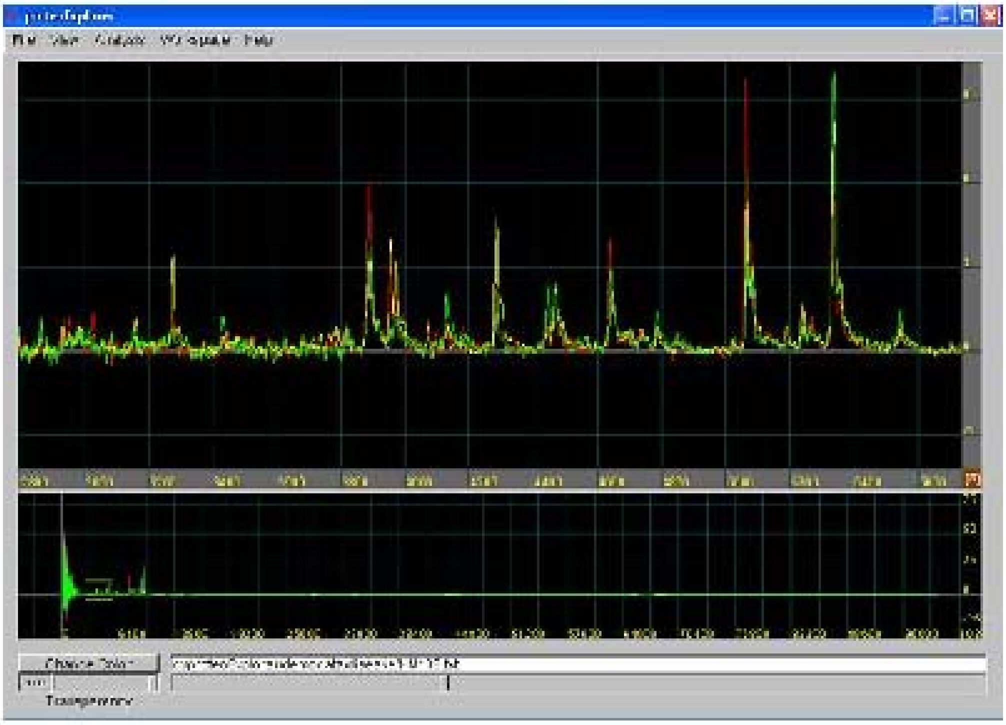

The transparency can be tuned from 0 to 1 using the Transparency Toolbar. The transparency is 1 in the plot above, which means all three spectra are shown with the same maximum clarity.

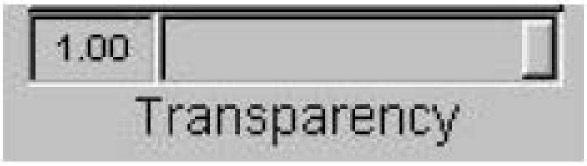

1.00

Transparency

By tuning the Display Toolbar, one can select a particular spectrum of interest. In the following example, the green spectrum is the chosen spectrum and its file name appears in the File Directory. By tuning the transparency down to 0.2, the other unselected spectra (red and yellow) will fade away as seen in the screen shot below.

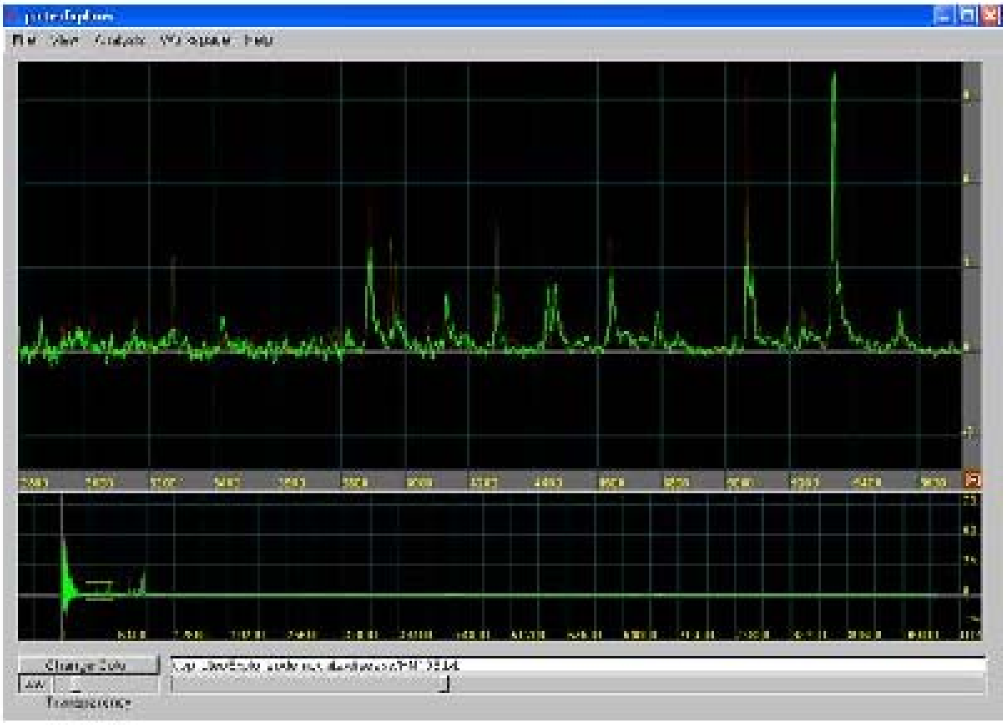

Change Display Order of Opened Spectra

View → Reverse Display Order: Change the display order. In the previous example, three spectra are opened and the colors are set in the order of green, yellow and red. Thus the green one is always shown on top.

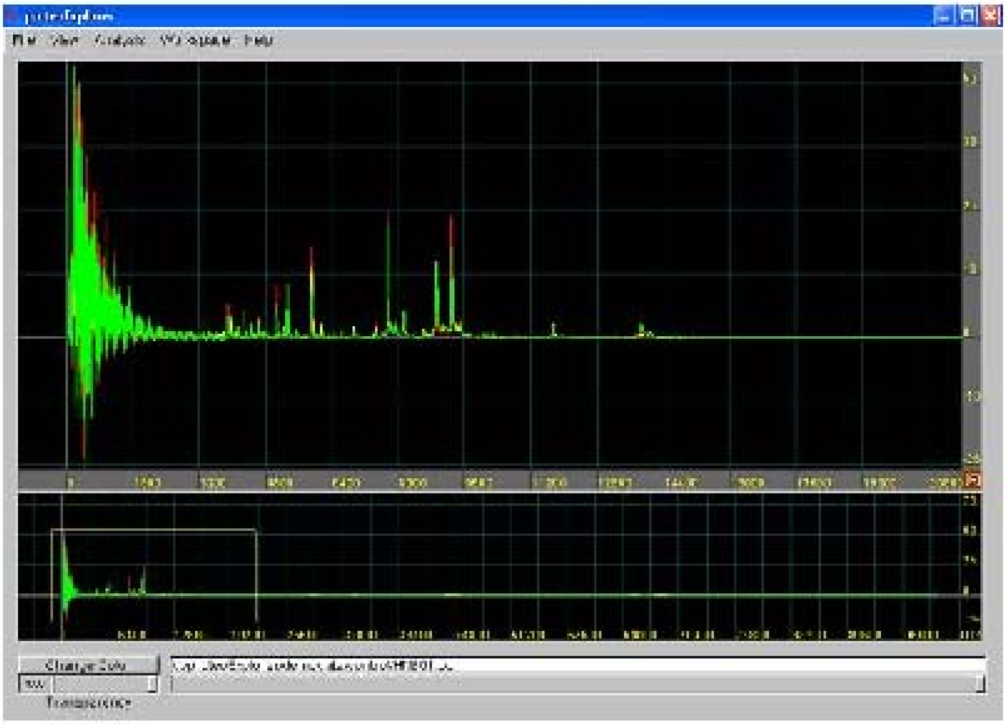

Checking the Reverse Display Order will reverse the display order, which means, the red spectrum will be on top and the green one will be on the bottom.

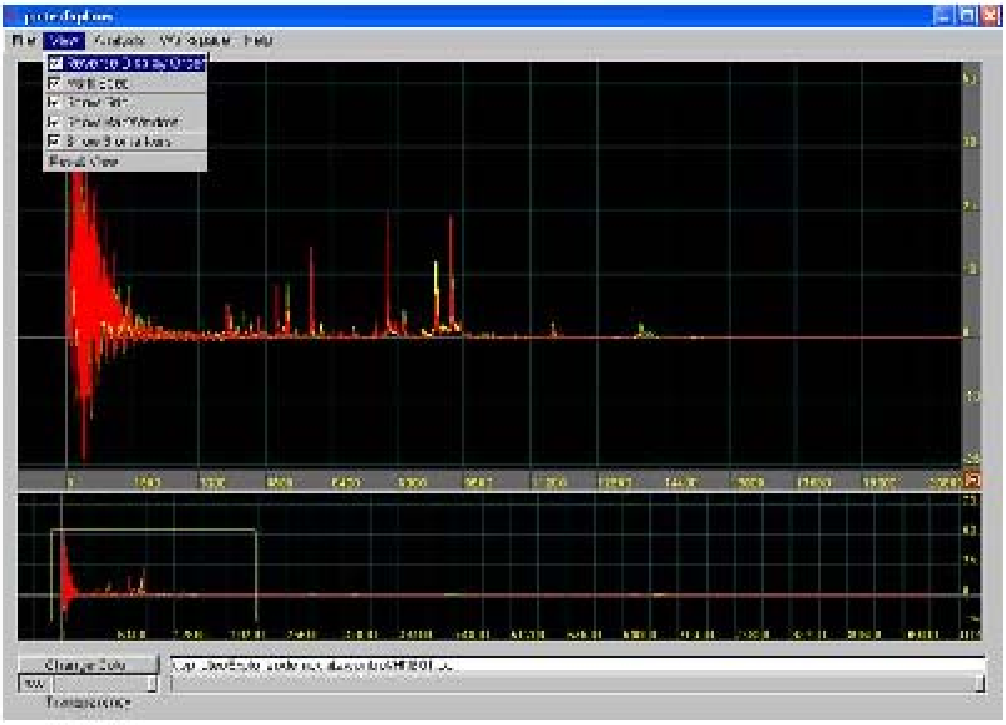

Hide/Show Grid

View → Show Grid: If uncheck this option, the grid will disappear.

Hide/Show Map Window

View → Show Map Window: The user may choose to show the Map Window or not.

Reset View

View → Reset View: Reset View will set the spectra on display to the their original scale.

A.2.6 Reset and start over

File → Unload Spectrum: Release one selected spectrum.

File → Reset: Release all spectra and back to the status when you open the software (with no spectrum on display).

A.2.7 Workspace

Save all the spectra opened in the Main Window and the display options such as zoom, color and the transparency. By loading the workspace, it is convenient to recover the display options without setting them again. The workspace is in xml format.

A.3 Data analysis

A.3.1 Data preprocessing

To perform preprocessing, click on Analysis → Preprocessing in the manual bar of main GUI to open the Preprocessing sub-window. The Preprocessing sub-window has two parts, the top portion is for spectra visualization and the bottom portion for preprocessing parameter selection. Preprocessing consists of three sequential steps: smoothing, baseline correction and normalization. In all cases, smoothing is a required first processing step to filter out noise. Depending on whether baseline has been corrected during the generation of the mass spectrum or not, which is indicated by the absence or presence of negative intensity values in the mass spectrum, baseline correction is an optional step. Normalization should be performed on smoothed and baseline corrected mass spectrum and is also necessary for all cases.

Use the **Preprocessing Window** to (1) Open a single mass spectrum and tune the parameters for each processing step by visualizing the effects of different parameter settings on the given spectrum; (2) Save selected parameters into a profile for the subsequent batch processing; (3) Choose the dataset/folder one wish to format using the selected parameter setting; (4) Apply the saved preprocessing parameter profile to the chosen dataset/folder and format the entire dataset/folder using the given parameter setting automatically.

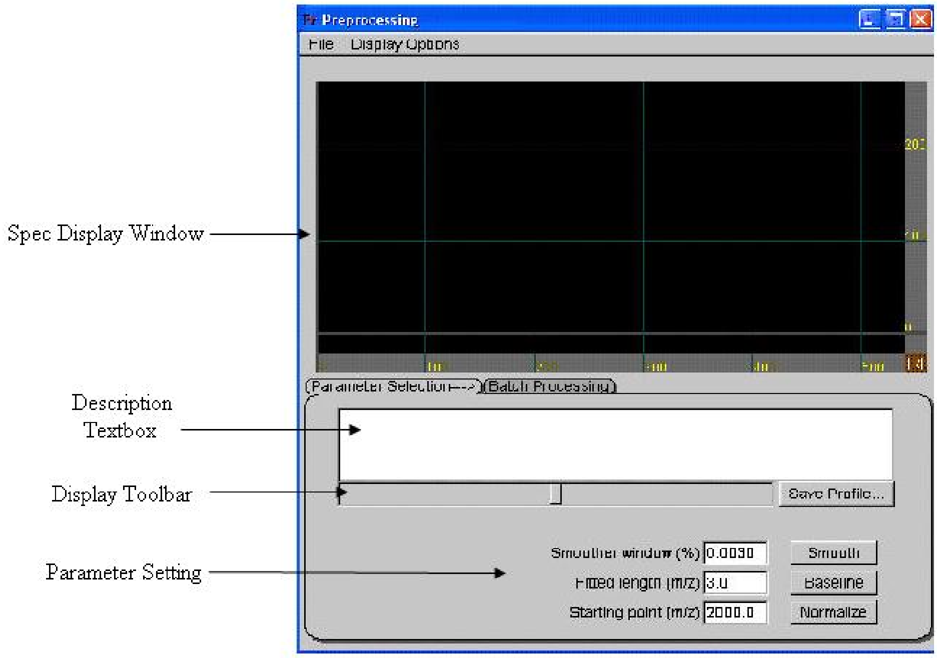

Smoother window (%) 0.0030
Fitted length (m/z) 3.0
Starting point (m/z) 2000.0

For the above 4 steps, the parameter setting steps (1 & 2) are done using the **Parameter Selection** sub-page; and the batch processing steps (3 & 4) are done with the **Batch Processing** sub-page. Details are given below. First, we introduce the layout of the **Preprocessing Window**.

Display a single spectrum

File → Open Last Selected: the selected spectrum is highlighted when multiple spectra are displayed in the Main Window, display that highlighted spectrum in the Preprocessing Window.

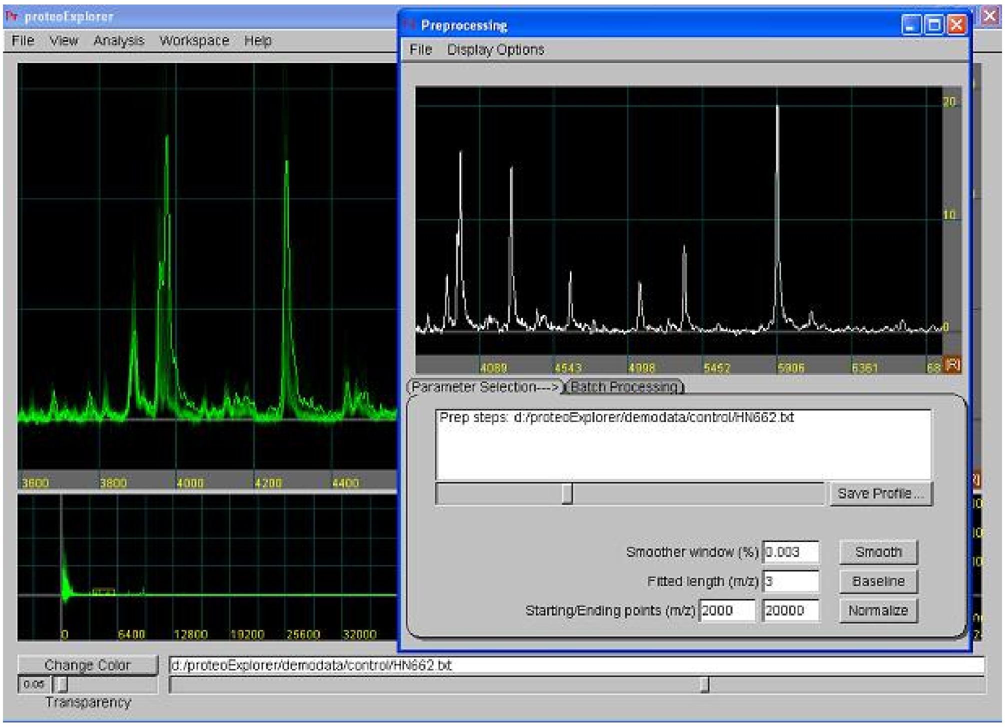

Prep steps: d:/proteoExplorer/demodata/control/HN662.txt

Smoother window (%) 0.003

Fitted length (m/z) 3

Starting/Ending points (m/z) 2000 20000

0.05

d:/proteoExplorer/demodata/control/HN662.txt

File → Open New Spectrum: open a spectrum from the directory dialog directly.

Display Options → Show All: show all spectra at each preprocessing step. The current preprocessed spectrum is highlighted. In the following example, one spectrum is smoothed with the parameter 0.003% and baseline corrected with the parameter 3. The three spectra: raw, smoothed and smoothed baseline corrected, are displayed simultaneously in the visualization window. One can tune the Display Toolbar to highlight the desired spectrum.

The raw spectrum:

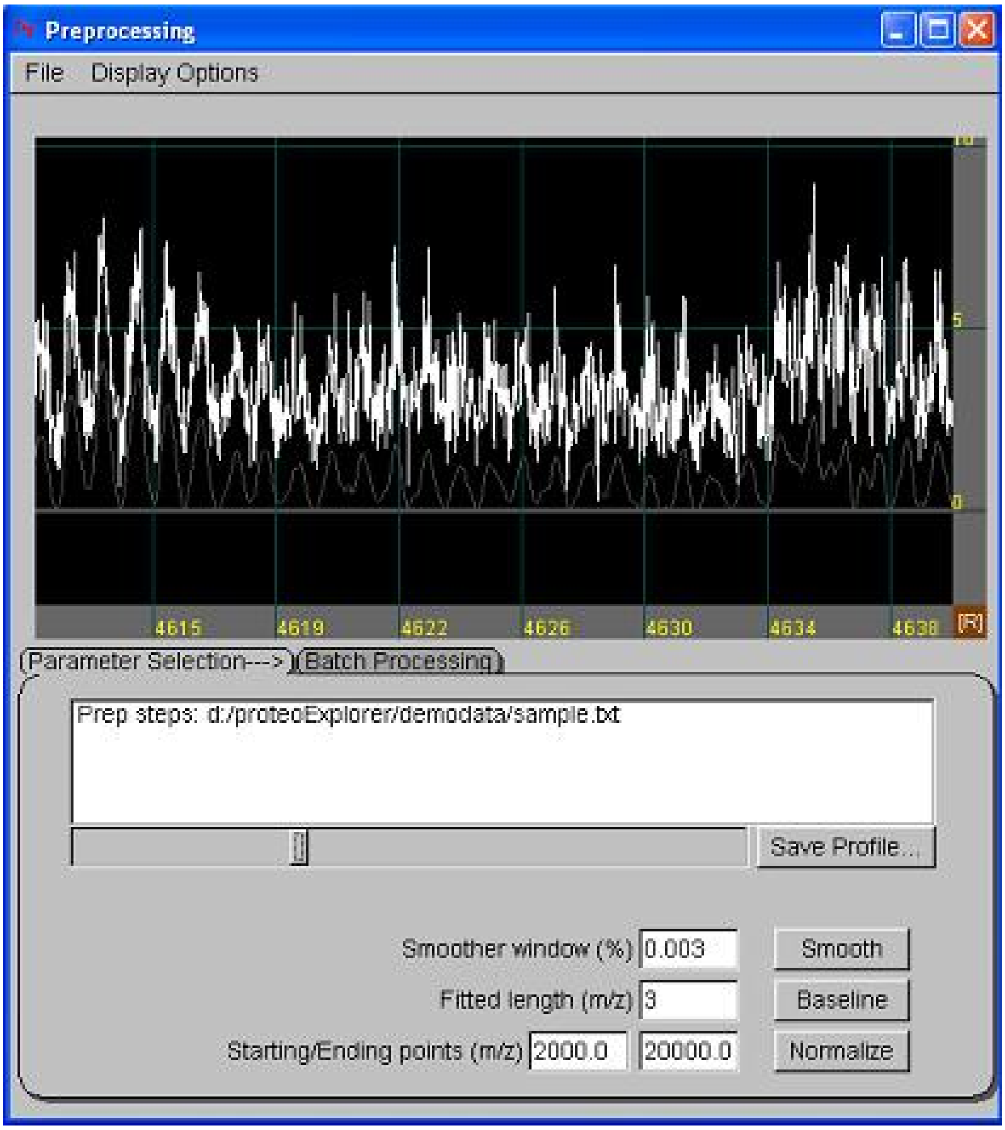

Prep steps: d:/proteoExplorer/demodata/sample.txt

Smoother window (%) 0.003

Fitted length (m/z) 3

Starting/Ending points (m/z) 2000.0 20000.0

The smoothed spectrum:

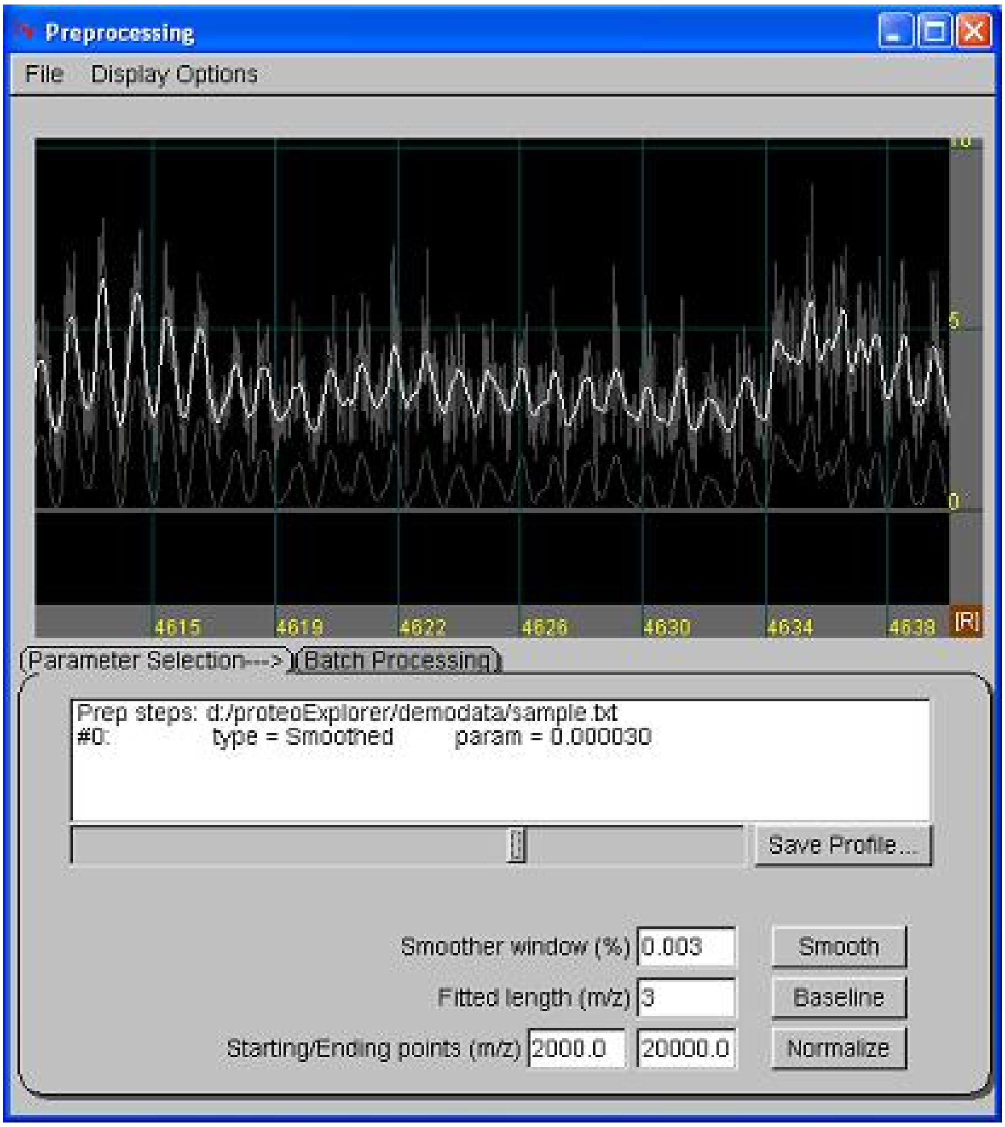

Prep steps: d:/proteoExplorer/democlata/sample.txt
#0: type = Smoothed param = 0.000030

Smoother window (%) 0.003

Fitted length (m/z) 3

Starting/Ending points (m/z) 2000.0 20000.0

The smoothed and baseline corrected spectrum:

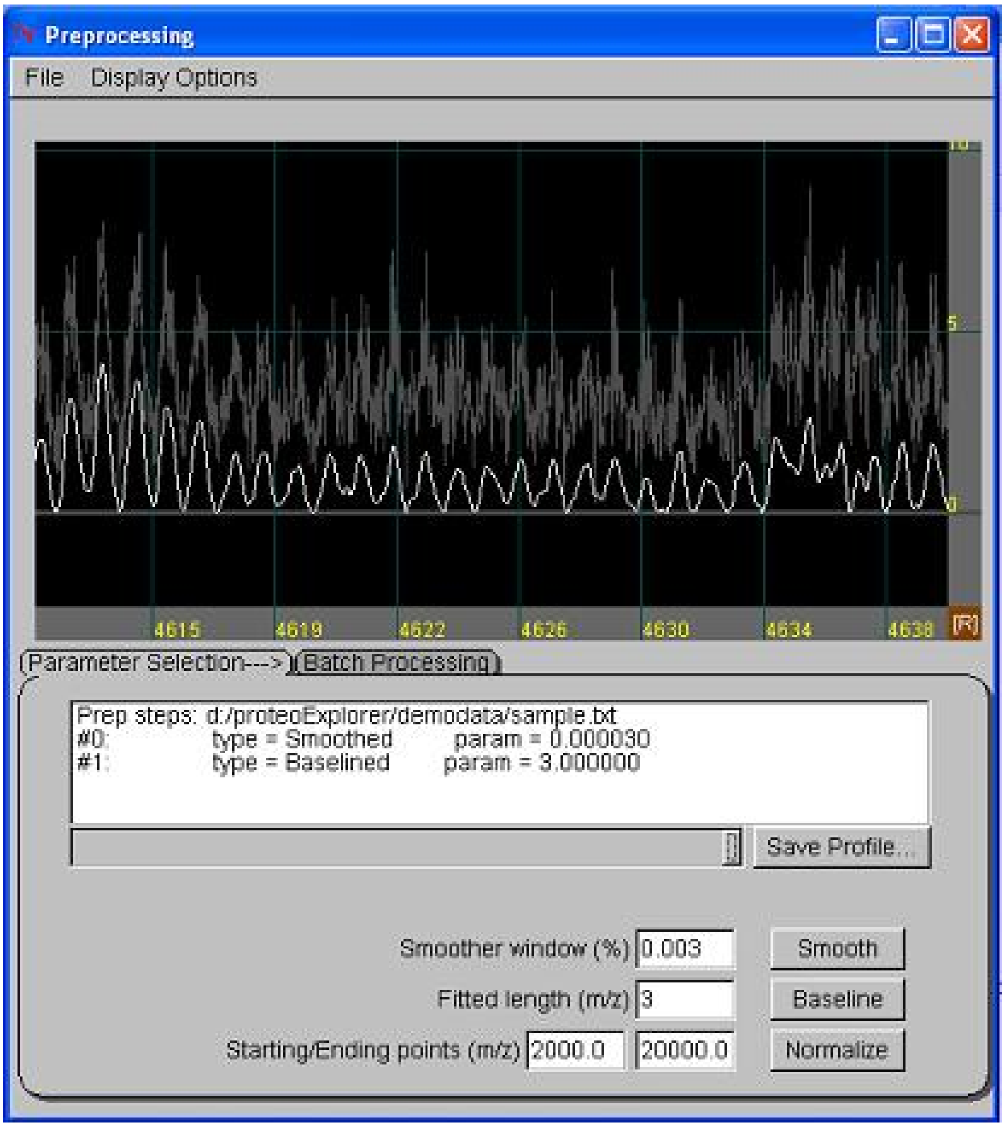

```
Prep steps: d:/proteoExplorer/demodata/sample.txt
#0:            type = Smoothed        param = 0.000030
#1:            type = Baselined       param = 3.000000
```

Smoother window (%) 0.003

Fitted length (m/z) 3

Starting/Ending points (m/z) 2000.0 20000.0

The preprocessed spectra with different parameters can also be displayed simultaneously. By comparing those spectra, you can determine the best parameter profile.

Parameter Selection Page

Description Textbox: identify the spectrum, the preprocessing steps and the parameters.

Display Toolbar: select the target spectrum. It is highlighted and its location will be displayed in the Description Textbox.

Parameter Setting:

Smoothing: input the percentage of all data points. It determines the width of the Gaussian Smoother Window at each m/z.

Baseline Correction: input the Fitted Length for the convex hull algorithm to fit the baseline.

Normalization: given the Starting/Ending Points of the m/z range, each spectrum is divided by the average intensity of its range. If the Starting Point is zero and the Ending Point is larger than the maximum m/z, use all data points in the entire range to take the average. The default value is 2,000/20,000, which means we use data points with $2,000 < m/z < 20,000$ only.

Save Profile...: the preprocessing parameters in the Description Textbox will be saved in a .prp file. The file will be used later in the Batch Processing Page to preprocess an entire dataset/folder.

Batch Processing Page

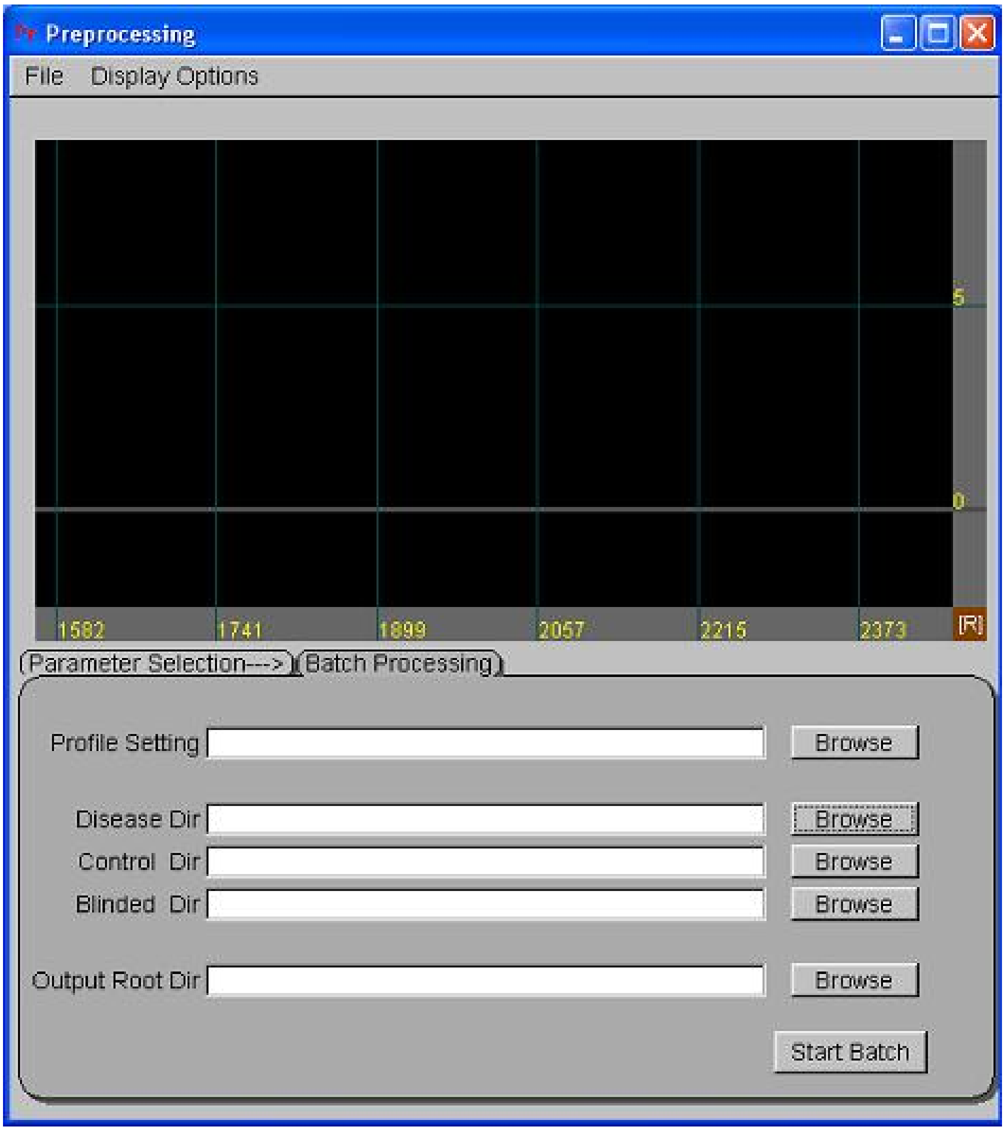

Profile Setting: the location of the .prp file with the preprocessed parameters. By default it is the file saved most recently in the Parameter Selection Page.

Disease Dir: the directory of training data set of subjects with certain disease or abnormality.

Control Dir: the directory of training data set of normal control subjects.

Blinded Dir: the directory of blinded/testing data set with a blinded mixture of diseased and control subjects.

Output Root Dir: by default it has the same parent directory as the Input Dir. A subdirectory of the Output Root Dir is created according to the preprocessing steps. The three groups of preprocessed spectra will be output to this subdirectory.

For Example, there are three groups of spectra A, B and C. The preprocessing step is smoothing with the parameter 0.003%.

Then Disease Dir is 'dir1/A/', Control Dir is 'dir1/B/', Blinded Dir is 'dir1/C/' and Output Root Dir: 'dir1/Preprocessed/'.

The preprocessed spectra are output to the subdirectory of the Output Root Dir:

Disease: 'dir1/Preprocessed/Smoothed(3.e-005)/A/'.

Control: 'dir1/Preprocessed/Smoothed(3.e-005)/B/'.

Blinded: 'dir1/Preprocessed/Smoothed(3.e-005)/C/'.

A.3.2 Biomarker detection

Select Analysis → Biomarker Detection. There are two types of biomarkers: Maximum Peak Intensity and Peak Area.

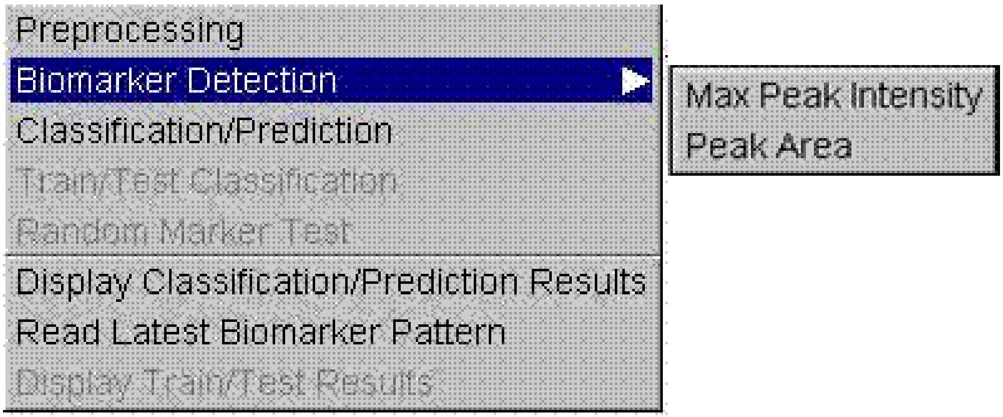
Preprocessing
Biomarker Detection
Classification/Prediction
Train/Test Classification
Random Marker Test
Display Classification/Prediction Results
Read Latest Biomarker Pattern
Display Train/Test Results
Max Peak Intensity
Peak Area

After you choose either Maximum Peak Intensity or Peak Area, the Biomarker Detection sub-window will pop-up automatically. Similar to the Preprocessing sub-window, it has two parts, the top portion for spectrum visualization and the bottom portion for parameter selection.

Peak detection consists of three steps: Identification, Refinement and Alignment. First, the rise and fall within the neighborhood of each m/z point is identified as a peak. Then, the noise level is determined within the noise window. The peak above the noise level is called a refined peak. After performing the peak identification and refinement on each spectrum, the program will then align the peaks across all spectra in the training and test data sets.

Use the Biomarker Detection Window to (1) Open a single mass spectrum and tune the parameters for peak detection; (2) Save selected parameters into a profile for the subsequent batch processing; (3) Choose the dataset/folder one wishes to format using the selected parameter setting; (4) Apply the saved parameter profile to the chosen dataset/folder and format the entire dataset/folder using the given parameter setting automatically.

For the above 4 steps, the parameter setting steps (1 & 2) are done using the Parameter Selection sub-page; and the batch processing steps (3 & 4) are done with the Batch Processing sub-page. Further details are given below.

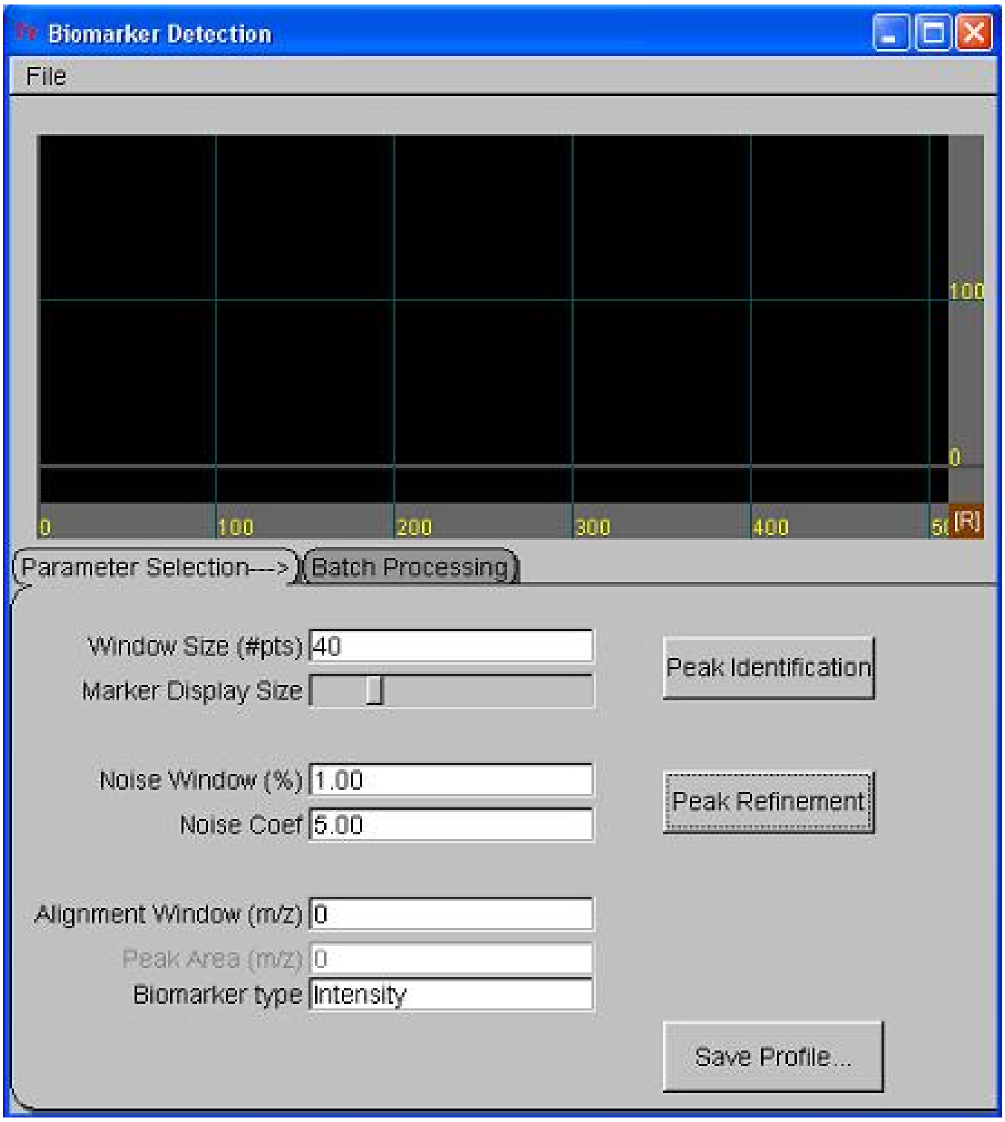

Window Size (#pts) 40

Noise Window (%) 1.00

Noise Coef 5.00

Alignment Window (m/z) 0

Peak Area (m/z) 0

Biomarker type Intensity

Parameter Selection Page

Peak Identification: within the neighborhood of each m/z, identify the local maximum or rise and fall as a peak. Window Size means the number of points within the neighborhood. Click Peak Identification button and the peaks are displayed in green squares, you can tune the Marker Display Size.

Peak Refinement: The noise level is calculated by the points in the Noise Window. You need to input a percentage. The number of points in the Noise Window is the input percentage*total number of points. At each m/z:

noise = mean + Noise Coef*standard deviation

where Noise Coeff is proportional to the signal/noise ratio.

Click Peak Refinement and a yellow noise boundary line will appear. Peaks below the noise level are represented by red squares and discarded for the ensuing classification/prediction analysis. Peaks above the noise level are represented by green squares and are termed refined peaks. The refinded peaks will be used for further classification/prediction.

Peak Alignment: align peaks across all samples within the Alignment Window. This parameter is the window size and should be a positive number.

Peak Area: if you choose Peak Area in the Biomarker Detection menu, this item will be activated. Input the width of the interval to calculate the peak area. If you input zero, it is equivalent to detect the Maximum Peak Intensity.

Save Profile...: all parameters will be saved in a .pek file. The file will be used later in the Batch Processing Page to perform peak detection on an entire dataset/folder.

Batch Processing Page

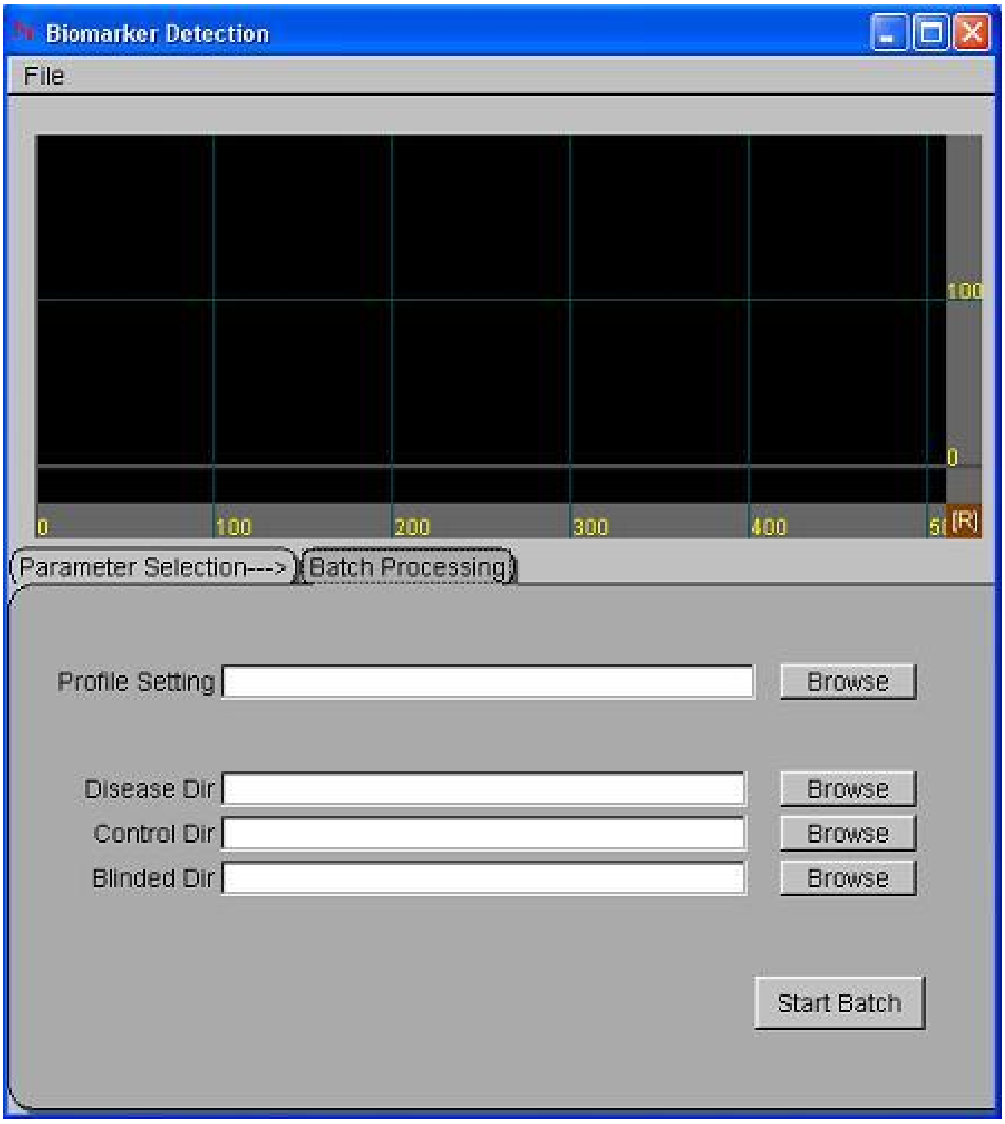

Profile Setting: the location of the .pek file with parameters in peak detection. By default it is the file saved most recently in the Parameter Selection Page.

Disease Dir: the directory of training data set of subjects with certain disease or abnormality.

Control Dir: the directory of training data set of normal control subjects.

Blinded Dir: the directory of blinded/testing data set with a blinded mixture of diseased and control subjects.

We recommend the user to use the preprocessed spectra for biomarkers detection and the ensuing classification/prediction analysis. Thus the above input directories should be the output directories in Preprocessing. A subdirectory named 'PeakAligned(*)' is created automatically in each input directory, where * are selected parameters. The spectra with detected biomarkers are output to this subdirectory.

Example: following the example in Data Preprocessing.

Disease Dir: 'dir1/Preprocessed/Smoothed(3.e-005)/A/'.

Control Dir: 'dir1/Preprocessed/Smoothed(3.e-005)/B/'.

Blinded Dir: 'dir1/Preprocessed/Smoothed(3.e-005)/C/'.

The output directories are:

Disease: 'dir1/Preprocessed/Smoothed(3.e-005)/A/PeakAligned(*)/'.

Control: 'dir1/Preprocessed/Smoothed(3.e-005)/B/PeakAligned(*)/'.

Blinded: 'dir1/Preprocessed/Smoothed(3.e-005)/C/PeakAligned(*)/'.

A.3.3 Classification/Prediction

Select Analysis → Classification / Prediction. We perform the Z/T test to select significant biomarkers. The Bonferroni's method is applied for multiple-test correction to determine the experimentwise critical value. Using the significant biomarkers, we train the classifiers with the training sets (e.g. disease and control) and then predict the identity of those in the blinded/testing data set (e.g. test).

Batch Processing Directory

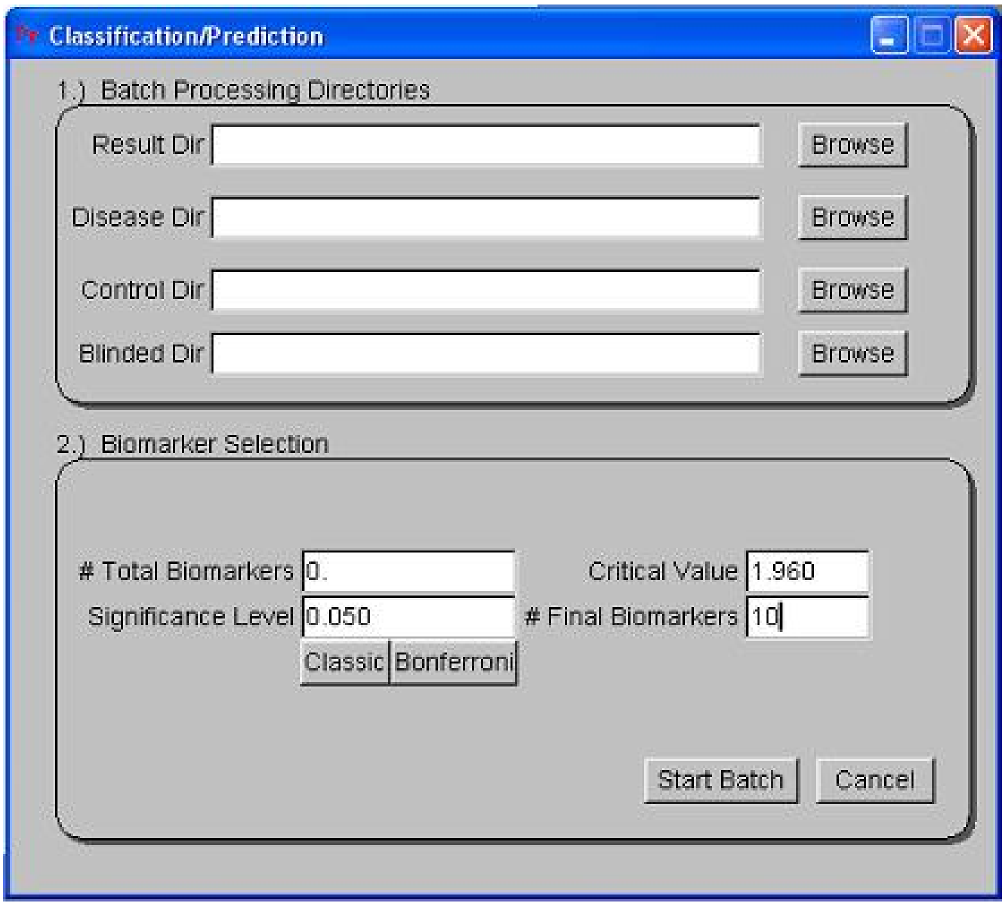
Classification/Prediction

1.) Batch Processing Directories

Result Dir

Disease Dir

Control Dir

Blinded Dir

2.) Biomarker Selection

Total Biomarkers 0.

Critical Value 1.960

Significance Level 0.050

Final Biomarkers 10

Result Dir: the directory of the output results.

Disease Dir: the directory of training data set of subjects with certain disease or abnormality.

Control Dir: the directory of training data set of normal control subjects.

Blinded Dir: the directory of blinded/testing data set with a blinded mixture of diseased and control subjects.

Use the output directories from the Biomarker Detection step C i.e. the PeakAligned directories embedded inside the preprocessed spectra directories.

Example: following the previous example.

Disease Dir: 'dir1/Preprocessed/Smoothed(3.e-005)/A/PeakAligned(*)/'.

Control Dir: 'dir1/Preprocessed/Smoothed(3.e-005)/B/PeakAligned(*)/'.

Blinded Dir: 'dir1/Preprocessed/Smoothed(3.e-005)/C/PeakAligned(*)/'.

The PeakAligned directories will have a suffix which is the value of the Peak Area size chosen in the Biomarker Detection step. For example, peak data generated using the Maximum Peak Intensity method will have output directories labeled as PeakAligned(0.). Peak data generated using the Peak Area method with a chosen area size of 10 will have output directories labeled as PeakAligned(10.).

Biomarker Selection

Set the parameters for the Z/T test to select the significant biomarkers.

Number of Total Biomarkers: the number of biomarkers detected. It is determined by any input directory. For the Maximum Peak Intensity or Peak Area method, this is the number of refined peaks identified in the Biomarker Detection step.

Significant Level: the significant level of the Z/T test. It is 0.05 by default. This significance level refers to either the level of a single test at each biomarker selected or the experimentwise significance level for all biomarker selected depends on whether you click the Classic or Bonferroni button below.

Critical Value: select biomarkers above the critical value of the Z/T tests. There are two methods to calculate the critical value, Classic for the single marker test and Bonferroni for the multiple-test correction to ensure the experimentwise error rate of all biomarkers selected. Click either button will set the corresponding critical value automatically.

Number of Final Biomarkers: the number of biomarkers with the top largest absolute Z/T values. They will be in your final model. (On rare occasions, the number of biomarkers exceeding the critical value threshold might be less than the number of markers you have entered. This could occur when you use the Bonferroni threshold. In this case, the minimum of the number of available markers and your chosen number will be used for the subsequent classification/prediction.)

Output Description

The output is in the directory Result Dir. The summary is in an html file entitled ClassificationReport.htm. A suffix of the date and time the report is generated will be attached to the file name to avoid any confusion. Select Analysis → Display Classification/Prediction Results to open it. The biomarkers are saved in a file named 'Biomarkers.pat'. Open a spectrum in the Main Window and then select Analysis → Read Latest Biomarker Pattern to visualized the pattern. The biomarkers are displayed in red bars.

A.3.4 Visualized biomarker pattern

The user can visualize the selected biomarker pattern with the individual spectrum or the average spectrum. Open the spectrum in the Main Window before reading the biomarker file and then select File → Read Biomarker Pattern. The biomarkers are displayed in red bars.

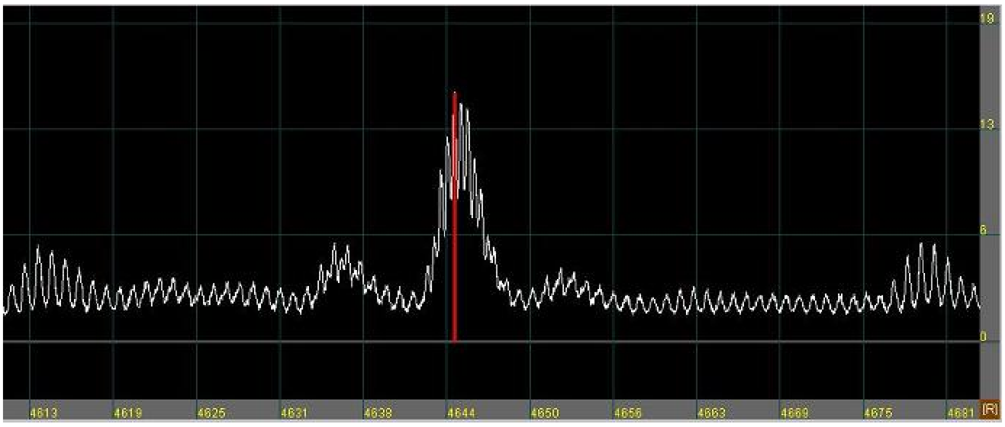

A.4 Example of head and neck data

A.4.1 Data description

	Training	Training	Testing
Status	HNSCC (disease)	Normal (control)	Blinded (test)
Number of Subjects	73	76	49

Each spectrum has 34,378 data points. All spectra should be saved in the same parent directory:

A.4.2 Data preprocessing

Select Analysis → Preprocessing to open the preprocessing sub-window, display a spectrum by select File → Open New Spectrum. For instance, we open a spectrum with the sample ID 11 in the disease group. The Description Textbox displays the location of the file: '/proteoExplorer/demodata/disease/HN011.txt'.

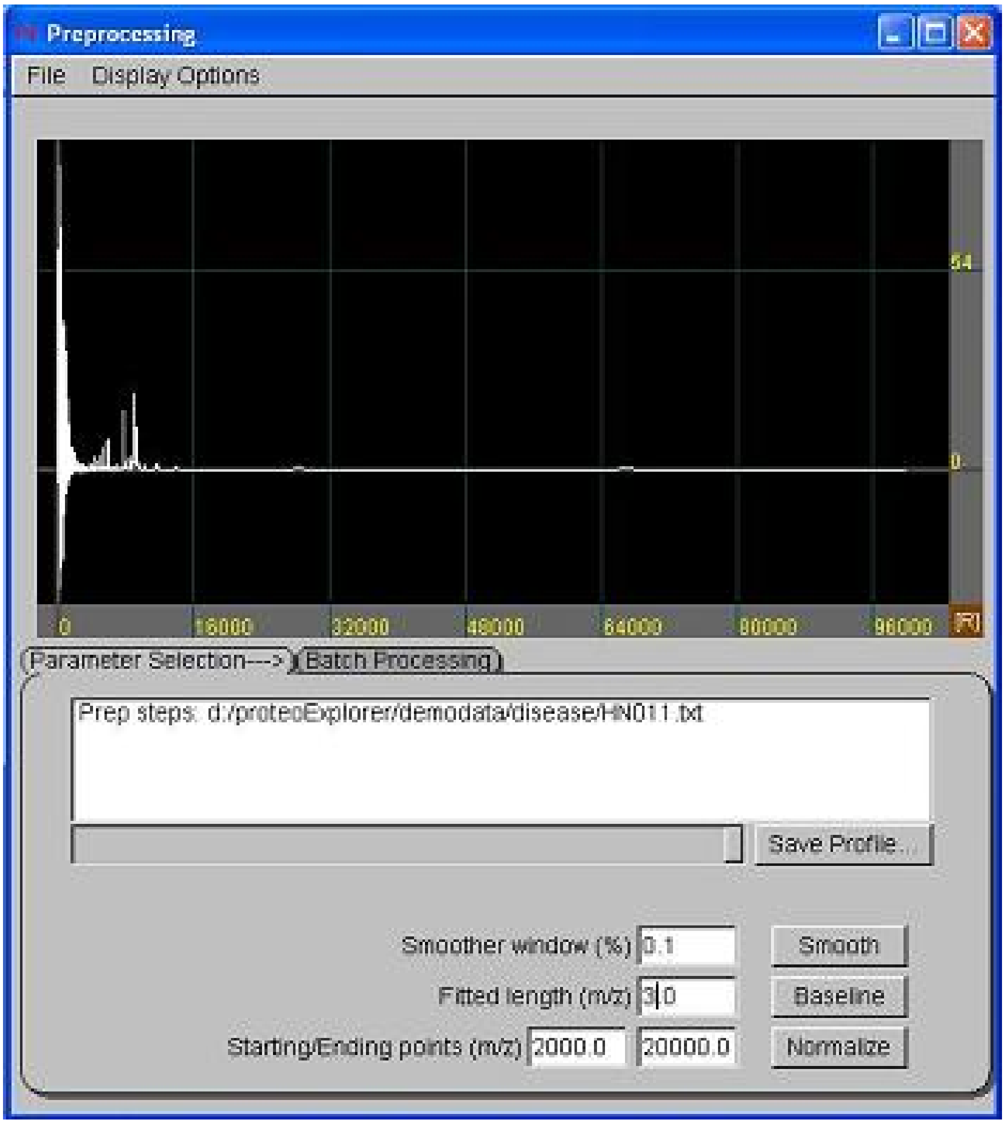

Prep steps: d:/proteoExplorer/demodata/disease/HN011.txt

Smoother window (%) 0.1

Fitted length (m/z) 3.0

Starting/Ending points (m/z) 2000.0 20000.0

Click **Smooth** on the bottom to do smoothing, the default parameter is 0.1%, which means the smoothing window contains 34 points (0.1% * 34378 = 34.37). The description of this preprocessing step, '#0: type = Smoothed param = 0.001' is displayed in the Description Textbox. Select Display Options → Show All, one can zoom in to see the change of the preprocessed spectrum. All the spectra in each preprocessing step will be displayed simultaneously and the most recent preprocessed spectrum (smoothed) is highlighted. The difference can also be seen by tuning the Display Toolbar below the Description Textbox.

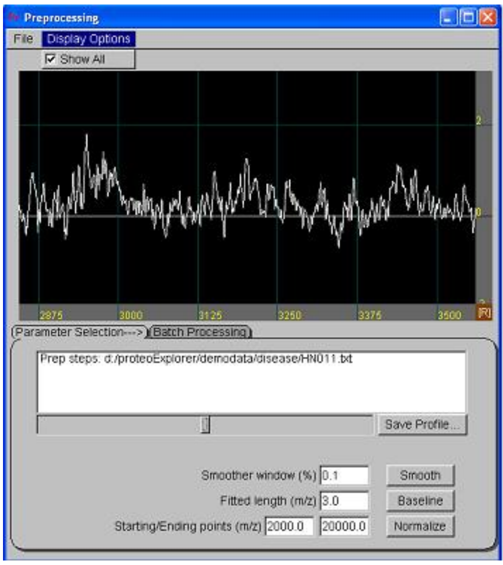

Prep steps: d:/proteoExplorer/demodata/disease/HN011.txt

Smoother window (%) 0.1

Fitted length (m/z) 3.0

Starting/Ending points (m/z) 2000.0 20000.0

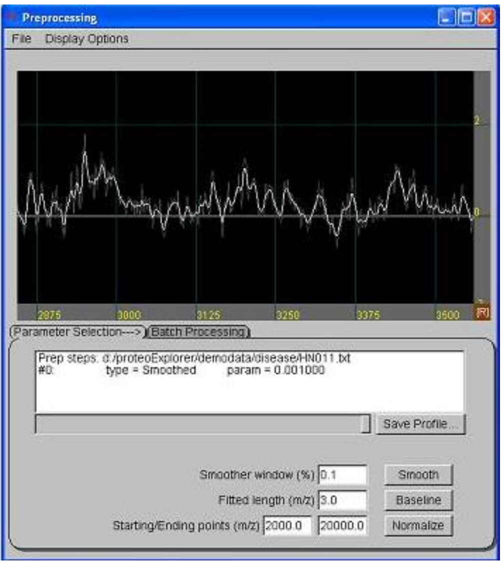

```
Prep steps: d:/proteoExplorer/demodata/disease/HN011.txt
#0:          type = Smoothed        param = 0.001000
```

Smoother window (%) 0.1

Fitted length (m/z) 3.0

Starting/Ending points (m/z) 2000.0 20000.0

Next, we can perform the baseline correction and the normalization by clicking Baseline and Normalize respectively. In this case, we notice that the baseline is already corrected and there are some negative values. Thus we perform normalization only. The m/z range between 2,000 and 20,000 is selected because there is noise in the range of m/z below 2,000 and almost zero for m/z above 20,000.

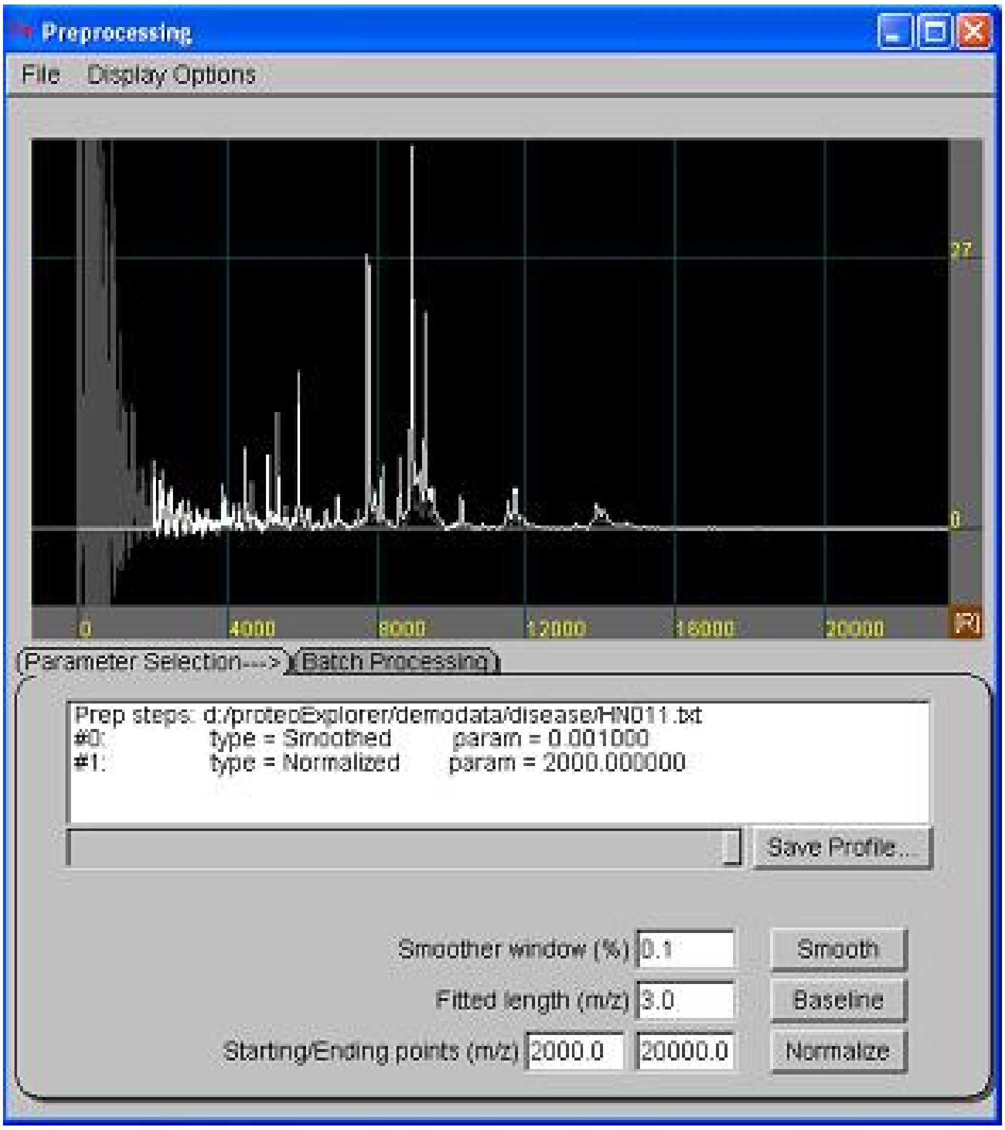

```
Prep steps: d:/proteoExplorer/demodata/disease/HN011.txt
#0:         type = Smoothed      param = 0.001000
#1:         type = Normalized    param = 2000.000000
```

Smoother window (%) 0.1

Fitted length (m/z) 3.0

Starting/Ending points (m/z) 2000.0 20000.0

Click Save Profile..., select the directory and type the name of the file to save the preprocessing parameters. The file has the extension name 'prp'. Should you decide to create and rename a new directory, please press the ENTER key on your key board after typing the name of the new folder created to confirm the new folder name. For example, create a new directory '/para' and save the parameters to '/proteoExplorer/para/prep1.prp'. (Note, you only need to type prep1, the .prp extension will be added automatically.) Click OK in the 'Choose a save location' dialog, the Parameter Selection Page will change to Batch Processing Page automatically and the most recent saved parameter filename will appear in the Profile Setting textbox automatically as well.

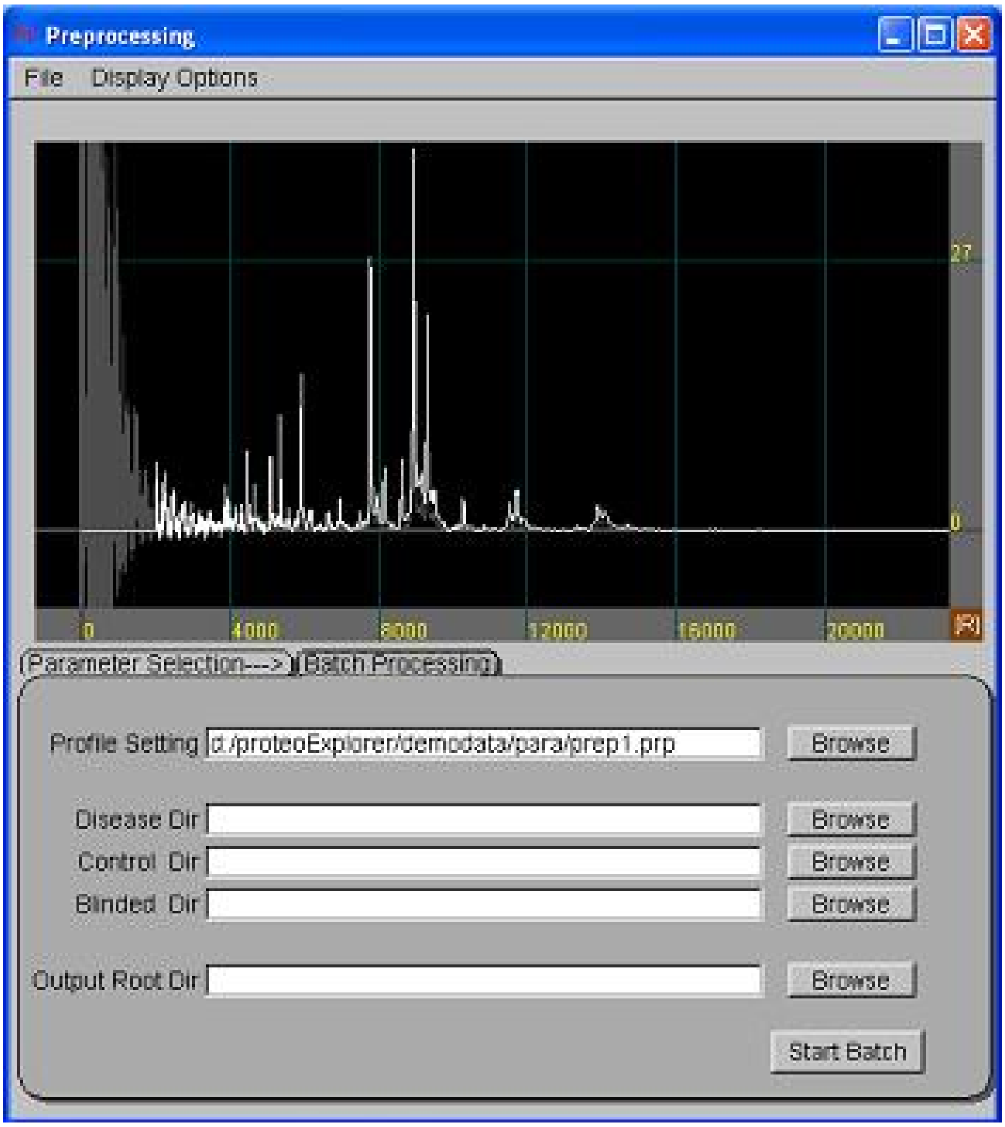

Profile Setting d:/proteoExplorer/demodata/para/prep1.prp

Disease Dir

Control Dir

Blinded Dir

Output Root Dir

We will now perform preprocessing on the three groups of spectra. Click the Browse button to choose the directory for each group.

Head&Neck Cancer (disease): '/proteoExplorer/demodata/disease/'.

Normal Control(control): '/proteoExplorer/demodata/control/'.

Blinded(test): '/proteoExplorer/demodata/test/'.

The Output Root Dir will be '/proteoExplorer/demodata/Preprocessed/' automatically. Click Start Batch to start the preprocessing procedure.

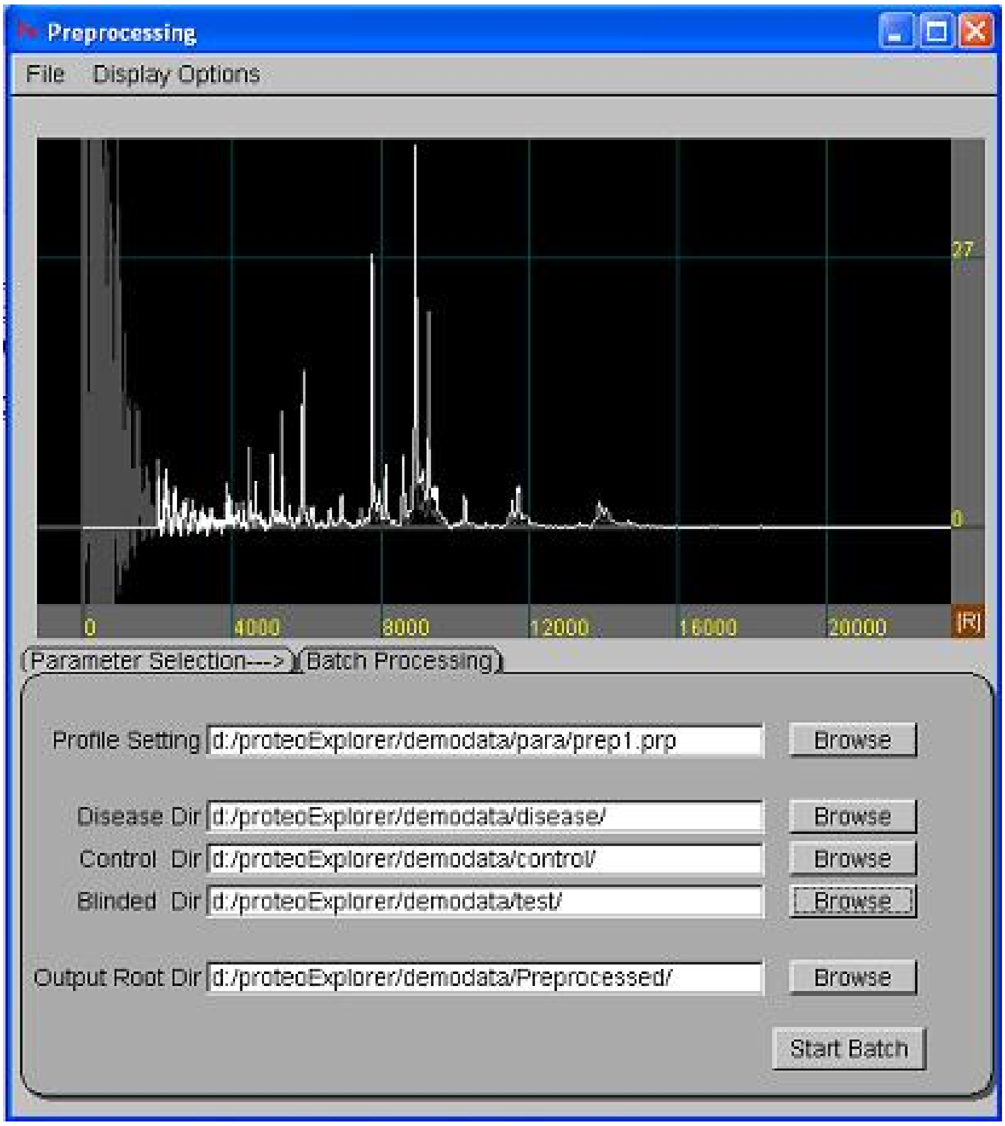

Profile Setting d:/proteoExplorer/demodata/para/prep1.prp

Disease Dir d:/proteoExplorer/demodata/disease/

Control Dir d:/proteoExplorer/demodata/control/

Blinded Dir d:/proteoExplorer/demodata/test/

Output Root Dir d:/proteoExplorer/demodata/Preprocessed/

A subdirectory of '/proteoExplorer/demodata/Preprocessed/' is created and named 'Smoothed(1.e-003)Normalized(2.e+003,2.e+004)'. The name contains the parameters for smoothing and normalization. The preprocessed spectra are saved in this subdirectory as follows:

Head&Neck Cancer (disease):

'/proteoExplorer/demodata/Preprocessed/.../disease/'.

Normal Control (control):

'/proteoExplorer/demodata/Preprocessed/.../control/'.

Blinded (test):

'/proteoExplorer/demodata/Preprocessed/.../test/'.

A.4.3 Biomarker selection

Maximum Peak Intensity

Select Analysis → Biomarker Selection → Maximum Peak Intensity to open the sub-window to generate the peak data based on the maximum intensity of each peak. First open a (preprocessed) spectrum and tune the parameters in the Parameter Selection Page to detect, refine and align the peaks. The spectrum with the sample ID 011 in the disease group is used as an example. Since we recommend to use the preprocessed spectra, open the spectrum 'HN011.txt' in the directory:

'/proteoExplorer/demodata/Preprocessed/.../disease/'.

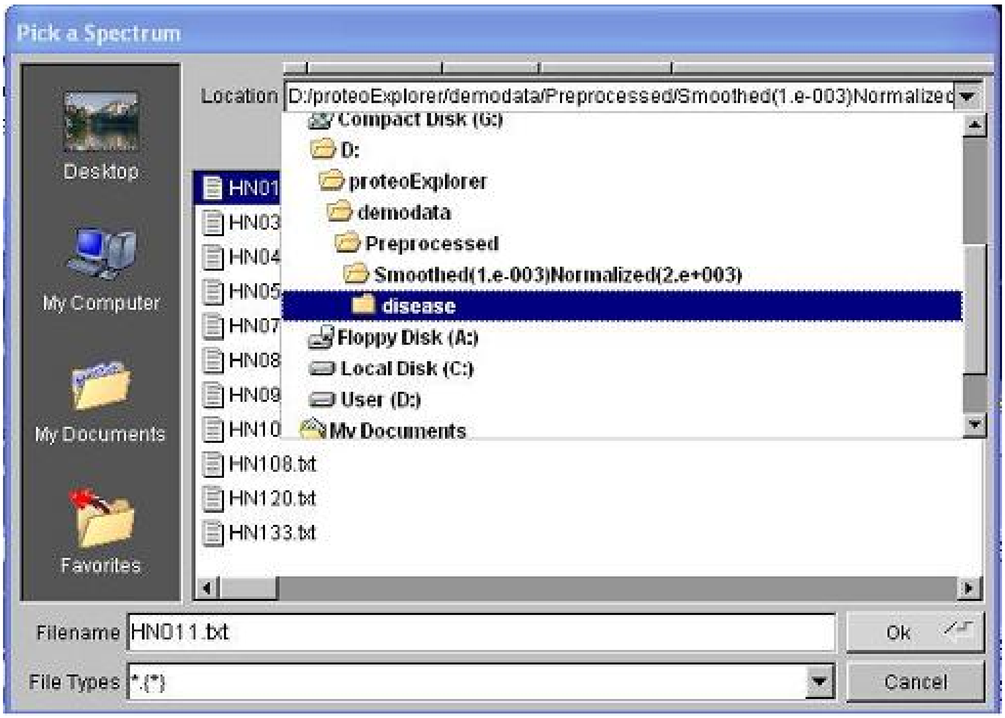

Location D:/proteoExplorer/demodata/Preprocessed/Smoothed(1.e-003)Normalized

Filename HN011.txt

File Types *.(*)

Click Peak Identification to identify peaks. The green squares indicate the identified peaks and their display size is tunable.

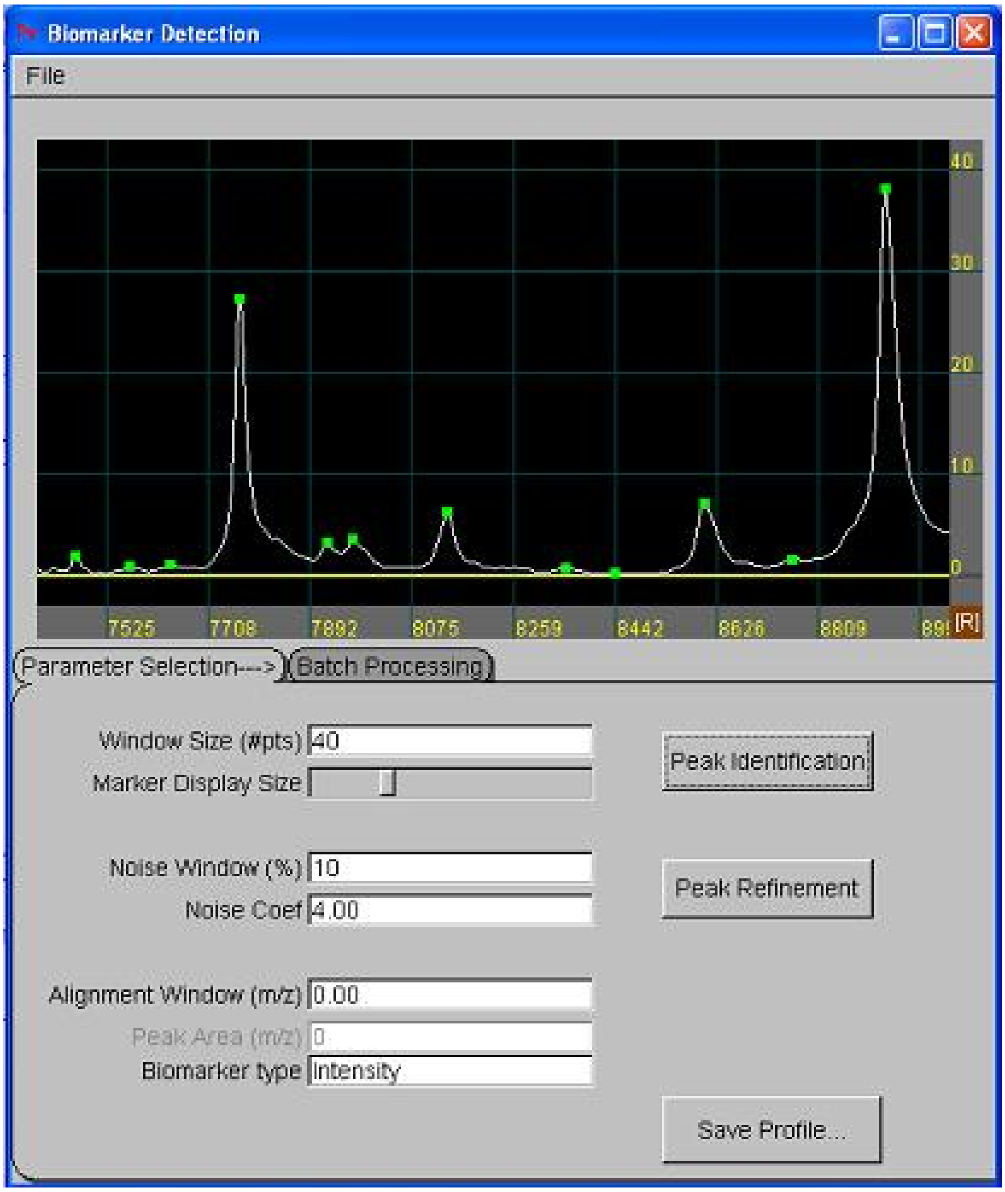

Window Size (#pts) 40

Noise Window (%) 10

Noise Coef 4.00

Alignment Window (m/z) 0.00

Peak Area (m/z) 0

Biomarker type Intensity

Click Peak Refinement to refine peaks. The yellow line indicates the noise level and the peaks below the noise level are denoted by red squares and are discarded for the ensuing classification/prediction analysis. The green squares are refined peaks that are saved for future analysis.

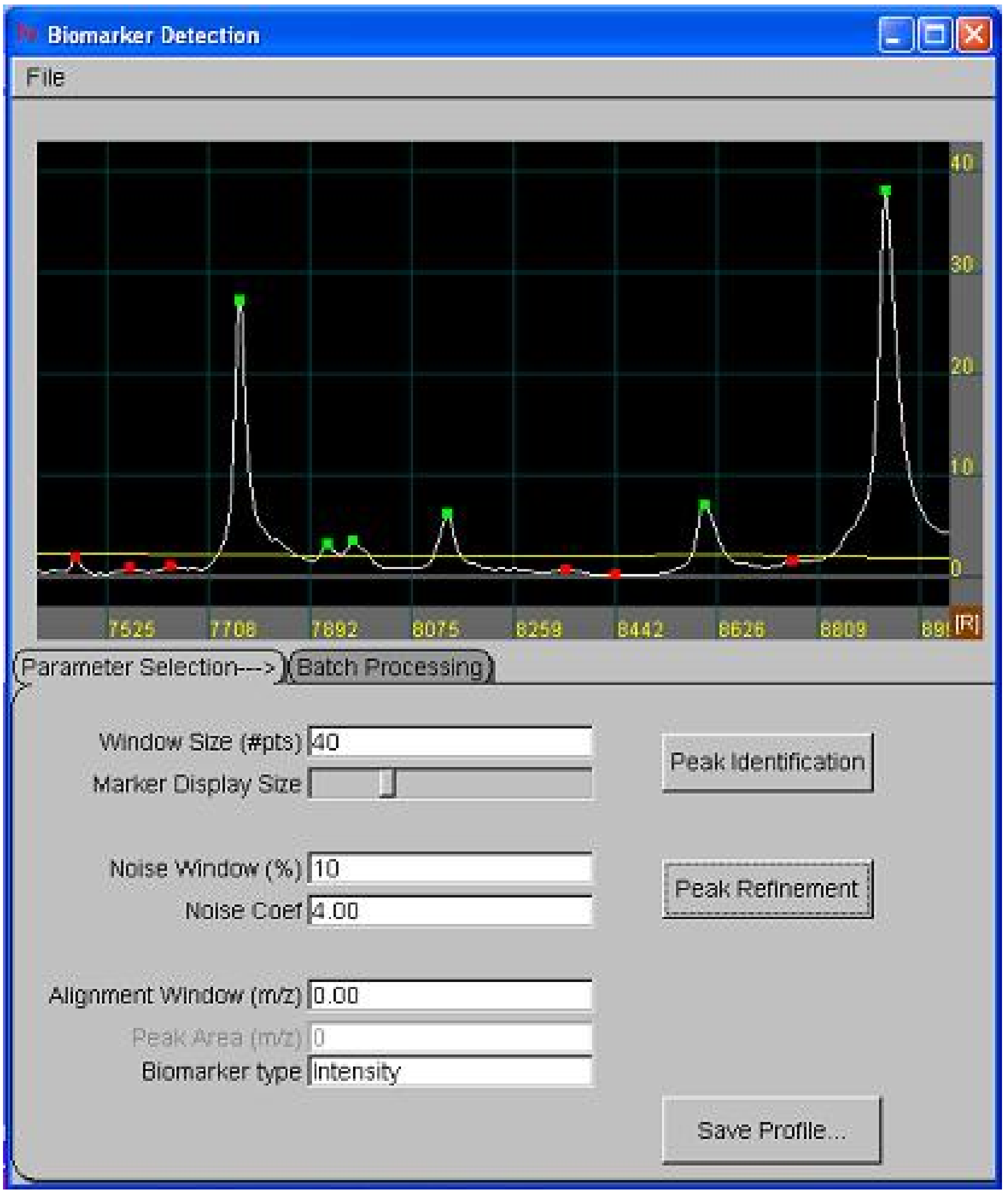

Window Size (#pts) 40

Noise Window (%) 10

Noise Coef 4.00

Alignment Window (m/z) 0.00

Peak Area (m/z) 0

Biomarker type Intensity

Set the parameter Alignment Window, it is the peak shift width with 10 m/z. The alignment window for each peak is indicated by two grey vertical lines.

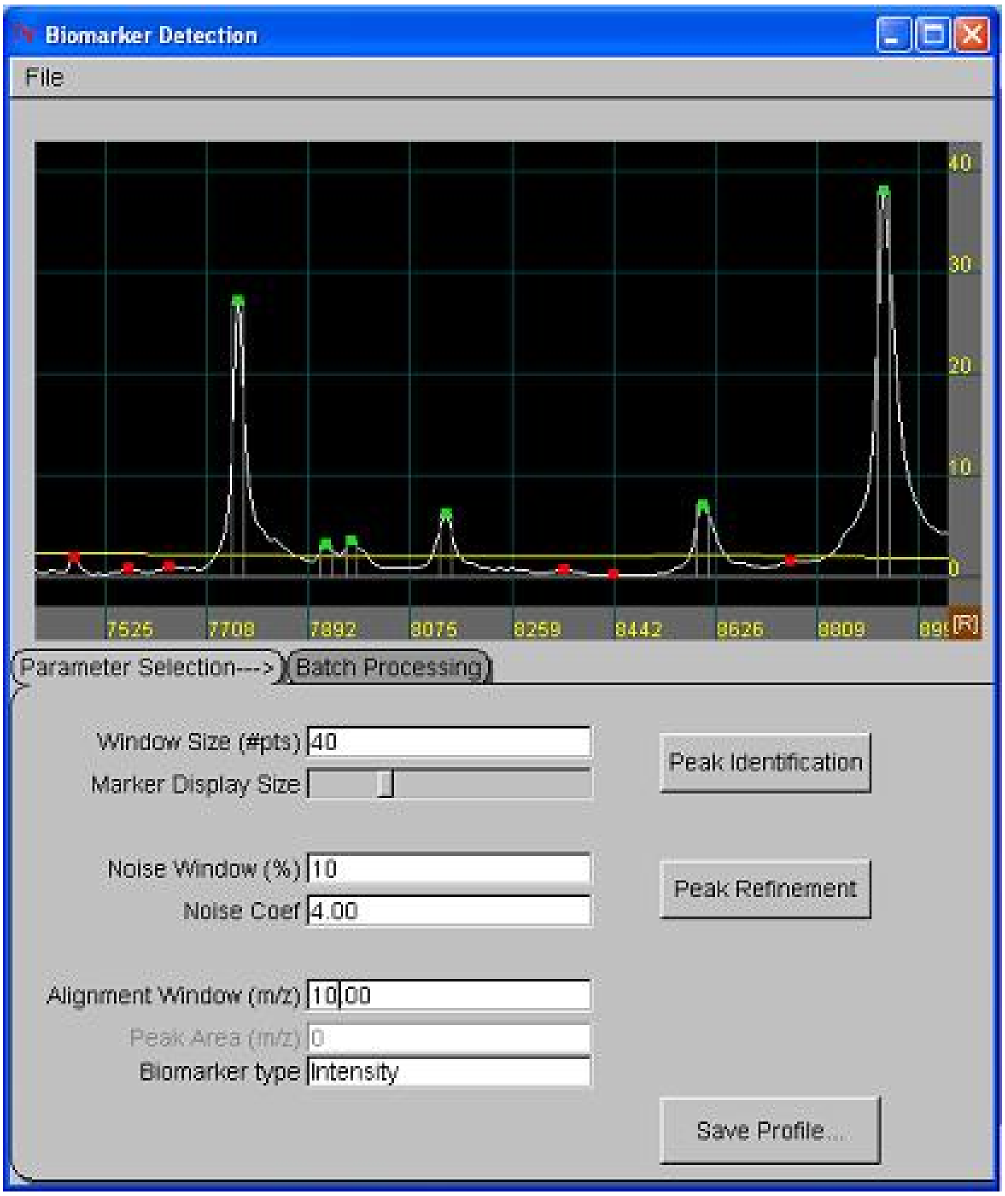

Window Size (#pts) 40

Marker Display Size

Noise Window (%) 10

Noise Coef 4.00

Alignment Window (m/z) 10.00

Peak Area (m/z) 0

Biomarker type Intensity

Click Save Profile... to save the parameter settings into a file with the extension 'pek'. We save this file to '/proteoExplorer/para/peak1.pek'. Now the Parameter Selection Page will change to the Batch Processing Page and the location of this peak parameter file will appear in the Profile Setting textbox automatically.

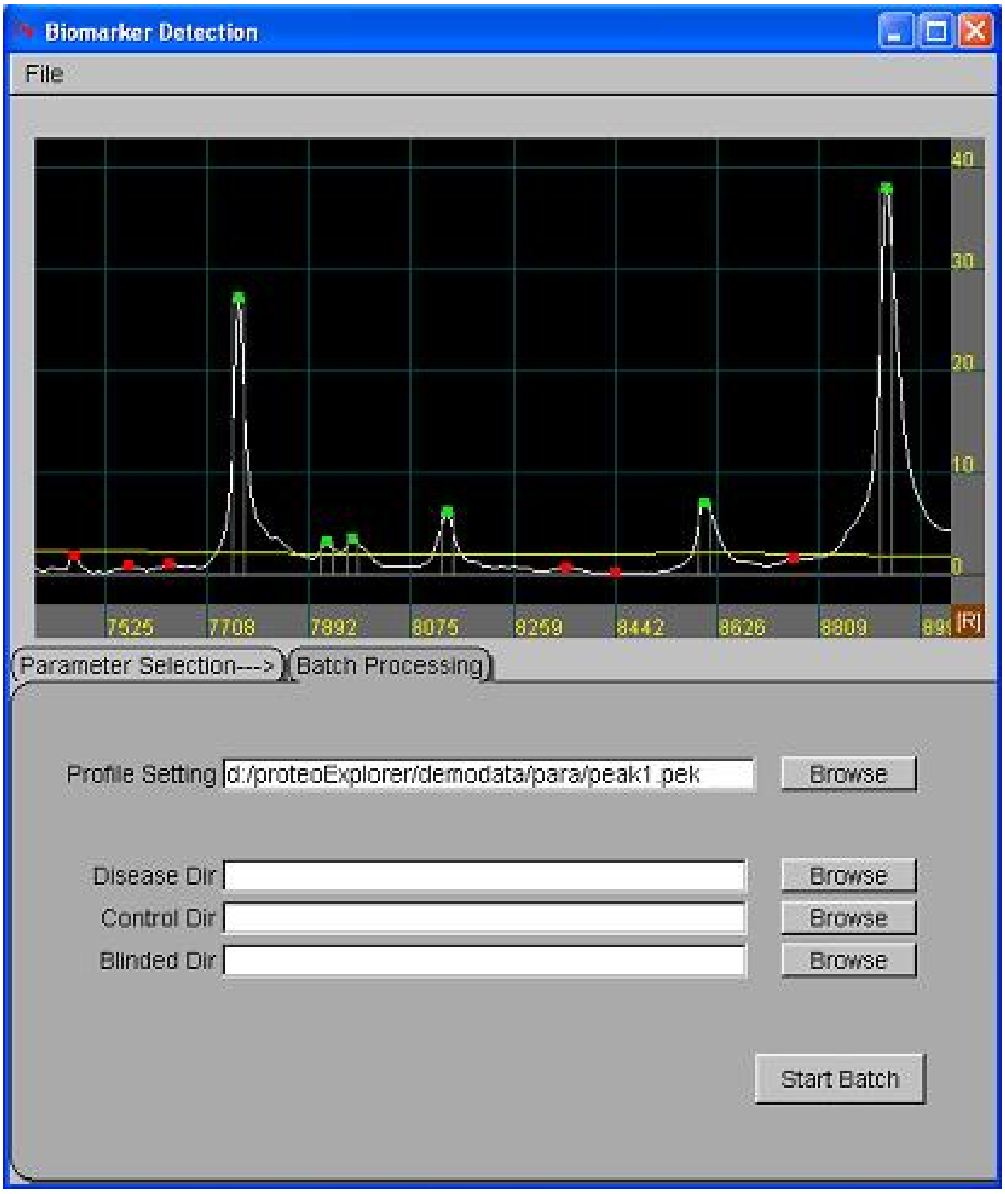

Profile Setting d:/proteoExplorer/demodata/para/peak1.pek

Disease Dir

Control Dir

Blinded Dir

Choose the directory of preprocessed spectra as the input directories. They are the same as the output directories in the preprocessing step:

Input Dir:

Head&Neck Cancer (disease):

'/proteoExplorer/demodata/Preprocessed/.../disease/'.

Normal Control (control):

'/proteoExplorer/demodata/Preprocessed/.../control/'.

Blinded (test):

'/proteoExplorer/demodata/Preprocessed/.../test/'.

The refined and aligned maximum peak intensity data/spectra are saved to subdirectories PeakAligned(*), where * represents the parameters in the Parameter Selection page.

Output Dir:

Head&Neck Cancer (disease): '.../disease/PeakAligned(40.,10.,4.,10.,0.)/'.

Normal Control (control): '.../control/PeakAligned(40.,10.,4.,10.,0.)/'.

Blinded (test): '.../test/PeakAligned(40.,10.,4.,10.,0.)/'.

Peak Area

Same as Maximum Peak Intensity except there is one more parameter to choose. Input the interval width to determine the area in the Peak Area textbox.

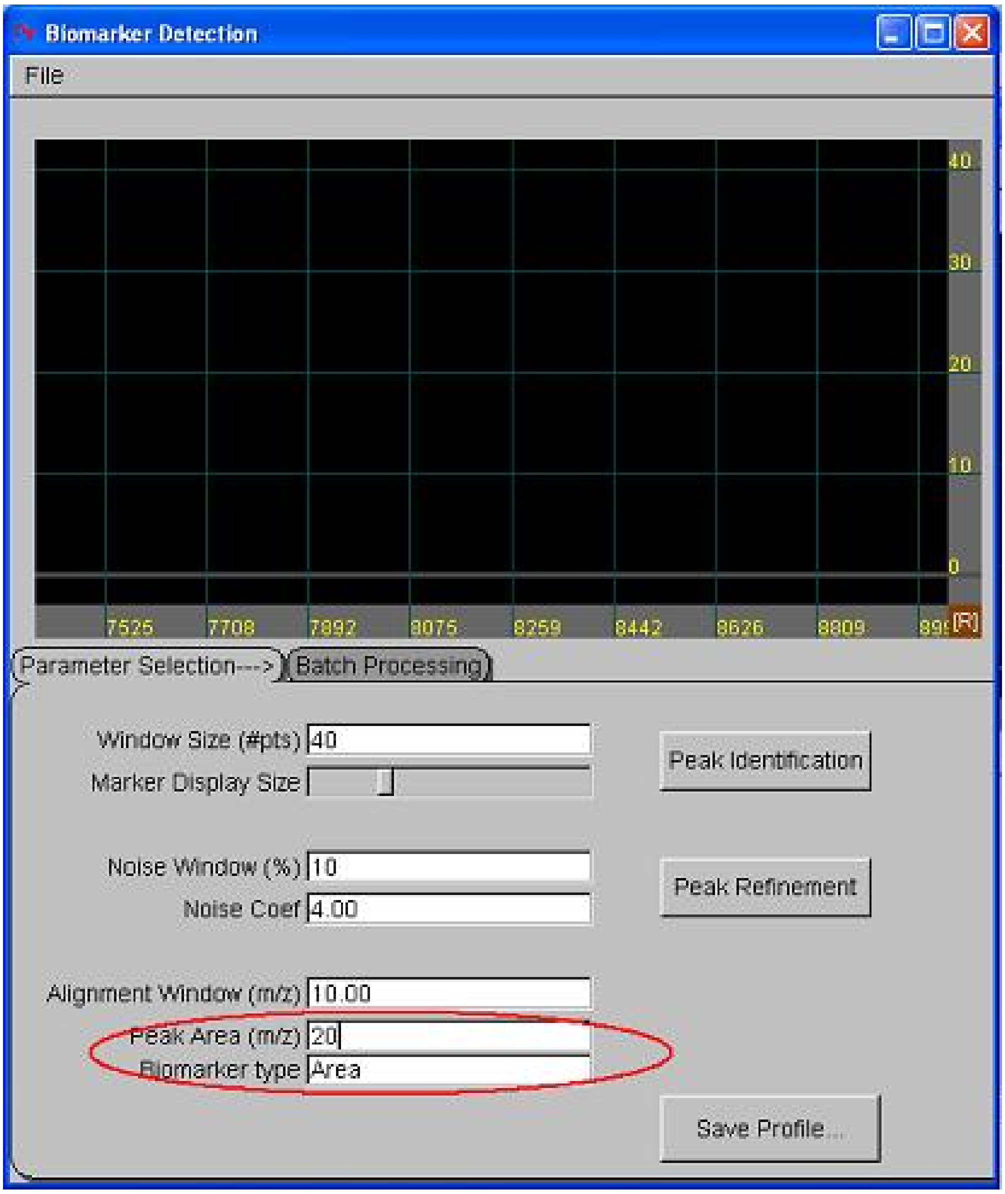

Window Size (#pts) 40

Noise Window (%) 10

Noise Coef 4.00

Alignment Window (m/z) 10.00

Peak Area (m/z) 20

Biomarker type Area

Save profile to a pek file and the output directories will be as following:

Head & Neck Cancer (disease): '.../disease/PeakAligned(40.,10.,4.,10.,20.)/'.

Normal Control (control): '.../control/PeakAligned(40.,10.,4.,10.,20.)/'.

Blinded (test): '.../test/PeakAligned(40.,10.,4.,10.,20.)/'.

A.4.4 Classification/Prediction

Select Analysis → Classification/ Prediction. First, choose the Result Dir to output results. Then choose the the directory of three groups of spectra.

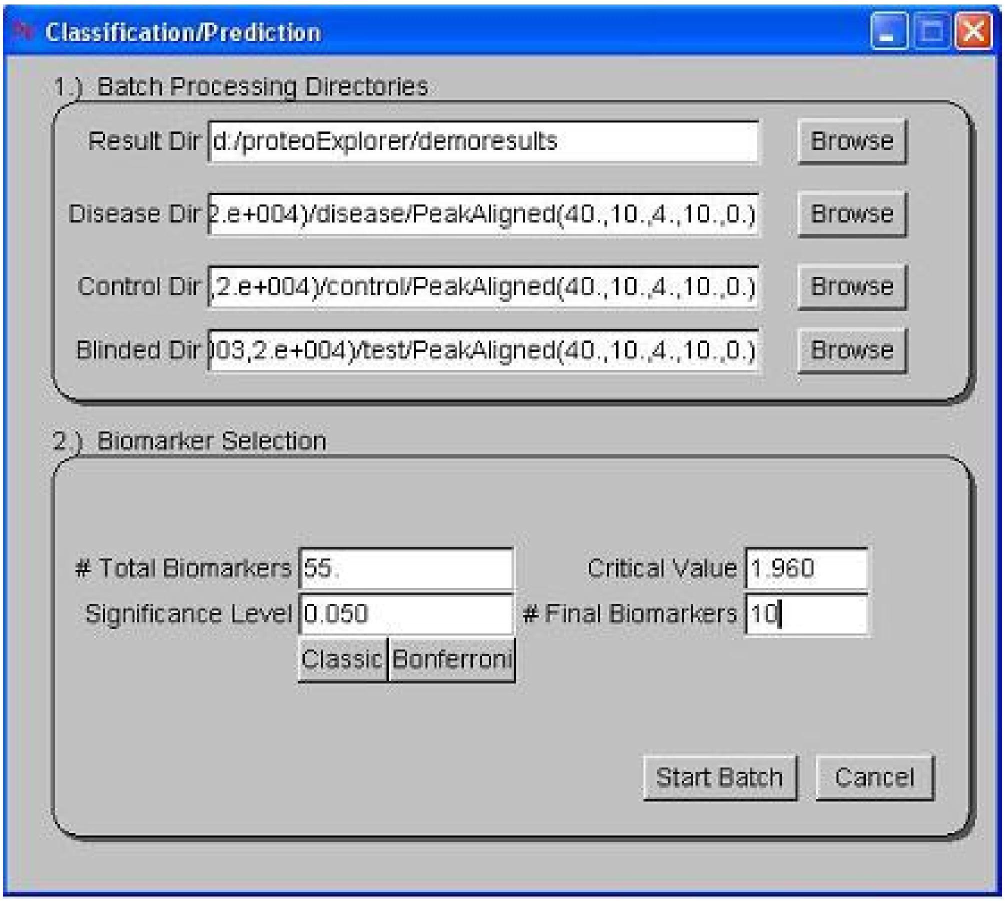

1.) Batch Processing Directories

Result Dir d:/proteoExplorer/demoresults

Disease Dir 2.e+004)/disease/PeakAligned(40.,10.,4.,10.,0.)

Control Dir ,2.e+004)/control/PeakAligned(40.,10.,4.,10.,0.)

Blinded Dir 03,2.e+004)/test/PeakAligned(40.,10.,4.,10.,0.)

2.) Biomarker Selection

Total Biomarkers 55.

Critical Value 1.960

Significance Level 0.050

Final Biomarkers 10

We choose Maximum Peak Intensity as the biomarkers, thus the input directories are the same as the output directories in the corresponding Biomarker Detection step:

Disease Dir: '.../disease/PeakAligned(40.,10.,4.,10.,0.)/'.

Control Dir: '.../control/PeakAligned(40.,10.,4.,10.,0.)/'.

Blinded Dir: '.../test/PeakAligned(40.,10.,4.,10.,0.)/'.

No. of Total Biomarkers is 47, which means there are 47 refined and aligned peaks. Select the Significant Level (alpha) which is 0.05 (2-sided) by default. Click Classic or Bonferroni to determine the corresponding Critical Value for the Z/T test. The Critical Value is 3.273 if we choose Bonferroni's method to ensure an exprimentwise significance level of 0.05 (2-sided).

The No. of Final Biomarkers entered is 10, which means we wish to use the top 10 biomarkers with the large absolute Z/T values as our final model. If we want to select all significant markers, input the maximum number (47 in this example) in No. of Final Biomarkers, and the number of significant biomarkers can be seen in the output file.

Now we are ready to click Start Batch to perform the classification and prediction using the given training and testing data sets. An html file entitled 'ClassificationReport***.htm' will be output to the Result Dir, select Analysis → Display Classification/ Prediction Results to open it. Please note that *** is the generation date and time of this html output file to avoid confusion. In the output file, the summary of training result is listed in the first table and the detail classification result of each spectrum is in the 2nd table. The selected biomarkers are also given.

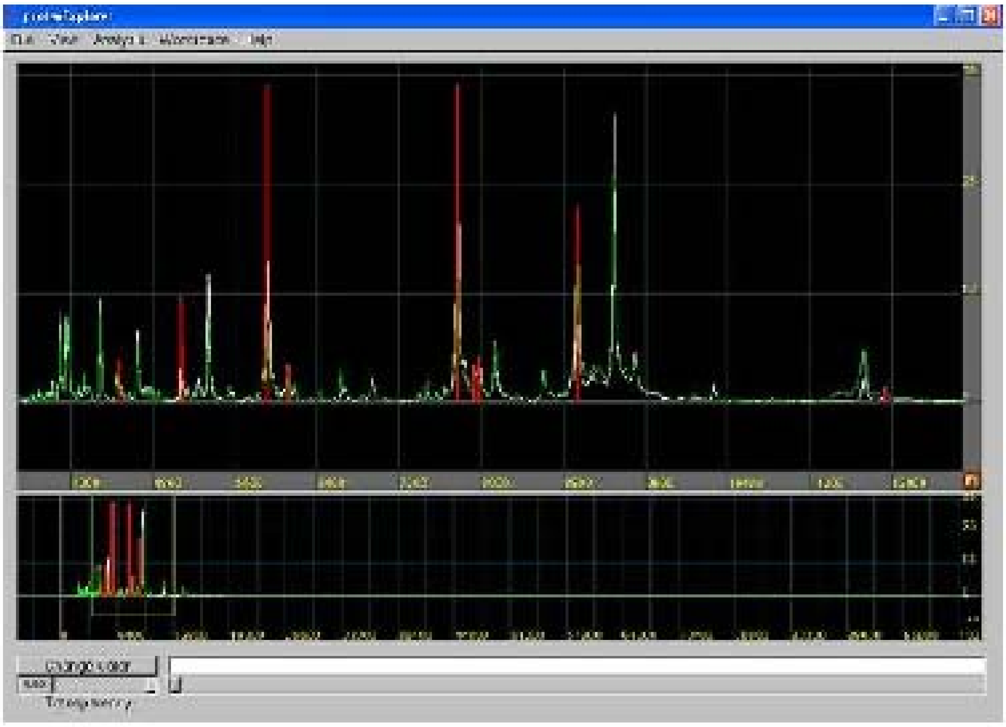

A file named ’Biomarker.pat’ is generated in Result Dir and save the biomarker pattern. To look at the positions of selected biomarkers, open any spectrum first and then select Analysis → Read Latest Biomarker Pattern to open ’Biomarker.pat’ or select File → Read Biomarker Pattern to locate the file. In the figure below, the average spectra of the two groups are displayed, the green one is for disease and the white one for control, the red bars denote the selected biomarkers.